Chemical modifications of DNA activate the cGAS/STING-signaling pathway even in the presence of the cytosolic exonuclease TREX1

Dissertation
zur
Erlangung des Doktorgrades (Dr. rer. nat.)
der
Mathematisch-Naturwissenschaftlichen Fakultät
der
Rheinischen Friedrich-Wilhelms-Universität Bonn

vorgelegt von

Christina Mertens
aus
Bergisch-Gladbach

Bonn, März 2015

Angefertigt mit der Genehmigung der Mathematisch-Naturwissenschaftlichen Fakultät
der Rheinischen Friedrich-Wilhelms-Universität Bonn.

1. Gutachter: Prof. Dr. Gunther Hartmann
2. Gutachter: Prof. Dr. Michael Hoch

Tag der Promotion: 12.08.2015
Erscheinungsjahr: 2015

Die vorliegende Arbeit wurde im Zeitraum von Mai 2011 bis März 2015 am Institut für Klinische Chemie und Klinische Pharmakologie der Rheinischen Friedrich-Wilhelms-Universität Bonn unter Leitung von Prof. Dr. Gunther Hartmann und Betreuung durch Prof. Dr. Winfried Barchet angefertigt.

Hiermit erkläre ich an Eides statt,

- dass ich die Arbeit ohne fremde Hilfe angefertigt und andere Hilfsmittel als die in der Dissertation angegebenen nicht benutzt habe; insbesondere, dass wörtlich oder sinngemäß aus Veröffentlichungen entnommene Stellen als solche kenntlich gemacht worden sind,

- dass ich mich bis zu diesem Tage noch keiner Doktorprüfung unterzogen habe. Ebenso hat die von mir vorgelegte Dissertation noch keiner anderen Fakultät oder einem ihrer Mitglieder vorgelegen,

- dass ein Dienststraf- oder Ehrengerichtsverfahren gegen mich weder geschwebt hat noch gegenwärtig schwebt.

Bonn, März 2015

(Christina Mertens)

Für meine Familie

Acknowledgement

I would like to express my gratitude to **Prof. Dr. Gunther Hartmann** and the Institute of Clinical Chemistry and Clinical Pharmacology for giving me the possibility to complete this work.

Especially, I would like to thank **Prof. Dr. Winfried Barchet** for his support and supervision throughout my research project. He was significantly involved in the success of my experiments.

I would like to thank **my reviewers** for their efforts reading and examining this work. I know that they are very busy, and thus, I am even more grateful that they could spare a bit of their time for my thesis and me.

I am also very grateful to the whole Barchet group, notably to **Volker Böhnert, Dr. Nadine Gehrke, Soheila Riemann, Malte Stasch** and **Dr. Thomas Zillinger**, who were always willing to give me any help I needed.

Moreover, I would like to thank **Dr. Tobias Bald** from the Institute of Dermatology for his help with the ear injection experiments.

Additionally, I owe **my friends** a debt of gratitude for encouraging me to continue on with this work and never give up. In particular, I am very much obliged to **Christian Pipper** who was of great help in difficult times.

My family I would like to thank for support in all phases of life. This work is dedicated to you!

Last but not least, I would like to thank all who looked closely at the final version of this thesis.

Thank you!

Table of contents

Summary

To recognize pathogen threats, the innate immune system is equipped with pattern recognition receptors (PRRs) that bind to and are activated by pathogen-associated molecular patterns (PAMPs). Most PAMPs are conserved across species of microbes but at the same time not present in the host, allowing for the efficient discrimination between endogenous and foreign material. However, viruses rely on the host transcriptional and translational machinery to produce every viral component, and therefore do not really contain foreign molecules. It has become apparent that viruses instead are mainly detected via their nucleic acid genomes in the endosomes or cytosol of the host cell. However, virus sensing based on their nucleic acids comes at the risk of erroneous recognition of self-DNA - a process that leads to autoinflammation and possibly autoimmune disease. In particular, the receptor cGAMP synthase (cGAS) detects the mere presence of any DNA in the cytosol by binding its sugar phosphate backbone, and thus shows no apparent preference for sequence or specific molecular structures.

Within this work, evidence is provided that specific damage-associated DNA modifications strongly enhance cGAS-dependent innate immune activation. DNA modifications occurring after UV irradiation, incubation with cytostatic agents, ROS exposure or as a consequence of neutrophil extracellular trap (NET) release were shown to potentiate the interferon (IFN) release in response to cytosolic DNA. However, this differential immune response was not due to higher affinity binding of the modified DNA to cGAS itself, but rather due to an impaired degradation by the cytosolic exonuclease TREX1. Resistance to TREX1 promoted an accumulation of the modified DNA in the cytosol, leading to a prolonged activation of the cGAS/STING-signaling pathway and the release of type I IFN.

One well-known autoimmune disease driven by autoantibodies recognizing double-stranded DNA is lupus erythematosus (LE). Using the lupus-prone mouse model MRL/lpr, UV-damaged DNA (UV-DNA) was shown to be able to induce lupus-like lesions. Thus, UV-DNA could be a potential cause for the phototoxicity often observed in LE patients. Moreover, intravenous administration of UV-DNA induced a type I IFN response in MRL/lpr mice, which could be linked to F4/80-positive monocytes/macrophages.

Together, these data show that under certain conditions self-DNA is transformed into a damage-associated molecular pattern (DAMP) that provides an additional layer of information to distinguish danger and damage from healthy states

1. Introduction

1.1. The Immune System

The immune system (from Latin immunis = free or untouched) is the combination of various defense systems that evolved to protect higher organisms against pathogens, foreign substances and abnormal cells. In vertebrates, the immune system can be divided into innate and adaptive immune system.

The innate immune system is of ancient origin and found in all organisms in some form. Its features are germline encoded and recognize and respond to general molecular patterns that are ideally essential to pathogens but foreign to the host. As such, the receptors and effectors of the innate immune system are immediately available and can provide the first line of defense. Cells of the innate immune system include natural killer (NK) cells, mast cells, neutrophils, eosinophils, basophils, monocytes/ macrophages, and dendritic cells (DC). These cells are responsible for the identification and removal of foreign substances, the recruitment of further immune cells to the site of infection and finally the activation of the adaptive immune system for a more specific immune response.

The adaptive immune system is antigen-specific, since it makes use of DNA recombination and somatic hypermutation to generate a vast diversity of antigen-specific receptors (Brack et al., 1978; Schatz et al., 1992). Exposure to pathogens bearing a particular antigen leads to the selective expansion of cells which can recognize them. After initial exposure, it can take several days until the adaptive immune system becomes protective. However, during this primary immune response, memory cells are generated that remain inside the body and can initiate a rapid secondary immune response if the body encounters the same threat again. Cells of the adaptive immune system include B and T lymphocytes (B and T cells). The main function of B cells involves the production of specific antibodies that can either neutralize their target directly or tag the pathogen for attack by other immune cells. CD4-positive T helper (T_H) cells assist other immune cells by secreting cytokines that regulate or support immunologic processes, while CD8-positive cytotoxic T (T_c) cells destroy host cells that are infected by viruses or have become malignant.

One important link between innate and adaptive immune system are professional antigen presenting cells (APCs) such as DCs or macrophages from the innate immune system. They internalize pathogens and digest them into smaller fragments, which are then presented on Major Histocompatibility Complex (MHC) class II molecules to T_H cells from the adaptive immune system. The interaction of the T cell receptor (TCR) with the antigen-MHC class II complex then leads to the activation of the T cell, but only if also an additional co-stimulatory signal is provided by the APC. To ensure that the adaptive immune system is only activated in

case of pathogen invasion or danger, APCs only upregulate the co-stimulatory signals if their pattern recognition receptors (PRRs) have been activated by pathogen associated molecular patterns (PAMPs).

1.2. Pattern Recognition Receptors

The innate recognition of foreign substances and structures is based on a limited number of receptors encoded in the germline. The so-called pattern recognition receptors (PRRs) recognize pathogen-associated molecular patterns (PAMPs) that are frequently found on pathogens, but ideally absent on host molecules (Janeway, 1989a/b; Gordon, 2002; Janeway and Medzhitov, 2002). There are different classes of PRRs. However, this work will focus on signaling PRRs that recognize nucleic acids (NAs) within the cytosol and subsequently trigger intracellular signaling cascades, which result in the expression of pro-inflammatory cytokines, chemokines, antimicrobial proteins and antiviral molecules (Takeuchie and Akira, 2010).

1.2.1. Immune Sensing Of Nucleic Acids

The recognition of nucleic acids (NAs) is especially important for the detection of viral infections, since viruses make us of the cellular host machinery for replication and have not many other features suitable for identification. Safeguards such as specific NA modifications or the location of the PRRs ensure that self-NAs do normally not cause an immune response. In the endosome, toll-like receptors (TLRs) detect RNA and DNA species, while RIG-I-like receptors (RLRs) and various DNA sensors detect NAs in the cytosol.

1.2.1.1. Endosomal Toll-like Receptors

The membrane bound toll-like receptors (TLRs) are the best-characterized PRR family (Gürtler and Bowie, 2013). They contain an extracellular leucine rich repeats (LRRs) domain, which is important for ligand recognition (Martin and Wesche, 2002), and an intracellular Toll/ interleukin-1 receptor homology (TIR) domain, necessary for the recruitment of adapter proteins and intracellular signaling. The TLR-family members TLR3, TLR7, TLR8 and TLR9 are located in the endosomes of immune cells, where they detect different NA species. The compartmentalization of these receptors appears to be a safeguard which better allows the distinction between ‘self’ and ‘non-self’ NAs, since endogenous NAs do normally not occur inside the endosomes (Barton et al., 2006).

TLR3 was originally identified as a receptor that recognizes polyinosine-polycytidylic acid (poly(I:C)), a synthetic analog of double stranded (ds) RNA. Later, it was shown that TLR3 also detects naturally occurring dsRNA that is derived from protozoa and fungi (Aksoy et al., 2005; Carvalho et al., 2012), present in the genome of dsRNA viruses, or generated during replication or transcription of various single stranded (ss) RNA and DNA viruses (Alexopoulou et al., 2001; Weber et al., 2006). TLR7 and TLR8 are structurally related and are both sensors for ssRNA

(Heil et al., 2004; Lund et al., 2004). In humans, TLR7 expression is restricted to plasmacytoid DCs (pDCs) and B cells (Krug et al., 2001). In contrast, it is widely expressed in murine cells. TLR8 is found in human monocytes, macrophages and myeloid DCs (mDC), where it seems to complement the absence of TLR7 (Krug et al., 2001; Hornung et al., 2002). In mice, TLR8 is found in splenic DC subsets and pDCs, yet its precise function there is not known (Jurk et al., 2002; Alexopoulou et al., 2012).

TLR9 recognizes unmethylated CpG motifs in dsDNA that occur approximately once per 16 bases in bacteria. In vertebrates these motifs are much less frequent and usually highly methylated (Bird, 1986). Stacey and colleagues showed that the methylation of CpG motifs blocked the immune stimulatory properties of bacterial DNA (Stacey et al., 1996). In addition to its endosomal localization, CpG methylation is a further reason why under normal circumstance vertebrate DNA does not trigger a TLR9-dependent immune response. In mice, TLR9 is expressed by B cells, monocytes, macrophages, pDCs and conventional DCs (cDCs), while, in humans, it is only found in pDCs and B cells (He et al., 2013).

For the activation of TLR3, TLR7, TLR8 and TLR9, acidification of the endosome is required in order to degrade pathogens and make their nucleic acids accessible. Upon recognition of their respective foreign NA ligands, TLRs dimerize to build homo- or heterodimers (Kawai and Akira, 2007). For TLR7, TLR8 and TLR9 signal transduction is initiated by the recruitment of the adapter protein myeloid differentiation factor 88 (MyD88) (Medzhitov et al., 1998; Kawai et al., 1999), while TLR3 makes use of the TIR domain-containing adapter molecule (TRIF) (Kawai et al., 2001; Hoshino et al., 2002; Yamamoto et al., 2003).

These adaptor molecules bind to the TIR domain of the TLRs (**Figure 1**), which in turn results in the phosphorylation of interferon regulatory factors (IRF) 3 and 7 (Schoenemeyer et al., 2005; Takaoka et al., 2005; Kawai et al., 2004). Once phosphorylated, IRFs translocate from the cytoplasm to the nucleus, where they act as transcription factors and cause the induction of type I IFNs and IFN-dependent genes (Fujita et al., 1989; Harada et al., 1996; Marié et al., 1998; Sato et al., 2000). TLR signaling also results in an activation of the nuclear factor kappa-light-chain-enhancer of activated B-cells (NFκB)-dependent signaling pathway, which is important for the induction of pro-inflammatory cytokines such as IL-1, IL-6 and tumor necrosis factor alpha (TNF-α). Moreover, extracellular signal-regulated kinase (ERK), the mitogen activated protein kinase (MAPK) p38 and Jun N-terminal kinase (JNK), are activated by the TLR signaling pathway (Ninomiya-Tsuji et al., 1999; Sakurai, 2012). Together, ERK, p38 and JNK activate the transcription factor activating protein-1 (AP-1), which then leads to the expression of pro-inflammatory cytokines.

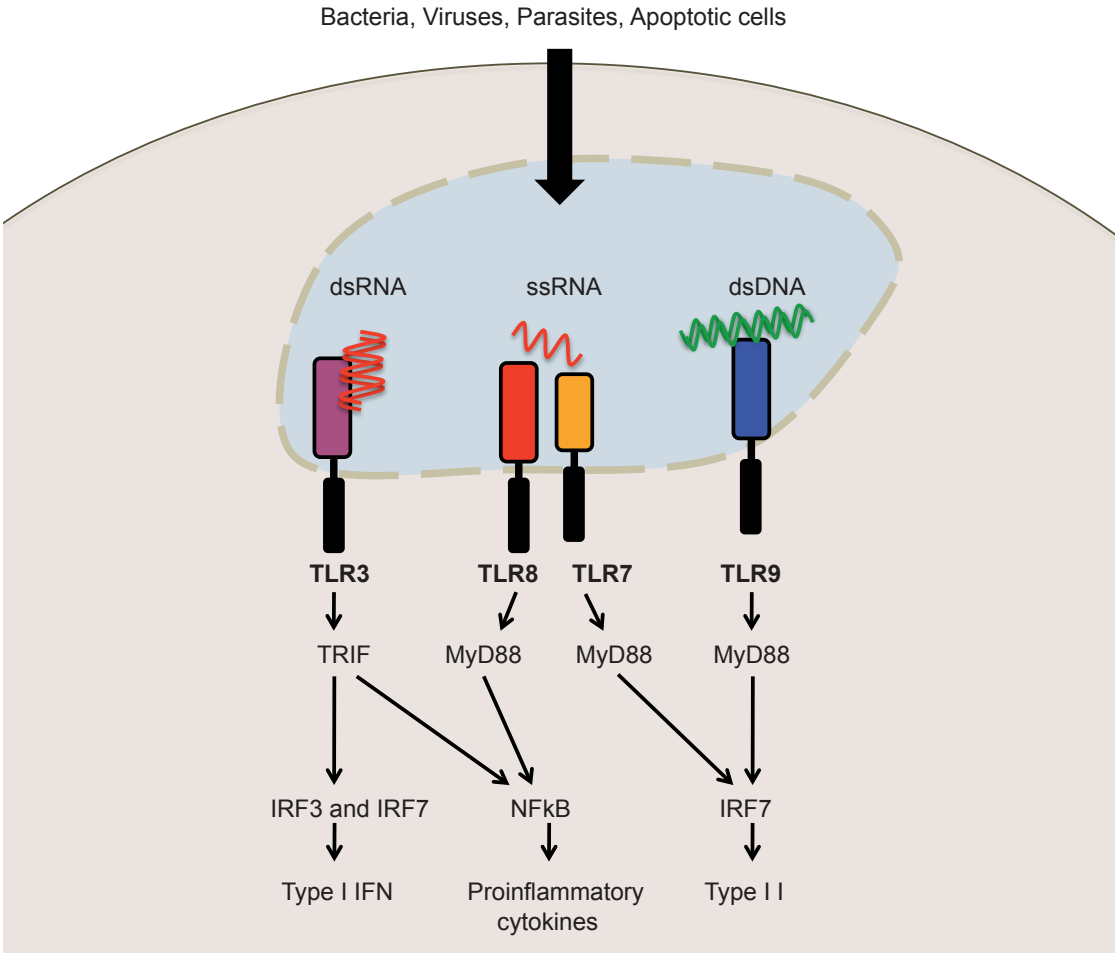

Figure 1: Endosomal Toll-like receptors (adapted from Krieg, 2010)

The endosomal Toll-like receptors TLR3, TLR7/8, and TLR9 detect dsRNA, ssRNA, or unmethylated CpG DNA, respectively. Activation leads to the recruitment of the adaptor proteins TRIF (TLR3) or MyD88, which signal via IRFs and NFkB transcription factors leading to the upregulation of type I IFNs and inflammatory cytokines.

1.2.1.2. Cytosolic RNA Sensing By RIG-I-like Receptors

Apart from endosomal sensing by TLRs, pathogenic RNA is also detected in the cytosol by RIG-I-like receptors (RLRs). RLRs are ubiquitously expressed and include Retinoic acid inducible gene-I (RIG-I), Melanoma differentiation- associated gene 5 (MDA5) and Laboratory of genetics and physiology 2 (LGP2) (Yoneyama et al., 2004; Kang et al., 2002; Andrejeva et al., 2004). Both, RIG-I and MDA5, contain a C-terminal RNA helicase domain with RNA-dependent ATPase activity and two N-terminal caspase-recruitment domains (CARDs) required for downstream signaling (**Figure 2**). LGP2 does not contain a CARD-domain and is thought to act as a primary regulator of the RIG-I/ MDA5-inititated signaling pathway (Miyoshi et al., 2001; Yoneyama et al., 2005). Signaling occurs through CARD interactions with the interferon promoter-stimulating factor 1 (IPS-1) adaptor protein (also known as mitochondrial antiviral signaling protein (MAVS), virus-induced signaling adaptor (VISA) or CARD adaptor inducing IFN-β (CARDif)), which recruits RIG-I and MDA5 to the outer membrane of the mitochondria (Kawai et al., 2005; Meylan et al., 2005; Seth et al., 2005; Xu et al., 2005). Receptor-adaptor interaction results in the

activation of IRF3 and IRF7, which then translocate to the nucleus where they induce the transcription of type I IFN genes. IFNs then upregulate the expression of IRF3, IRF7, RIG-I and MDA5 in a positive feedback loop. In addition, RLR signaling also leads to the activation of the transcription factors ATF2, c-Jun (Yoshida et al., 2008) and NFκB, which then cause the expression of pro-inflammatory cytokines.

RIG-I and MDA5 both detect viral RNA, but they have different ligand specificity. The synthetic dsRNA poly(I:C) was the first ligand described for RIG-I (Yoneyama et al., 2004). Two years later, it was shown that the 5′-triphosphate end of RNA (3pRNA) of *in vitro* transcribed RNA or generated by viral polymerases is responsible for RIG-I–mediated detection of RNA molecules (Hornung et al., 2006; Pichlmair et al., 2006). Consistent with this notion, RIG-I recognizes ssRNA viruses that exhibit prior or during their replication phase a 5´- triphosphate in their RNA genome, including hepaciviruses and members of the Paramyxoviridae, Rhabdoviridae, and Orthomyxoviridae virus genera (Kato et al., 2006). In 2009, Schlee and colleagues specified the ligand for RIG-I as a 5′-triphosphate short blunt end dsRNA structure (3pRNA) as contained in the panhandle of negative strand viral genomes (Schlee et al., 2009).

The cytoplasmic presence of 3pRNA allows discrimination between self and viral RNA, because free 5′-triphosphates are normally absent from self-RNA as a result of substantial posttranscriptional modifications (Hornung et al., 2006; Pichlmair et al., 2006). However, some dsRNAs lacking a 5´-triphosphate have also been proposed to act as RIG-I agonists (Takahasi et al., 2008; Kato et al., 2008). Additionally, it was shown that small self-RNA produced by the antiviral endoribonuclease RNase L could also activate the RIG-I signaling pathway (Malathi et al., 2007). In contrast to RIG-I antagonists, little is known about MDA5 specific ligands. MDA5 is associated with the recognition of Picornaviridae (Kato et al., 2006), murine norovirus (McCartney et al., 2008) and murine hepatitis virus (Roth-Cross et al., 2008). A subset of viruses, including dengue virus, West Nile virus and reovirus, was shown to be recognized by both MDA5 and RIG-I (Loo et al., 2008). Comparison of RIG-I and MDA5 interaction with poly(I:C) suggests that the length of dsRNA is important for differential recognition by RIG-I and MDA5. Long poly(I:C) fragments are recognized by MDA5, whereas RIG-I shows a preference for shorter RNA fragments (Kato et al., 2008).

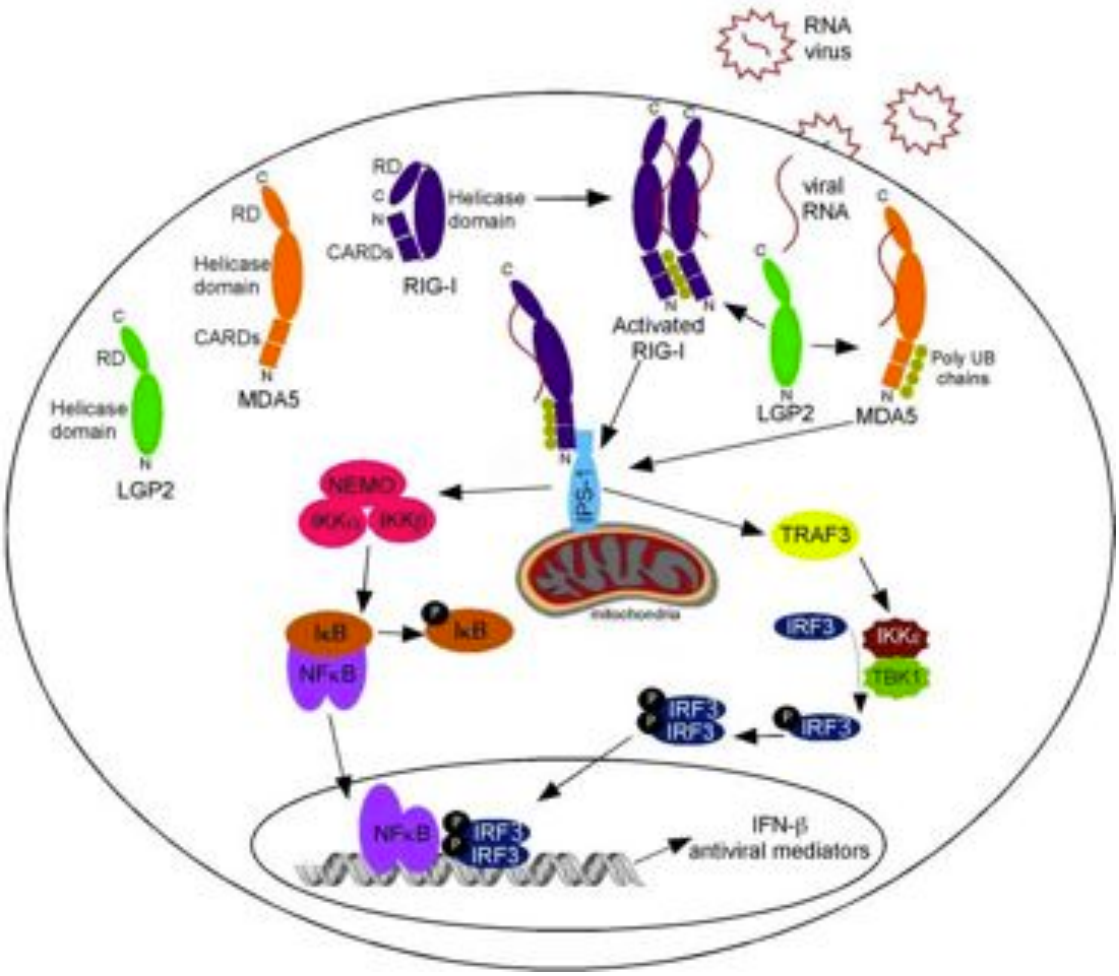

Figure 2: RLR signaling (Bruns and Hovarth, 2012)

Upon ligand binding, RIG-I and MDA5 recruit the adaptor protein IPS-1, which activates TANK-binding kinase 1 (TBK1) and inhibitor of nuclear factor kappa-B kinase (IKK). This results in the activation of NFkB and IRF transcription factors, which translocate to the nucleus and induce antiviral genes.

1.2.1.3. Cytosolic DNA Sensing

Ten years ago, it was shown that cytosolic DNA could activate the immune system in a TLR9-independent fashion (Okabe et al., 2005; Yasuda et al., 2005). Before any cytosolic DNA receptor was discovered, it became clear that the signaling cascade comprises TBK1 and IRF3 (Ishii et al., 2006; Stetson and Medzhitov, 2006). Later, the endoplasmatic reticulum (ER)-resident transmembrane protein STING (stimulator of interferon genes), also known as MITA (mediator of IRF-3 activation), was identified as crucial adaptor upstream of TBK1 (Ishikawa and Barber, 2008; Zhong et al., 2008; Sun et al., 2009; Ishikawa et al., 2009). STING functions as a scaffold protein to specify and promote the phosphorylation of IRF3 by TBK1 (Tanaka and Chen, 2012). Over the years many cytosolic DNA receptors upstream of STING have been suggested (**Figure 3**).

DNA-dependent activator of IRFs (DAI) was the first cytosolic DNA receptor candidate to be discovered (Takaoka et al, 2007; Wang et al., 2008). It was shown to trigger type I IFN expression in murine L929 fibroblasts upon dsDNA-binding and TBK1-IRF3 interaction.

Furthermore, the interaction of DAI with Receptor-interacting protein (RIP) 1 and 3 was described to activate NFκB (Kaiser et al., 2008; Rebsamen et al., 2009). However, DAI was dispensable for DNA-induced responses in many human cells and DAI-knockout mice responded normally to DNA (Lippmann et al., 2008; Ishii et al., 2008). Thus, a restricted and maybe cell-type specific role for DAI in DNA recognition was suggested.

RNA polymerase (Pol) III was the second cytosolic DNA receptor described. Prior to that, Pol III was only known to transcribe transfer RNAs and other small non-coding RNA molecules. But in 2009, it was shown that Pol III is also able to transcribe AT-rich dsDNA into 3pRNA, which is then recognized by RIG-I (Ablasser et al., 2009; Chiu et al., 2009). However, transfection of AT-poor dsDNA did not result in the production of type I IFNs, indicating a limited role of Pol III in the recognition of cytosolic DNA.

In the same year, the PYHIN protein absent in melanoma 2 (AIM2) was identified by four independent groups as a sensor of cytosolic DNA (Bürckstümmer et al., 2009; Fernandes-Alnemri et al., 2009; Hornung et al., 2009; Roberts et al., 2009). Upon DNA sensing, AIM2 recruits the adaptor protein ASC (apoptosis-associated speck-like protein containing a CARD) as well as caspase-1 in order to form the AIM2 inflammasome, which then cleaves pro-IL-1β and pro-IL-18 into their mature forms. Thus, AIM2 was shown to induce the release of IL-1ß and IL-18 in response to DNA, but does not have a role in the induction of type I IFNs.

Another PYHIN protein called IFN-inducible protein 16 (IFI16) was also suggested as DNA sensor, since it induced a STING-dependent IFN-ß response upon DNA binding (Unterholzner et al., 2010). In accordance with that, knockdown of human IFI16 or its murine ortholog in mice, p204, inhibited DNA and DNA-virus induced gene induction in a variety of cell types (Duan et al., 2011; Conrady et al., 2012; Horan et al., 2013).

In 2011, a central kinase in the DNA damage response (DDR), DNA-dependent protein kinase (DNA-PK), was described to result in the activation of NFκB and IRFs, and in the production of IFNs (Brzostek-Racine et al. 2011). Thus, a link between viruses creating DNA breaks during integration or lytic replication and the induction of an IFN response was made. DNA-PK consists of a catalytic subunit and its binding partners Ku70 and Ku80. Together, they bind to DNA breaks, promote cell cycle arrest, and thus, allow DNA damage repair. Zhang and colleagues demonstrated via knockdown that Ku70 plays a role in the DNA-induced production of IFN-λ1 in HEK293 cells (Zhang et al. 2011a). In another study, Ferguson et al. showed that the DNA-PK complex is required for the production of IFN-ß, ISGs and IL-6 in response to HSV-1 and Modified Vaccinia Ankara infection (Ferguson et al., 2012). However, Ku70 had only an effect on type III but not on type I IFNs, and additionally, the DNA-PK complex was shown to be dispensable for the IFN response to intracellular DNA in murine bone marrow (bm)-derived macrophages (Stetson and Medzhitov, 2006).

Mre11 (Meiotic recombination 11), another DNA damage factor has also been suggested as STING-dependent cytosolic DNA sensor, since murine bmDCs and mouse embryonic fibroblasts

(MEFs) had defects in dsDNA-induced type I IFN production after Mre11 knockdown (Kondo et al. 2013). However, Mre11 was dispensable for type I IFN production in response to pathogens such as HSV-1 and *Listeria monocytogenes* (Kondo et al. 2013), posing in question the physiological role of Mre11 during infection.

Members of the DExD/H box helicase protein family have also been implicated in the sensing of cytosolic DNA. In 2010, Kim and colleagues described DHX9 and DHX36 as MyD88-dependent DNA sensors in the cytosol of pDCs (Kim et al., 2010). DHX36 induced IRF7 nuclear translocation and IFN-α production in response to CpG-A oligodeoxynucleotides (ODNs), while DHX9 led to NFκB activation and TNF-α/ IL-6 production after stimulation with CpG-B ODNs. Furthermore, pDCs in which DHX9 or DHX36 were knocked down showed a significantly reduced cytokine response to the DNA virus HSV (Kim et al., 2010). However, DHX9 and DHX36 were also described to sense RNA and induce MAVS- and TRIF- dependent signaling (Zhang et al., 2011a/b). Thus, DHX9/ 36 might not be real DNA sensors, but rather act further downstream in different NA recognition pathways (Paludan and Bowie, 2013).

In 2011, Zhang et al. demonstrated that the helicase DDX41 could bind both DNA and STING. Furthermore, a reduction of DDX41 expression correlated with a reduced type I IFN response to DNA and DNA viruses in mDCs and human monocytes (Zhang et al., 2011c). DDX41 has also been shown to bind the bacterial cyclic dinucleotides (CDNs) cyclic di-AMP and cyclic di-GMP (Parvatiyar et al. 2012). CDNs act as second messengers in bacteria and stimulate a STING-dependent immune response (Barker et al. 2013; Burdette et al. 2011; Jin et al. 2011; McWhirter et al. 2009). Before DDX41 was identified, Burdette and colleagues demonstrated that STING could sense CDNs directly (Burdette et al. 2011). Later, Parvatiyar et al. proposed that DDX41 works upstream of STING. They demonstrated a specific and direct interaction of cyclic di-GMP and STING with immunoprecipitation and immunoblot analysis. Furthermore, knockdown of DDX41 expression in mouse and human cell lines as well as in different primary cells resulted in a reduced induction of IFN-β and TNF in response to CDNs or *Listeria* bacteria. Thus, they suggested that DDX41 assists STING in binding to CDNs (Parvatiyar et al. 2012).

The binding of dinucleotides to STING has recently also been suggested as major step in the sensing of cytosolic DNA. In 2013, the group of Zhijian J. Chen identified cyclic GMP-AMP (cGAMP) as an endogenous second messenger that is produced in many different cell types following DNA stimulation (Wu et al. 2013; Sun et al. 2013). It binds to and activates STING, resulting in the phosphorylation and dimerisation of IRF3. With quantitative mass spectrometry and classical protein purification strategies the human C6ORF150 and the mouse protein E330016A19 were identified as enzyme that synthesizes cGAMP, and then renamed cyclic GMP-AMP synthase (cGAS) (Sun et al. 2013). Overexpression of cGAS induced IFN-ß expression, whereas knockdown of cGAS inhibited IFN-ß induction by DNA transfection or DNA virus infection (Sun et al., 2013; Ablasser et al. 2013; Zhang et al. 2013). The binding of cGAS to DNA and the production of cGAMP in a DNA-dependent manner have further been supported by

detailed structural analysis of the enzyme in the presence and absence of DNA (Civril et al. 2013; Diner et al. 2013; Gao et al. 2013a/b). It was shown that the binding of DNA to cGAS results in conformational changes that make the catalytic pocket accessible to its substrate. Thus, cGAS could be a DNA receptor in its own right.

As already mentioned, there were a lot of cytosolic DNA receptor candidates described over the last years. Up to now, it remains unclear if “the one“ has already been found and how the different candidates are linked together. Possible explanations for the high number of candidates might be functional redundancy, as well as cell type or ligand specificity of certain receptors. It is also conceivable that different receptors act over time, meaning that some may be more important in the initial sensing of intracellular DNA, while others take over this function at a later date. In addition, it might be that some proposed cytosolic DNA sensors are not real receptors, since detailed molecular mechanisms of the signaling pathways are often missing. The only proposed cytosolic DNA receptor that provides a clear molecular mechanism for signaling and STING activation is the enzyme cGAS. Thus, further investigation in this field is absolutely necessary (Unterholzer, 2013).

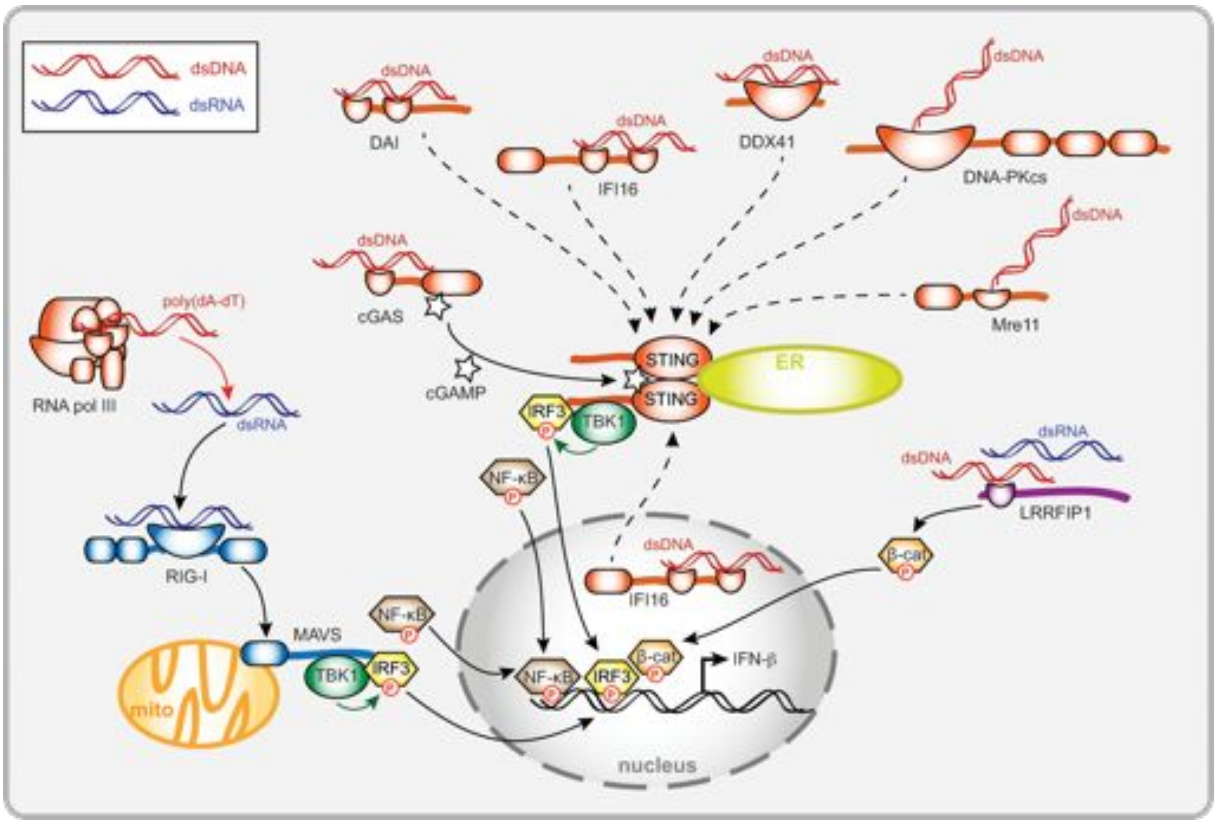

Figure 3: Possible cytosolic DNA receptors (Unterholzner, 2013)

Multiple cytosolic DNA sensors have been proposed to activate a STING-dependent signaling pathway that leads to the activation of the transcription factors IRF3 and NFκB, and the induction of type I IFN. Of these candidates, only RNA polymerase III initiates a STING-independent pathway involving the transcription of poly(dA:dT) to dsRNA, which is then sensed by RIG-I.

1.3. Type I Interferon System

PRRs can induce the production of various proinflammatory cytokines, such as interleukin-1 (IL-1), IL-6, IL-12 and TNF-α. However, the focus of this study lies on interferons (IFNs), which stimulate an "antiviral state" to block viral replication and to interfere with cellular and virus processes. 60 years ago, IFNs were described as antiviral cytokines released by virus infected cells and named after their ability to "interfere" with viral replication (Isaacs and Lindenmann, 1957).

Based on their receptor, IFNs are typically divided into three classes. Type I IFNs bind to the IFN-alpha receptor (IFNAR) that is composed of IFNAR1 and IFNAR2 chains (de Weerd et al., 2007). Human type I IFNs include IFN-alpha, -beta, -delta, -epsilon, -kappa and -omega (Roberts et al., 1998; Liu, 2005; LaFleur et al., 2001; Adolf, 1995). Interferon-gamma is the only type II IFN and binds to IFN-gamma receptor (IFNGR) consisting of IFNGR1 and IFNGR2, whereas IFN-lambda is a type III IFN and signals through a receptor complex consisting of IL10R2 and IFNLR1 (Kotenko et al., 2003; Sheppard et al., 2003).

All IFNs fight pathogens and tumor cells, however IFN-α and IFN-ß are the substantial mediators of anti-viral immunity. The IFN-β gene is only present as a single copy in humans and mice (Weissmann and Weber, 1986). Transcriptional activation of IFN-ß requires activating transcription factor 2 (ATF2)/c-Jun, NFκB, and the interferon regulatory factors (IRF) 3 and 7. These transcription factors build up together an enhanceosome of regulatory elements (Goodbourn and Maniatis, 1988; Leblanc et al., 1990; Du and Maniatis, 1992; Carey, 1998) that recruits co-activators, chromatin- remodeling proteins and the transcriptional machinery to the promoter region to initiate gene expression.

The IFN-α gene family consists of more than a dozen members. Their promoters include sequences that are known to bind members of the IRF transcription factor family (Fujita et al., 1988; Miyamoto et al., 1988). Particularly important for the transcription of IFN-α are IRF3 and 7 (Sato et al., 2001).

By interacting with IFNAR, type I IFNs initiate the Janus kinase (JAK)- signal transducer and activator of transcription (STAT) signaling pathway (Platanias, 2005). JAK1 and Tyrosine kinase 2 (TYK2) bind to the activated IFNARs and phosphorylate both STAT1 and STAT2. As a result, an IFN-stimulated gene factor 3 (ISGF3) complex forms that is made of STAT1, STAT2 and IRF9. The ISGF3-complex translocates to the nucleus where it binds to IFN-stimulated response elements (ISREs) within the promoters of IFN- stimulated genes (ISGs). The first ISGs were discovered more than 30 years ago (Larner et al., 1984; Knight and Korant, 1979), and over time, more than 300 ISGs were discovered by microarray studies. ISGs have antiviral, antiproliferative, and immunomodulatory properties (de Veer et al., 2001). Protein kinase R (PKR) is a classical ISG (Feng et al., 1992; Lee and Esteban, 1993). It phosphorylates the alpha subunit of the eukaryotic translation initiation factor eIF2 (Hovanessian, 1989), which in turn stops the initiation of protein synthesis and prevents viral replication (Hershey, 1989). Moreover,

PKR phosphorylates IkB that normally sequesters the transcription factor NFkB in the cytosol (Zamanian-Daryoush et al., 2000). Upon phosphorylation, IkB releases NFkB, which can then travel to the nucleus and becomes activated. In turn, NFkB upregulates the expression of IFNs and with the help of this positive feedback loop the antiviral signal spreads further. Another IFN-induced enzyme is ribonuclease (RNase), which destroys all RNA within the cell. It thereby reduces protein synthesis, and thus, causes apoptosis of the host cell (Dougherty et al., 1981).

Another function of IFNs is the upregulation of co-stimulatory molecules and the enhanced expression of MHC class I and MHC class II molecules. In turn, more viral peptides are presented to cytotoxic T cells, causing the enhanced killing of infected cells. Additionally, more helper T cells are activated which then coordinate the activity of other immune cells (Zhou, 2009). But IFNs cannot only indirectly affect T cell responses by acting on APCs, they can also directly promote T cell activation and keep the activated T cells alive (Conrad, 2003). Additionally, all IFNs are capable of activating NK cells, and increasing their cytotoxicity through the induction of TNF-related apoptosis-inducing ligand (TRAIL) (Sato et al., 2001).

To limit the extent and duration of type I IFN responses, regulatory molecules are also induced by IFNs as part of a negative feedback loop. The suppressor of cytokine signaling (SOCS) proteins 1 and 3 compete with STATs for binding to IFNAR and suppress JAK activity (Fenner et al, 2006), whereas USP18, a type I IFN-inducible ubiquitin specific peptidase, binds to IFNAR2 and blocks the interaction between JAK1 and IFNAR (Malakhova et al., 2006). Another mechanism that suppresses type I IFN-mediated responses is the downregulation of cell surface IFNAR. Internalization of IFNAR is induced by various pro-inflammatory cytokine signaling pathways such as IL-1, TLRs, immunoreceptor tyrosine-based activation motif (ITAM)-associated receptors and oxidative or metabolic stress (Fuchs et al., 2013; Bhattacharya, et al., 2013; Huynh et al., 2012; Huangfu et al., 2011). TLR stimulation and crosslinking of ITAM-associated receptors can also activate protein tyrosine phosphatases SHP-1, SHP-2 and PTP-1B, which dephosphorylate JAK1, STAT1 and TYK2 (You et al., 1999; Myers et al., 2001). In addition, specific miRNAs were shown to regulate the type I IFN response (Nazarov, et al., 2013; Liu et al., 2009; Gracias et al., 2013).

1.4. UV Radiation

UV radiation (UVR) can be divided into UV-A (315-400 nm), UV-B (280-315 nm) and UV-C (100-280 nm) light. Due to the absorption of short-wave UVR below 310 nm by atmospheric oxygen and the blockage of mid-range UVR by the ozone layer, only UV-A (95 %) and 5-10 % of UV-B reach the earth surface. UV-C is usually completely filtered off by the stratospheric ozone layer (van der Leun, 2004).

Even though UV radiation constitutes only 10 % of the sunlight, it has a high energetic potential and can ionize molecules and thereby induce chemical reactions (Maverakis et al., 2010). The depth of penetration into the skin correlates with the wavelength of radiation. Long-wave UV-A

can penetrate deep into the dermis and affect fibroblasts and matrix metalloproteinases, as well as DCs, T cells, mast cells and endothelial cells. UV-A is also the main cause of photoaging of the skin, with irregular pigmentation, enlarged capillary vessels, hornification and reduced elasticity of the connective tissue (Krutmann, 2003). Moreover, UV-A can induce an immediate pigment darkening that involves oxidative modification of melanin (Beitner, 1988). Both UV-A and UV-B are able to induce tanning, although UV-B is more efficient. UV-B reaches only the epidermis and affects keratinocytes, Langerhans cells and melanocytes (Kindl and Raab, 1998). However, it possesses much more energy than UV-A, and it is mainly UV-B that causes sunburn. If keratinocytes are too long exposed to UV-B, they undergo apoptosis as a protective mechanism against the carcinogenic effect of irreversibly and severely damaged DNA. Those cells are known as sunburn cells (SBCs) (Kerr et al., 1972). Chronic UVR exposure however cannot be compensated by SBCs. It is a strong environmental mutagen and can result in fatal cancer (Brash et al., 1991). However, for the photo-isomerisation of 7-dehydrocholesteral and ergosterol to previtamin D2 and D3, UV-B is indispensable (Norman, 1998; Okamura et al., 1993).

UV-C provides the highest energy and has a very strong mutagenic potential. Due to strong attenuation by the atmosphere, no significant UV-C radiation on earth results from natural sources. However, studies with UV-C lamps have shown that UV-C can irritate the skin and induce sunburn (Maverakis et al., 2010).

1.4.1. UV- induced DNA Damage

The skin is the organ that is mainly affected by solar UV radiation. One of the most important chromophores is the epidermal DNA with its aromatic bases that absorb the radiation energy. Since DNA has an absorption maximum at 260 nm, UV-C lamps are widely used to study UV radiation induced DNA damage (Batista et al., 2009).

DNA damage is induced by the absorption of UV photons that generate lesions usually referred to as photoproducts. The most common photoproducts are cyclobutane pyrimidine dimers (CPDs) and (6-4) pyrimidine-pyrimidone photoproducts (PP) (Ravanat et al., 2001) (**Figure 4**). CPDs are formed from the photo (2 + 2) cycloaddition of the 5,6-double bond of two adjacent pyrimidine nucleotides (Torizawa et al., 2004). Thus, there are thymidine-thymidine (T-T), thymidine-cytosine (T-C), cytosine-thymine (C-T) and cytosine-cytosine (C-C) CPDs, with T-T dimers occurring most frequently (Setlow and Carrier, 1966). (6-4)-PPs arise from the linkage of the C6 position of the 5´- pyrimidine to the C4 position of the 3´- pyrimidine in an adjacent pair (Rosenstein and Mitchell, 1987). They can be further transformed to Dewar valence isomers by photoisomerization (Taylor et al., 1988). Several studies showed that CPDs are at least three times more often formed than (6-4)-PPS after UV-C irradiation, (Mitchell, 1988; Kao et al., 1993), but the formation ratio varies and is related to the specific DNA sequence and UV wavelength. After UV-A or UV-C radiation CPDs are especially formed at T-T sequences (Sage, 1993),

whereas T-C sequences are more susceptible to (6-4)-PPs and occur after UV-C radiation (Lippke et al., 1981). Both, CPDs and (6-4)-PPs cause a conformational change of the DNA double helix that results in the blockage of replication and transcription processes. The replication arrest leads to the production of DNA double-strand breaks (DSBs) at the sites of collapsed replication forks (Limoli et al., 2002; Batista et al., 2009). Furthermore, replication stresses and free radicals may also cause DSBs by preventing the topoisomerase-mediated DNA religation (Strumberg et al., 2000; Box et al., 2001; Ohnishi et al., 2009; Banáth and Olive, 2003).

DNA cannot only be damaged directly by UV irradiation, but also indirectly through the generation of ROS. Upon UV exposure, the radiation energy is absorbed by photosensitizers like porphyrins, bilirubin, melanin, flavins, pterins, vitamins, NAD(P)H, trans-urocanic acid and tryptophan (Wondrak et al., 2005), which are promoted to an excited singlet state and undergo intersystem crossing with oxygen to initially produce superoxide (O_2^-). Superoxide is biologically toxic and known to denature enzymes, lipids and also DNA. Thus, an enzyme called superoxide dismutase (SOD) rapidly converts superoxide into hydrogen peroxide (H_2O_2), which is then further processed by an enzyme named catalse that catalyzes the decomposition of H_2O_2 to water and oxygen. Hydrogen peroxide does not directly cause DNA damages but it can be transformed into hydroxyl radicals ($HO^{\cdot}$), which are highly reactive (Halliwell and Aruoma, 1991). Next to superoxide and hydrogen peroxide, ROS include also hypochlorous acid (HOCl), ozone (O_3) and singlet oxygen ($1O_2$), which can be easily converted into radicals or have an oxidative effect themselves.

The DNA damages by ROS comprise single and double strand breaks, DNA base modifications or DNA-protein crosslinking, depending on whether DNA bases or deoxyribose are attacked (Ward, et al., 1987; Hönigsmann and Dubertret, 1996). Particularly critical are base modifications, since they result in mutations if not repaired immediately. Among the oxidatively modified bases, 8-hydroxy-2'-desoxy-guanosine (8-OHG), respectively 8-oxo-2'-desoxy-guanosine (8-oxoG), are the most abundant and best investigated (**Figure 5**) (Kasai et al., 1984; Floyd et al., 1988; Kasai, 1997). 8-OH-G is formed by many agents with different mechanisms of action (Kohda et al., 1980; Kohda et al., 1990; Kasai et al., 1992; Epe et al., 1996). It base pairs preferentially with adenine rather than cytosine and thus generates GC-TA transversion mutations after replication (Grollman and Moriya, 1993; Kasai, 1997; Wood et al., 1990).

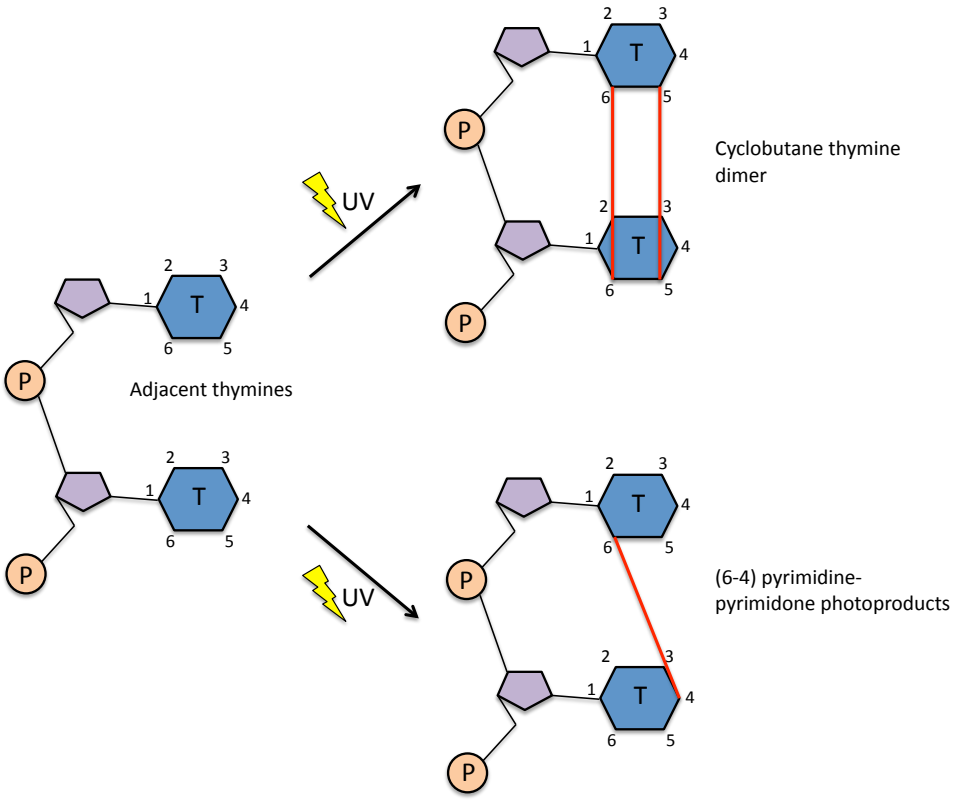

Figure 4: Cyclobutane Thymine Dimers and (6-4)-Pyrimidine-Pyrimidone Photoproducts

Upon UV irradiation two main classes of DNA photoproducts are formed: Cyclobutane pyrimidine dimers (CPDs) and (6-4) pyrimidine-pyrimidone photoproducts ((6-4)-PPs). CPDs contain a four membered ring arising from the photo (2 + 2) cycloaddition of the 5,6-double bond of two adjacent pyrimidines. (6-4)-PPs are formed by the linkage of the C6 position of a 5´- pyrimidine, to the C4 position of a 3´- pyrimidine.

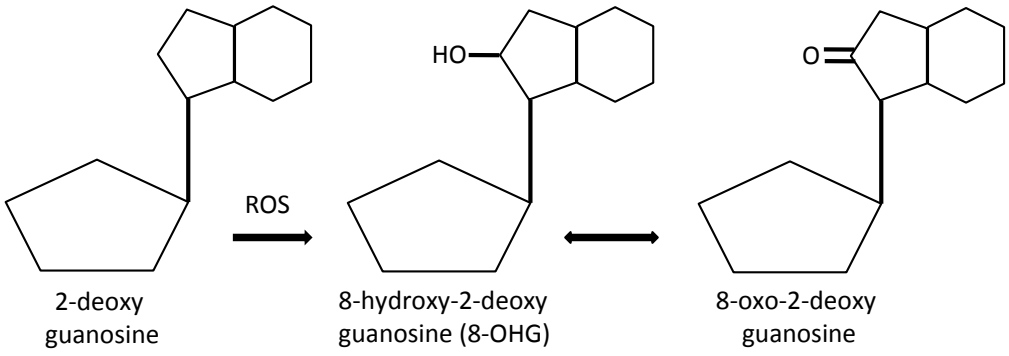

Figure 5: Oxidation of guanosine (adapted from 8-OHG EIA ELISA kit manual)

8-hydroxy-2-deoxy guanosine (8-OHG) or 8-oxo-2-deoxy guanosine are produced by the oxidative damage of DNA by reactive oxygen species (ROS) and serve as an established marker of oxidative stress.

1.4.2. Repair Of UV-induced DNA Damages

To prevent malignant transformation, cells have evolved a variety of mechanisms to detect and repair DNA damages. The tumor suppressor gene p53 controls the integrity of the DNA during the cell cycle and becomes activated in response to various stressors, one being UV irradiation (Maltzman and Czyzyk, 1984). P53 can activate DNA repair proteins and arrest growth at the G1/ S regulation point, so that the repair proteins have enough time to fix the DNA damage (Kuerbitz et al., 1992). One mechanism to repair UV damage is called photoreactivation or "light repair“. Photolyase enzymes specifically bind to CPDs or (6–4)-PPs and reverse the damage by using the energy of light. Antenna molecules like methenyltetrahydrofolate or 8-hydroxy-7,8-didemethyl-5-deazariboflavin transfer the absorbed energy to a deprotonated reduced flavin adenine dinucleotide which then donates an electron to the pyrimidine dimer, resulting in the splitting of the dimer into two monomeric units (Cook, 1970; Sutherland, 1974; Kim et al., 1992). Photoproducts are also repaired through processes that do not relate on light and are much more complex. Nucleotide excision repair (NER) and base excision repair (BER) pathways handle DNA single strand breaks (Hedge et al., 2008), which can then be filled by different polymerases and ligases. Double-strand breaks are either repaired through nonhomologous end joining (NHEJ), which does not require a homologous template and can rejoin broken DNA ends directly end-to-end, or through homologous recombination repair (HRR), which is dependent on homology to guide repair (Moore and Haber, 1996, Pastwa and Błasiak, 2003). If DNA damage cannot be repaired, the cellular DNA damage response (DDR) activates apoptotic pathways.

1.4.3. UV-induced Apoptosis

Overexposure to UV irradiation often results in keratinocytes undergoing apoptosis as a protective mechanism against the carcinogenic effects of UV light (Daniels et al., 1961). Apoptosis is also known as programmed cell death and characterized by a sequence of ordered events leading to the elimination of cells without releasing harmful substances into the surrounding area (Kerr et al., 1972). This is contrary to necrosis, which is an unordered and accidental form of cell death caused by external factors and characterized by cellular swelling and rupture, often leading to inflammation (Wyllie et al., 1980). Mechanisms of UV-induced apoptosis include (i) UV-induced DNA damages followed by p53 activation and leakage of the pro-apoptotic factor cytochrome c from mitochondria; (ii) UV-induced death receptor (DR) activation, resulting in caspase cascades and the translocation of pro-apoptotic proteins of the Bcl-2 family like Bax (bcl-2- associated x protein) to mitochondria, which causes the release of cytochrome c; (ii) UV-induced overproduction of ROS, which then damage proteins and DNA, and additionally increase the release of cytochrome c from impaired mitochondria (Lee et al., 2013). A failure in the clearance of apoptotic cells can result in the exposure of self-antigens, including self-DNA, which under certain circumstances might become immunogenic.

1.5. Deoxyribonucleases

Deoxyribonucleases (DNases) are enzymes that induce the degradation of DNA by catalyzing the hydrolytic cleavage of phosphodiester linkages in the DNA backbone. DNases are essential to maintain genome stability and to regulate immune responses by limiting the availability of NA-receptor ligands. They can be divided into endonucleases that cleave residues within the DNA strand and exonucleases that only cut at the DNA ends.

The three main types found in metazoans are DNase I, DNase II and DNase III (also known as three prime repair exonuclease 1, short TREX1). DNase I is an endonucleases that yields 5´-phosphate-terminated polynucleotides with a free hydroxyl group at the 3´end. Its function is waste management and the fragmentation of DNA during apoptosis (Samejima and Earnshaw, 2005).

DNase II is also an endonuclease and performs best at an acidic pH (Catchside and Holmes, 1947). Lysosomal localization and ubiquitous tissue distribution alluded to a role in the degradation of exogenous DNA encountered by phagocytosis (Odaka and Mizuochi, 1999). In 1998, Krieser and Eastman reported that overexpression of DNase II was sufficient to induce cell death in Chinese hamster ovary cells (Krieser and Eastman, 1998). However, loss-of-function analyses in *C. elegans*, *Drosophila* and mice have failed to demonstrate any requirement for DNase II in the induction or procession of apoptosis (Evans and Aguilera, 2003).

DNase III/ TREX1 is the most prominent DNA 3'–5' exonuclease in mammalian cells and especially found in the cytosol. Even though this enzyme was first purified in 1969 (Lindahl et al. 1969), its gene was not identified before 1999 (Höss et al., 1999; Mazur and Perrino, 1999). TREX1 has a preference for ssDNA or mispaired 3' termini and generates 5' mono- or dinucleotides (Höss et al., 1999; Mazur and Perrin, 1999; Bebenek et al., 2001). Based on homology with known editing enzymes and its exonuclease function, TREX1 was suggested to have a role in DNA replication or gap filling during DNA repair (Brucet et al., 2007). However, TREX1 knockout mice did not confirm a role of TREX1 in DNA editing, since they did not show higher numbers of spontaneous mutations. Instead, they displayed an autoimmune-like inflammatory myocarditis and a dramatically reduced lifespan (Morita et al., 2004).

1.6. Lupus Erythematosus

Impaired clearance of apoptotic cells is strongly correlated with the progression of the autoimmune disease systemic lupus erythematosus (SLE) (Franz et al., 2006). It is thought that an inadequate clearance of apoptotic cells leads to a prolonged disposition of chromatin-protein complexes in the extracellular space, which results in the generation of autoantibodies that are especially directed against nuclear antigens (antinuclear antibodies = ANA) (Lahita, 1992; Tan, 1989). Since the immune system looses the ability to distinguish self from non-self, it starts to attack the body’s own cells and tissues, resulting in inflammation and tissue damage. The name lupus erythematosus (latin for wolf and redness) comes from two characteristic symptoms: a

distinct rush as well as skin lesions in the face of lupus patients. Due to this typical butterfly rash that is provoked by UV exposition, lupus was initially thought to be a skin disease (Biett, 1824). Only 48 years later, lupus was found to have also a systemic character (Kaposi, 1872).

The two major forms of lupus are cutaneous LE (CLE) and systemic LE (SLE). If only the skin is affected, the disease is classified as CLE. Generally, CLE is histologically characterized by a lympho–histocytic interface dermatitis due to lymphocytes that enter the endothelium and cause apoptosis of basal keratinocytes (Clark et al., 1973; Sepehr et al., 2010). Based on clinical morphology, average duration of skin lesions and histopathologic examination, CLE can be further subdivided into chronic, subacute and acute CLE (Fabbri et al., 2003).

The most common form of lupus is SLE, which can affect many organ systems, including skin, kidney, joints, central nervous system, blood vessels, heart and lungs. SLE can cause different clinical symptoms that might vary from mild to severe forms. Common complaints include fever, joint paints, muscle aches, fatigue, skin alterations as well as kidney, lung or heart problems (Tan et al., 1982). Changes in the skin are not limited to CLE patients, but are also found in SLE patients, especially after exposure to UV light. This photosensitivity is a symptom found in up to 83 % of LE patients (Sanders et al., 2003) and can result in cutaneous lesions with variable severity, but also in inflammation of different inner organs.

Characteristical laboratory abnormalities in SLE include the increase of the blood sedementation rate, elevated antibody numbers, anemia, thrombocytopenia and the appearance of autoantibodies (Parodi and Rebora, 1997; Tan, 1989; Tan et al., 1982). Almost all SLE patients are positive for ANAs that bind to contents of the cell nucleus. The subtypes of ANAs are found to different extent in Lupus patients (**Table 1**) and can together with autoantigens form immunocomplexes that accumulate at the dermoepidermal junction and finally activate the complement system. This so-called Lupus band contains all major immunoglobulin classes (IgG, IgM, and IgA) and various complement components (Burnham et al., 1963; Crowson et al., 2009).

Percentage	Autoantibody
40-90 %	anti-dsDNA antibodies
10-30 %	anti-Sm antibodies
40-60 %	anti-SSA/Ro and anti-SSB/La antibodies
20%	anti-Histon antibodies
30-40 %	anti-Cardiolipin antibodies
30-40 %	anti-rRNP and anti-snRNP antibodies

Table 1: Characteristic autoantibodies in SLE (according to Tan et al., 1982)

Because SLE is characterized by large amounts of autoantibodies, the loss of B cell tolerance is believed to be important for the initial phase of the disease. B cells can additionally function as autoantigen-presenting cells for T cells, and worsen the disease by the release of cytokines and chemokines (Lund, 2008), which then amplify autoimmunity through innate and adaptive immune system dysregulation (Marian and Anolik, 2012). Not only B cells, but also plasmacytoid

dendritic cells (pDCs) can be activated by co-stimulation of TLRs and Fc receptors via immune complex binding. Upon activation, they secrete large amounts of IFN-α, which then leads to the activation and maturation of DC subsets and stimulation of both T and B cells (Rönnblom et al, 2001). Indeed, high IFN levels (Kariuki et al., 2010) as well as mutations of genes involved in TLR and IFN signaling pathways (e.g. IRAK1, IRF5, and STAT4) were identified as SLE risk variants (Kariuki et al., 2010; Remmers et al., 2007; Harley et al., 2008; Jacob et al., 2009). However, there remains a need for further research in the etiology of LE. It is supposable that, next to age and gender, other genetic factors play a predisposing role in the onset and progression of the disease. Likely candidates are certain HLA haplotypes (HLA-B8, -DR2, -DR3 und -DQ2), but also mutations in the gene loci of TREX1 (Green et al., 1986; Rahman and Isenberg, 2008; Wakeland et al., 2001)

1.7. Lupus And Neutrophil Extracellular Traps

Neutrophils account for the largest group of white blood cells and provide the first line of defense of the innate immune system (Nathan, 2006). They have long been shown to be associated with SLE. However, their role in the pathogenesis of SLE was not clear until the discovery of neutrophil extracellular traps (NETs). NETs are web-like chromatin structures that are decorated with histones, myeloperoxidase, neutrophil elastase, cathepsin G, lactoferrin, LL-37 and HMGB1 (Brinkmann et al., 2004; Mantovani et al., 2011). They are released to immobilize and eventually kill invading microbes.

Sera of lupus patients often contain anti-neutrophil cytoplasmic antibodies (*ANCAs*) (Fauzi et al., 2004), which are directed against major components of NETs. Thus, an imbalance between NET formation and clearance was suggested to play a role in SLE. Indeed, two independent studies demonstrated that up to 65% of SLE patients have a decreased ability to degrade NETs (Hakkim et al., 2010; Leffer et al., 2012), and the persistence of NETs may lead to the production of autoantibodies against NETs and worsen the disease.

Different NET release mechanisms have been described over the last years. The major route of NET formation seems to occur as the result of NETosis, a specific type of cell death (**Figure 6 ii**) (Brinkmann et al., 2004; Steinberg et al. 2007). During NETosis, the chromatin decondenses into the cytoplasm while the plasma membrane remains intact. This allows the antimicrobial granular cargo to mix with the DNA. Afterwards, the plasma membrane bursts and the NETs are released. However, two other forms of NET generation were described to leave the cells viable so that they retain their ability to phagocyte pathogens (Yousefi et al., 2009; Yipp et al., 2012). Yousefi and colleagues explained the viability of the cells with the type of DNA released. They described that only mitochondrial DNA was extruded, while the nucleus remained intact (**Figure 6 iii**) (Yousefi et al., 2009). However, others showed that nuclear DNA was released by viable neutrophils through a vesicular mechanism (**Figure 6 i**) (Yipp et al., 2012). Experimentally, NETosis is usually induced by the addition of microorganisms or the protein kinase C (PKC)

activator Phorbol-12-myristate-13-acetate (PMA) (Brinkmann et al., 2004; Urban et al., 2006), but LPS, IL5/IFNγ + LPS/C5a/eotaxin, GM-CSF + LPS/ C5a, IL-8, glucose oxidase, H_2O_2, or TNF were also described to cause the release of NETs (Remijsen et al., 2011b).

To date, ROS such as superoxide generated by the NADPH oxidase Nox2 are thought to be the driving force for the formation of death mediated NETs. Especially, since patients with chronic granulomatosis, which have a nonfunctional NADPH oxidase, are not able to make NETs (Fuchs et al., 2007). Additionally, myeloperoxidase (MPO) seems to be required for the expulsion of NETs, but also this mechanism is not fully understood. Metzler et al. showed that neutrophils completely deficient in MPO fail to form NETs, while neutrophils from partially MPO-deficient donors maintained their ability to make NETs. Extracellular products of MPO did not rescue NET formation, suggesting that not downstream products of MPO, but the enzyme itself is responsible for NET expulsion (Metzler et al., 2011). Possibly, neutrophil elastase and MPO are required to partly degrade histones to allow decondensation of the chromatin (Papayannopoulos et al., 2010).

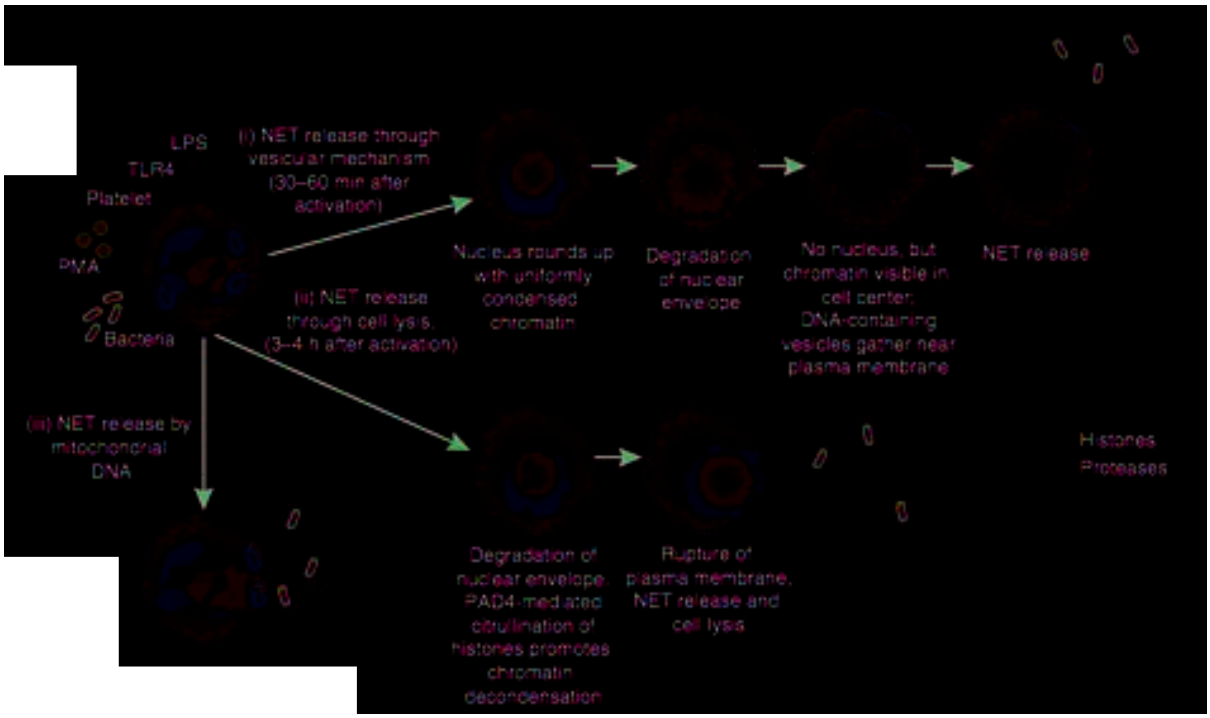

Figure 6: The formation of NETs (Phillipson and Kubes, 2011)

Different mechanisms of NET expulsion have been described. NETs can be released through DNA-containing vesicles that leave the cells viable (i), but they can also be withdrawn through a cell-death mediated mechanism (ii). Additionally, NET release by mitochondria has also been observed (iii).

1.8. The MRL/lpr Mouse Model

MRL/lpr mice develop a systemic autoimmune disease similar to SLE in humans. These mice are derived from inbreeding of strain MRL/Mp, which originates from crosses among the standard inbred strains LG/J, AKR/J, C3H/Di and C57BL/6 (The Jackson Laboratory). It is expected that 75 % of the genome is derived from strain LG/J (Harlan laboratory), which develops antinuclear antibodies and rheumatoid factor as well as renal disease (Peng et al,

1996). Thus, it is not remarkable that MRL/lpr mice also suffer from fatal renal disease characterized by glomerulonephritis, interstitial nephritis, vasculitis, and proteinuria (Kelley and Roths, 1985). With increasing age, high concentrations of several autoantibodies such as ANA and anti-dsDNA antibodies are found in MRL/lpr mice, resulting in large amounts of circulating immune complexes (Andrews et al, 1978; Hewicker et al, 1990). Since serum autoantibodies are not present at birth, a breakdown in tolerance must happen during lifetime, which might be explained by MRL/lpr being homozygous for the lymphoproliferation spontaneous mutation (Fas^{lpr}). The Fas^{lpr} mutation is a deletion in the structural gene for the Fas antigen (Watanabe-Fukunaga et al, 1992; Watson et al, 1992), a transmembrane receptor that upon ligand binding leads to apoptotic cell death mediated by caspases 3/8 activation (Waring and Müllbacher, 1999). The Fas-mediated apoptosis pathway plays an important role in the homeostasis of lymphocytes. Under normal conditions, T and B cells start to express the Fas ligand after activation and become progressively more sensitive to Fas-mediated apoptosis the longer they are activated (Hahne et al, 1996). The activation-induced cell death (ACID) is required to prevent an excessive immune response and eliminate autoreactive T and B cells. In MRL/lpr mice, the absence of the Fas antigen results in failure of lymphocytes to undergo programmed cell death (Watson et al, 1992). This accumulation of aberrant T and B cells comes along with a massive enlargement of lymph nodes and spleen. Other conspicuous symptoms are the development of skin rash and ear necrosis with increasing age. As observed in humans, female MRL/lpr mice develop more often clinical symptoms and die at an average age of 17 weeks of age, while males are less affected and die at an average age of 22 weeks. This compares to approximately 50 weeks in females on the C57BL/6J background (Roths, 1987). Cytokines seem to play an important role in the disease pathogenesis. Like in SLE patients, disease severity in MRL/*lpr* mice is linked to the Th1 cytokines IFN-gamma and IL-12, which stimulate different immune cells in the destruction of invading organisms and infected cells (Takahashi et al, 1996; Peng et al, 1997; Schwarting et al, 1999; Balomenos et al, 1998). Furthermore, IL-18 serum levels are increased in both SLE patients and MRL/*lpr* mice, stimulating IFN-gamma production, Fas-mediated cytotoxicity, and developmental regulation of Th1 (Nakanishi et al, 2001). TNF-alpha, another proinflammatory cytokine, was also found to be elevated in MRL/*lpr* mice (Yokoyama et al, 1995). Due to many analogies with human SLE patients, the MRL/lpr mouse is the most commonly studied mouse model of lupus.

1.9. Aim

The aim of this work was to uncover the molecular mechanism responsible for a phenomenon that had been observed in the Barchet laboratory. Previous experiments showed that direct and indirect UV irradiation greatly enhanced the immunostimulatory properties of DNA. *In vitro*, increased type I IFN and pro-inflammatory cytokine responses upon “UV-DNA” stimulation were observed in human monocytes, but also in murine myeloid DCs, macrophages and keratinocytes. Oxidative DNA modifications were identified as cause for the increased immunogenicity of UV irradiated DNA and it was shown that this DNA is recognized in the cytosol via STING. However, the mechanism behind the described phenomenon was not discovered.

<u>The aim of this thesis was to answer the following questions:</u>

- What is the molecular mechanism behind the observed phenomenon?
- Which DNA uptake facilitators (soluble factors or receptors) are responsible for the transport into the cytosol?
- What is the role of oxidatively damaged DNA in systemic lupus erythematosus (SLE) and the cutaneous form of lupus?
- Which cell types respond to oxidatively damaged DNA *in vivo*?

2. Material And Methods

2.1. Materials

2.1.1. Equipment

Equipment	Manufacturer
Analytical balance U4100-OD2.2	Sartorius (Göttingen)
Autoclave VX-150	Systec (Wettenberg)
Bacterial incubator	VWR International (Darmstadt)
Beakers	Schott (Mainz)
Cell culture incubator MCO-20AIC	Sanyo (San Diego, USA)
Centrifuges 5415 D, 5415 R, 5430 R, 5810 R	Eppendorf (Hamburg)
Centrifuge Galaxy mini	VWR (Darmstadt)
Electroporator Gene Pulser II	Bio Rad (Munich)
Electrophoresis Power Supply EV231	Peqlab (Erlangen)
ELISA reader Apollo LB912	Berthold (Bergisch-Gladbach)
ELISA Vacupette	VWR (Darmstadt)
Erlenmeyer flasks	Schott (Mainz)
Flex cycler	Analytic Jena (Jena)
Flow cytometer LSR II	BD Biosciences (Heidelberg)
Fluorescence Microscope Axiovert Observer	Carl-Zeiss (Göttingen)
Freezer (- 20°C), different models	AEG-Electrolux(Nürnberg),Siemens(Munich)
Freezer (-80°C) HFU 586 basic	Thermo Electron (Oberhausen)
Freezer (-150°C) ultra low freezer	Sanyo (San Diego, USA))
Freezing container	VWR (Darmstadt)
Fridge	AEG-Electrolux (Nürnberg)
Gel documentation system	Peqlab (Erlangen)
Gel chamber with gel tray and comb	Peqlab (Erlangen)
Ice machine AF20	Scotsman (Pogliano (I))
Lab dancer	VWR (Darmstadt)
Magnetic stirrer	VWR (Darmstadt)
Microbiological Safety Cabinet Type 1.8	Thermo Fisher Scientific (Schwerte)
Microscope Type Wilovert 30	Wilhelm Hund GmbH (Wetzlar)
Microwave NN-E205W	Panasonic (Hamburg)
Multichannel pipettes Ergonomic High-Performance (1-10 µl, 5-50 µl, 20-200 µl)	VWR (Darmstadt)
Neubauer counting chamber	Brand (Wertheim)
Nitrogen tank	Taylor Wharton (Mildstedt)
PCR Thermocycler "Flex-Cycler"	Analytik Jena (Jena)
pH-Meter HI8424	HANNA Instruments (Kehl am Rhein)
Pipetboy acu	Integra Biosciences (Fernwald)
Pipettes	Eppendorf (Hamburg)
Prepare cutlery	Labotec Labor-Technik (Göttingen)
Shaker KS 260 basic	IKA (Staufen)
Spectral photometer Nanodrop 1000	Peqlab (Erlangen)
Sterile Workbench	Thermo Fisher Scientific (Waltham MA, USA)
Suction pump Midisart 2000	Sartorius (Göttingen)
Thermomixer comfort	Eppendorf (Hamburg)
Threaded bottles	Schott (Mainz)
Ultrapure water purification system	Purelab classic ELGA (Celle)
UV-C irradiation device	Saalmann (Herford)
Vertical Gel electrophoresis system	Bio-Rad (München)
Volumetric flasks	Schott (Mainz)
Vortex Genius 2	Scientific Industries (New York, USA)
Wallac Envision 2104 Multilabel Reader	Perkin-Elmer (Waltham MA, USA)
Water bath Isotemp 210	Thermo Fisher Scientific (Schwerte)

2.1.2. Expendable Materials

Material	Manufacturer
Cell culture flasks	Sarstedt (Nürnbrecht)
Cell culture plates, flat- and round-bottom	TPP (Trasadingen (CH))
Cell culture plates	Sarstedt (Nürnbrecht)
Cell strainer (40 µm)	BD Biosciences (Heidelberg)
Cover slips (18 x 18 mm)	Marienfeld (Lauda-Königshofen)
Cryo tubes	Greiner Bio-One (Solingen)
Disposable cannulas Sterican (0,4 x 20 mm, 0,45 x 20 mm)	Braun (Melsungen)
Disposable gloves Dermaclean	Ansell Healthcare (Brussels (B))
ELISA plates	Greiner Bio-One (Solingen)
FACS tubes	Sarstedt (Nürnbrecht)
Falcon tubes	Greiner Bio-One (Solingen)
Microtainer tubes	BD Biosciences (Heidelberg)
Pipette tips	Greiner Bio-One (Solingen)
Pipette tips with aerosol filter	Biozym (Hess. Oldendorf)
Petri dishes	Greiner Bio-One (Solingen)
Plastic pipettes	Corning Costar (Bodenheim)
Reaction tubes (0,2 ml)	BIOplastics (Landgraaf (NL))
Reaction tubes (0,5 ml, 1,5 ml, 2 ml)	Eppendorf (Hamburg)
Sterile filter 500 ml Filter system	Corning Costar (Bodenheim)
Sterile filter (0,2 µm)	Whatman (Dassel)
Syringes Discardit II (2 ml, 5 ml, 10 ml)	BD Biosciences (Heidelberg)
Syringe filter (0,45 µm)	Thermo Fisher Scientific (Bonn)
Syringe Omnifix® F (1 ml)	Braun (Melsungen)

2.1.3. Chemicals

Chemical	Manufacturer
Acetic acid	Carl Roth (Karlsruhe)
Acetyl CoenzymeA	Genaxxon BioScience (Ulm)
Adenosine triphosphate (ATP)	Sigma-Aldrich (Steinheim)
Agarose	Applichem (Darmstadt)
Ampicillin	Carl-Roth (Karlsruhe)
Ampuwa	Fresenius (Bad Homburg)
Bacto Tryptone	BD Biosciences (Heidelberg)
Bacto Yeast Extract	BD Biosciences (Heidelberg)
BD OptEIA Substrate Reagent A and B	BD Biosciences (Heidelberg)
BD Pharmlyse	BD Biosciences (Heidelberg)
Blasticidine S Hydrochloride, 25mg	Carl Roth (Karlsruhe)
Bovines Serum Albumin (BSA)	Sigma-Aldrich (Steinheim)
Calcium chloride	Carl Roth (Karlsruhe)
Chloroform	Carl Roth (Karlsruhe)
Deoxynucleoside triphosphates (dNTPs)	Invitrogen (Karlsruhe)
Di-methylsulphoxide (DMSO)	Carl Roth (Karlsruhe)
Di-Sodiumhydrogen phosphate	Carl Roth (Karlsruhe)
Dithiothreitol (DTT)	Carl Roth (Karlsruhe)
DNA-Hybridisation buffer 10 x	New England Biolabs (Ipswich, GB)
DNA Loading Dye 6 x	Fermentas (St. Leon-Rot)
DreamTaq™ Green Buffer 10 x	Fermentas (St. Leon-Rot)
Dulbecco's Modified Eagle Medium (DMEM)	Gibco (Karlsruhe)
Dulbecco's PBS	PAA Laboratories (Pasching)
Dynabeads MyOne T1 Streptavidin, 2ml	Invitrogen (Karlsruhe)
ECL Western Blotting Substrate	Pierce Thermo Scientific (Rockford, USA)
Ethanol	Carl Roth (Karlsruhe)
Ethylendiamintetra acetic acid (EDTA)	PAA Laboratories (Pasching)
FastDigest® Buffer 10 x	Fermentas (St. Leon-Rot)
Fetal calf serum (FCS)	Gibco (Karlsruhe)

Ficoll	Biochrom (Berlin)
Geneticinedisulfate (G418)	Sigma-Aldrich (Steinheim)
Glucose	Sigma-Aldrich (Steinheim)
GM-CSF (murine)	Cell supernatant of J55811
HEPES	Carl Roth (Karlsruhe)
Hydrogen peroxide, 30 %	Carl Roth (Karlsruhe)
Isoflurane	Abbott (Wiesbaden)
Isopropanol (C_3H_8O)	Carl Roth (Karlsruhe)
Magnesium carbonate hydroxide	Carl Roth (Karlsruhe)
Magnesium chloride	Sigma-Aldrich (Steinheim)
Magnesium sulfate	Carl Roth (Karlsruhe)
MEM nonessential amino acids	Gibco (Karlsruhe)
MEM Sodium-Pyruvate 100 x	Gibco (Karlsruhe)
2-Mercaptoethanol	Carl Roth (Karlsruhe)
Optimem	Gibco (Karlsruhe)
Passive lysis buffer 5x	Promega (Madison, USA)
Penicillin/Streptomycin 100 x	Cambrex BioWhittaker (New Jersey, USA)
Phenol	Carl Roth (Karlsruhe)
Polybrene	Sigma-Aldrich (Steinheim)
Puromycine dihydrochloride	Sigma-Aldrich (Steinheim)
Potassium chloride	Carl Roth (Karlsruhe)
RPMI 1640	Gibco (Karlsruhe)
Sodium carbonate	Carl Roth (Karlsruhe)
Sodium chloride	Carl Roth (Karlsruhe)
Sodium dihydrogen phoshate-Monohydrate	Carl Roth (Karlsruhe)
Sodiumdodecyl sulfate (SDS)	Carl Roth (Karlsruhe)
Sodiumhydrogen carbonate	Carl Roth (Karlsruhe)
Sodium hydroxide	Carl Roth (Karlsruhe)
Sodium phosphate	Carl Roth (Karlsruhe)
SYBR® Safe DNA gel stain 40000 x	Invitrogen (Karlsruhe)
Tris-Acetate-EDTA (TAE) 50 x	Carl Roth (Karlsruhe)
Taq Buffer 5 x	Promega (Madison, USA)
Tricine	Carl Roth (Karlsruhe)
Tris	Carl Roth (Karlsruhe)
Tris-hydrochloride different pHs,1M	Carl Roth (Karlsruhe)
Trizol	Invitrogen (Karlsruhe)
Tryphan blue	Carl Roth (Karlsruhe)
Trypsin EDTA	Gibco (Karlsruhe)
Tween 20	Carl Roth (Karlsruhe)

2.1.4. ELISA

Human IFN-α ELISA (eBioscience (Vienna, Austria)):

- Monoclonal Coating Antibody to human IFN-alpha
- Human IFN-alpha Standard protein
- HRP-Conjugate anti-human IFN-alpha monoclonal antibody

Murine IFN-α ELISA (PBL Biomedical Laboratories (New Jersey, USA)):

- MAb to Mouse Interferon-Alpha, neutralizing, Clone RMMA-1
- Mouse Interferon-Alpha
- PAb to Mouse Interferon-Alpha, Rabbit Serum, neutralizing
- Donkey Anti-Rabbit F(ab)2-Peroxidase

2.1.5. Transfection Reagents

Transfection reagent	Manufacturer
Dotap	Carl Roth (Karlsruhe)
LipofectamineTM 2000	Invitrogen (Karlsruhe)
TransIT LT-I	Mirus (Madison, USA)

2.1.6. Enzymes

Enzyme	Manufacturer
DNase I	Roche (Mannheim)
DNase II, type V (bovine)	Sigma-Aldrich (Steinheim)
DNase II, type IV (porcine)	Sigma-Aldrich (Steinheim)
DreamTaq™ DNA Polymerase	Fermentas (St. Leon-Rot)
Fast AP	Fermentas (St. Leon-Rot)
Phusion High-Fidelity DNA Polymerase	New England Biolabs (Frankfurt a. M.)
Proteinase K	Sigma-Aldrich (Steinheim)
T4 DNA PK	Thermo Scientific (St. Leon-Rot)

2.1.7. Western Blot And FACS Antibodies

Antibody	Manufacturer
Monoclonal ANTI-FLAG M2 antibody	Sigma-Aldrich (Steinheim)
B220-PerCp-Cy5.5, Clone RA3-6B2	BD Biosciences (Heidelberg)
CD11b-APC, Clone M1/70	Biolegend (San Diego, USA)
CD11c-PE-Cy7, Clone HL3	BD Biosciences (Heidelberg)
CD4-BV421, Clone RM4-5	Biolegend (San Diego, USA)
CD8-PerCp-Cy5.5, Clone 53-6.7	Biolegend (San Diego, USA)
F480- BV421, Clone BM8	Biolegend (San Diego, USA)
GR-1-PerCp-Cy5.5, Clone RB6-8C5	BD Biosciences (Heidelberg)
Ly6C-APC, Clone AL-21	BD Biosciences (Heidelberg)

2.1.8. Kits

Kit	Manufacturer
HiPure Plasmid Filter Midiprep Kit	Invitrogen (Karlsruhe)
InnuPREP PCR Pure Kit	Analytic Jena (Jena)
MyBudget Gel Extraction Kit	Bio-Budget Technologies GmbH (Krefeld)
Pure Link Quick Plasmid Miniprep Kit	Invitrogen (Karlsruhe)

2.1.9. MACS Beads From Miltenyi Biotec

CD11b MicroBeads, mouse/ human
CD11c MicroBeads, mouse
CD3ε MicroBeads, mouse
CD19 MicroBeads, mouse
Monocyte isolation kit II, human

2.1.10. Oligonucleotides

Desalted and HPLC-purified oligonucleotide (ODNs) were purchased from Metabion (Planegg-Martinsried). The lyophilized ODNs were dissolved in Diethylpyrocarbonat (DEPC)-H_2O and stored at -20°C.

PCR

GFP-fw-(bio)	5´-(Biotin)-GGC CAC AAC CAT GGT GAG CA-3´
GFP-rev-full length	5´-TTA CTT GTA CAG CTC GTC CAT-3

Real-time-PCR

mbeta-actin_sgfw	5´-TCC AGC CTT CCT TCT TGG GT-3´
mbeta-actin_sgrev	5´-GCA CTG TGT TGG CAT AGA GGT-3´
mIFN-α4_sgfw	5´-AAG CCT GTG TGA TGC AGG A-3´
mIFN-α4_sgrev	5´-GCA CAG AGG CTG TGT TTC TTC-3´

2.1.11. Nucleic Acids

Poly(I:C) was purchased from Invitrogen (Karlsruhe) and poly(dAdT) was purchased from Sigma-Aldrich (Munich). They were dissolved in DEPC-H_2O with a concentration of 1 µg/ µl and stored at -20°C until use.

2.1.12. Media, Solutions, Substrates And Buffers

All solutions, buffer and culture media were stored at 4°C. FCS was inactivated by heat (30 minutes, 56°C) before use. Solutions were sterile filtrated or autoclaved.

Dulbecco's Modified Eagle's Medium (DMEM):
DMEM 41965
10 % (v/v) FCS
2 mM L-Glutamine
1 mM MEM Sodium-Pyruvate
100 U/ ml Penicillin/Streptomycin

DNase II Buffer:
80 mM Sodium acetate
25 mM MgCl2
adjusted to pH 5.0 with HCl

ELISA Assay Buffer (hIFN-α):
1 x PBS
2 % (v/v) FCS
0,05 % (v/v) Tween 20

ELISA Assay Buffer (mIFN-α):
1 x PBS
10 % (v/v) FCS
(0,05 % (v/v) Sodiumazide)

ELISA Coating Buffer (mIFN-α):
0,2 M Sodium phosphate pH 6,5
12,49 g Na_2HPO_4 and 15,47 g NaH_2PO_4 solved in H_2O
pH adjusted to 6,5 and filled up to 1 L with H_2O

ELISA Washing Buffer:
1 x PBS
0,05 % (v/v) Tween 20

FACS Buffer:
1 x PBS
2 % (v/v) FCS

Freezing Medium:
90 % (v/v) FCS
10 % (v/v) DMSO

HEPES Buffered Saline (HBS, 2 x):
4 g NaCl
0,18 g KCl
0,05 g Na2HPO4
2,5 g HEPES
0,5 g Glucose
250 ml H_2O
pH adjusted to pH 7,1 with NaOH

IBc Buffer:
10 ml of 0.1MTris–MOPS (pH 7,4)
1 ml of 0.1 M EGTA/Tris (pH 7,4)
20 ml of 1 M sucrose
Bring volume to 100 ml with distilled water
Adjust pH to 7,4

Laemmli Buffer (5 x):
10 % SDS
125 mM Tris-HCl pH 6.8
50 % Glycerol
4 % DTE
0.65 % BPB

Native Protein Purification buffer (5 x):
250 mM NaH2 PO4 pH 8.0
2.5 mM NaCl

Native Protein Binding Buffer (1 x):
20 mM Tris-HCl pH 7.9
500 mM NaCl
2 mM Imidazole
adjusted to pH 8.0

Native Protein Wash buffer (1 x):
20 mM Tris-HCl pH 7.9
500 mM NaCl
20 mM Imidazole

Native Protein Elution buffer (1 x):
20 mM Tris-HCl pH7.9
500 mM NaCl
250 mM Imidazole
adjusted to pH 8.0

Pull-down Lysis Buffer:
PBS
1% NP-40 Substitute
Proteinase inhibitor tablet from Roche

Pull-down Wash Buffer:
PBS
0,2 % NP-40 Substitute

RPMI Medium:
RPMI 1640
10 % (v/v) FCS
2 mM L-Glutamine
0,1 mM MEM nonessential amino acids
1 mM MEM Sodium-Pyruvate
100 U/ ml Penicillin/Streptomycin

Tail Buffer:
100 mM Tris
5 mM EDTA
0,2 % (v/v) SDS
200 mM NaCl

2.1.13. Primary Cells And Cell Lines

Cell name	Source
HEK293T cells	Human embryonic kidney cell line purchased from Invitrogen (Darmstadt)
Human primary cells	Isolated from Buffy Coats purchased from the Institute of experimental Hematology and Transfusion Medicine (Bonn)
Murine primary cells	Isolated from wild type or knockout mice
RMA cells	NK-cell hybridoma (H2Kb) (Gays et al., 2000)
THP1 cells	Human monocytic cell line from Sigma
129-Macrophages	Macrophage cell line generated from 129/SV wild type mice

2.1.14. Mice

C57BL/6J	Janvier (Saint Berthevin, France)
MRL/lpr	Harlan Laboratories (Indianapolis, USA)
Sting$^{Gt/Gt}$	Mice with point mutation (T596A) in STING that results in a null allele due to an isoleucine-to-asparagine substitution (I199N), made by Russel E.Vance
Tlr9$^{-/-}$	TLR9-deficient mice, provided by Dr. Andreas Limmer
Trex1 $^{-/-}$	TREX1-deficient mice, provided by Prof.Dr. Jörg Wenzel

2. 2. Methods

2.2.1. Cell Culture

2.2.1.1. General Preconditions

All operations were carried out under a laminar flow hood using disposable gloves, sterile devices, solutions and growth media. Cultivation of primary cells and cell lines took place in CO_2 incubators (5 % CO2 v/v) at 37°C and 95 % humidity.

2.2.1.2. Subculturing Of Cells

All cell lines were regularly passaged to assure the quality of the growth medium and to prevent overgrowth. The production of catabolic metabolites changes the pH value of the medium. By the use of purchasable Dulbecco's Modified Eagle's Medium (DMEM) and Roswell Park Memorial Institute (RPMI) media containing phenol red as pH indicator (pH 7.4 = light red) the wastage of the medium can be seen as a color change from red to yellow. The cells were split every other day.

2.2.1.3. Determination Of The Cell Number

To determine cell number and vitality, the cells were stained with tryphan blue and counted with the help of a Neubauer counting chamber (side length 1 mm, depth 0.1 mm). Tryphan blue is an acidic dye that only stains dead cells, while living cells are protected by their intact cell membrane and appear white under a microscope. To determine the number of living cells, the cell suspension was 1:5- 1:20 diluted with 0.04 % Tryphan blue in Phosphate buffered saline (PBS). 10 µl of this mixture were applied to the Neubauer counting chamber covered with a glass slip. Engravings mark a field with nine large squares of 1 mm². Living cells in four of these squares were counted under a microscope (magnification of 10) and subsequently the cell number was divided by four. The volume over a large square is 0.1 µl (area * depth = volume), thus, the cell number per ml can be estimated by multiplying the cell number per large square by the factor of dilution and 10^4.

2.2.1.4. Freezing And Thawing Of Cells

1 x 10^7 cells were frozen in 1 ml FCS with 10 % Dimethylsulfoxide (DMSO). The cryo tubes were put into a freezing container containing Isopropanol and placed at -80°C for 24 hours. For permanent storage the deep frozen tubes were transferred at -150°C. The cells were rapidly thawed at 37°C, then slowly diluted in 50 ml warm growth medium for washing and finally resuspended in fresh medium.

2.2.2. Isolation And Generation Of Cells

2.2.2.1. Preparation Of Murine Bone Marrow DCs

Bone marrow (bm) cells were isolated from the hind legs of mice and differentiated to DCs. Therefore, mice were sacrificed via cervical dislocation and the hind legs were detached from the hip without damaging the thighbone. Remaining muscles were removed and lower leg and thigh were separated by superextending the knee joint. The medullary canal was opened and the bone marrow was flushed out with the help of a syringe filled with medium. Afterwards, the cell suspension was centrifuged for five minutes with 300 x g at room temperature (RT); the sediment was taken up in 10 ml BD Pharmlyse and incubated for five minutes at RT. Subsequently, the cells were washed with medium and finally counted. For differentiation towards bmDCs, bm cells of one mouse were placed in five 10 cm-plates and cultivated for seven days in 15 ml RPMI- medium with 3 % granulocyte-macrophage colony-stimulating factor (GM-CSF). Afterwards, cells were harvested and counted. For following stimulation experiments, 2 x 10^5 cells were plated in each well of a 96-well plate in a volume of 150 µl.

2.2.2.2. Isolation Of Murine Spleen Cells

Mice were anaesthetized with Isoflurane and killed by cervical dislocation. After sterilization of the mouse, the spleen was isolated, freed from fat and placed into a cell strainer. Using the rounded end of the forceps, the spleen was mashed through the cell strainer into a petri dish filled with 1 x PBS. The cell strainer was rinsed with 10 ml PBS and the suspended cells were transferred into a 50 ml falcon. After centrifugation at 1500 rpm for 10 minutes at 4°C, erylysis was performed for five minutes at RT with Pharmlyse (BD).

2.2.2.3. Isolation Of Human Peripheral Blood Mononuclear Cells

Peripheral blood mononuclear cells (PBMC) were isolated from buffy coats kindly provided by the University Medical Center of Bonn. In a first step, the blood was equally distributed in 3 x 50 ml falcons and mixed 1:2 with 1x PBS. 14 ml Ficoll (Biochrom, Berlin) were overlaid with the blood/ PBS solution and centrifuged at 800 x g without brake for 20 minutes at RT. Ficoll is a sucrose gradient, which has a higher density than PBMCs, but a lower density than erythrocytes and granulocytes; thus, the blood- PBS solution was separated into four phases by centrifugation. The PBMCs were transferred into a new falcon and the volume was filled up to 50 ml with 0,9 % NaCl. After centrifugation (450 x g for 10 minutes at RT), an erylysis was performed for five minutes at RT with Pharmlyse (BD). Subsequently, the cells were washed with 0,9 % NaCl and then taken up into 50 ml RPMI before the number of PBMCs was determined. For stimulation experiments, 2 x 10^5 cells/ 96-well were used. Otherwise, the cells were subjected to MACS separation for the enrichment of monocytes.

2.2.2.4. Magnetic-activated Cell Sorting

Magnetic-activated cell sorting (MACS) is based on the incubation of cells with magnetic microbeads that are coated with antibodies against a particular surface antigen. Cells that express this antigen attach to the beads and stay on a column placed in a strong magnetic field, while other cells that do not express the particular antigen can flow through. With this method one can either deplete or enrich the cells of interest.

Human monocytes were isolated with the Human Monocyte Isolation Kit II from Miltenyi Biotec. With this kit, all cells of human PBMCs with the exception of monocytes are labeled with biotinylated antibodies. Anti-Biotin microbeads bind to these antibodies and hold the cells that are not of interest onto the column. Since monocytes were not labeled with an antibody, they can flow through the column and are collected. According to the user manual, human PBMCs were resuspended in 30 µl MACS buffer per 10^7 cells and incubated with 10 µl FcR-Blocking-reagent and 10 µl Biotin-ab-cocktail. After 10 minutes at 4°C, 30 µl MACS buffer and 20 µl anti-Biotin microbeads were added and the cells were further incubated for 15 minutes at 4°C. Thereafter, the cell suspension was washed with 2 ml MACS buffer and taken up in 500 µl MACS buffer per 10^8 cells. Next, the cell suspension was loaded onto a LS MACS column placed in the magnetic field of a MACS separator. The column was washed two times with 1 ml MACS buffer and the flow-through was collected in a fresh 50 ml falcon. The cells were taken up in 0,9 % NaCl and counted. For stimulation experiments, 2 x 10^5 cells/ 96-well were used.

Murine $CD3\varepsilon^+$ splenocytes were depleted with the MicroBead kit from Miltenyi Biotec. The cells were first labeled with 10 µL of CD3ε-Biotin per 10^7 cells for 10 minutes at 4°C, and subsequently magnetically labeled with 20 µl of Anti-Biotin MicroBeads per 10^7 cells for 15 minutes at 4°C. Thereafter, cells were applied onto a LD MACS column and unlabeled cells that passed through were collected.

Murine $CD19^+$ splenocytes were depleted with CD19 MicroBeads from Miltenyi Biotec. The cells were labeled with 10 µL of CD19 MicroBeads per 10^7 total cells for 15 minutes at 4°C and then loaded onto MS MACS columns. Unlabeled cells that passed through were collected.

2.2.2.5. Isolation Of Human Neutrophils From Fresh Blood

For the isolation of human neutrophils, 9 ml fresh blood were collected in an Ethylenediaminetetraacetic acid (EDTA) blood collection tube, layered over 5 ml Histopaque 1119 (Sigma) and centrifuged for 20 minutes at 800 x g and 21°C without brake. Afterwards, cells were resuspended in 2 ml PBS and laid over a five-layer Percoll gradient of 85-80-75-70-65 % Percoll (Sigma). After centrifugation at 800 x g for 20 minutes and 21°C (no brake!), neutrophils between the 65 and 85 % layers were harvested into a fresh falcon and washed with PBS. Remaining red cells were eliminated by erylysis for four minutes at RT. The isolated neutrophils were suspended in RPMI with 5 % FCS and directly used.

2.2.2.6. Isolation Of Murine Neutrophils From Bone Marrow

Murine neutrophils were isolated from bone marrow with the help of a Percoll gradient. Percoll consists of colloidal silica particles, which have been coated with polyvinylpyrrolidone (PVP). It is used to establish density gradients that can be used to isolate cells. For the isolation of neutrophils, marrow cavities of the tibias and femurs were flushed with PBS. After erylysis for five minutes at RT, the remaining cells were laid on a three-step Percoll gradient (55 %, 65 % and 75%) and centrifuged for 20 minutes at 1000 x g and 21°C without brake. Neutrophils recovered at the interface of the 65 and 75% fractions were >85% pure as assessed by fluorescence activated cell-sorting (FACS) analysis

2.2.3. Stimulation And Treatment Of Cells

2.2.3.1. Transfection Of Nucleic Acids

LipofectamineTM 2000 (Invitrogen) and TransIT-LT1 (Mirus) are reagents that allow the transfection of eukaryotic cells with nucleic acids or proteins. Hereby, the transfected substances reach predominantly the cytosol of a cell. For transfection of DNA, 1,2 µl TransIT-LT1 transfection reagent were diluted in 25 µl Optimem and incubated for five minutes at RT. Meanwhile, 400 ng DNA were diluted in 25 µl Optimem. Afterwards, the diluted reagent was added and the whole mixture was incubated for 20 minutes at RT to allow the formation of nucleic acid complexes. 45 µl of the nucleic acid mixture were then added to a 96-well plate containing 2 - 4 x 10^5 cells/ 150 µl medium per well. For transfection of 3pRNA, 100 ng 3pRNA and 0,2 µl Lipofectamine (Invitrogen) were used.

2.2.3.2. UV Irradiation Of Cells And DNA

For the irradiation of cells and nucleic acids with UV-A or UV-B light a Multitester SBB LT 400 (Saalmann, Herford) was used. Irradiation with UV-C light was done with an UV-crosslinker from Peqlab Erlangen (254 nm). Not more than 20 µl DNA per 96-well was placed in a round bottom plate without lid, irradiated with the desired UV doses and directly used for stimulation. Cells were irradiated in not more than 500 µl per 6-well and DNA was isolated after one hour.

2.2.3.3. HOCl/ H_2O_2-treatment Of Cells And DNA

0,5 -1 x 10^7 cells were placed in 6-well plates and treated with different concentrations of HOCl (10 µM, 100 µM, 1 mM) or H_2O_2 (100 µM, 1 mM, 10 mM). After 60 minutes incubation at 37°C, the cells were washed with 1 x PBS and then DNA was isolated like described. For direct H_2O_2-treatment of DNA, DNA was isolated of RMA-mOVA cells and incubated for three minutes with different amounts of HOCl/ H_2O_2 (1 µM, 10 µM, 100 µM). Afterwards, the DNA was precipitated with Ethanol. Therefore, 2/3 volume of 100 % Ethanol and 1/10 volume of Sodiumacetate was added to the DNA and five minutes incubated at -80°C. Next, the samples were centrifuged for

15 minutes with maximal speed at 4°C. The pellet was washed with 500 µl 70 % Ethanol and again centrifuged for five minutes. The supernatant was taken off and the DNA was dried at 37°C. At last, the DNA was taken up in H_2O or PBS.

2.2.3.4. Induction Of NETosis

NETosis of human and murine neutrophils was induced by an incubation in 40 nM Phorbol-12-myristate-13 acetate (PMA) for three hours at 37°C.

2.2.3.5. Incubation Of DNA With Human LL37 Peptide

To complex genomic DNA with the human cathelicidin LL37, the DNA was incubated with LL37 (Innovagen) in a ratio of 1:2 for 30 minutes at RT in a total volume of 20 µl. Afterwards, the volume was increased with 1x PBS to 100 µl and cells were stimulated with 45 µl/ 96-well.

2.2.4. Enzyme Linked Immunosorbent Assays

To determine the level of a specific antigen in a sample, often Sandwich-ELISAs are carried out. The principle of this method relies onto two antibodies that bind the same antigen. Importantly, they bind different epitopes so that they do not hinder each other. The first antibody is the coating or capture antibody. After its binding to a microtiter plate, remaining antigen-binding sites on the plate itself are blocked by the incubation with a buffer containing FCS or BSA. After a washing step, the samples are added and the capture antibody binds the specific antigen. Another washing step then ensures that unbound components of the samples are removed. Next, the second antibody named the detection ab is added to the wells and binds to the captured antigen. Thereby, an antibody-antigen-antibody complex (Sandwich) is generated. Either the detection ab itself is coupled to an enzyme which catalyzes the reaction of a given substrate into a detectable form, or a secondary ab is used which binds universally to the Fc-region of other antibodies and is coupled to an enzyme that allows the detection of the desired antigen. Often the enzyme HRP (horseradish peroxidase) is used which catalyzes the oxidation of tetramethylbenzidine (TMB) with H_2O_2 and stains the solution blue. This reaction is then stopped with an acid and the color changes from blue to yellow. For quantitative verification, standard rows with known antigen concentrations are added in addition to the other samples. With the help of a calibration curve one can then determine the amount of antigen being present in a specific sample.

2.2.4.1. Murine IFN-α ELISA

To determine the level of murine IFN-α in cell culture supernatants, the wells of a 96-well-ELISA-plate were coated with 50 µl of the primary antibody RMMA-1 (1 mg/ml) diluted 1:1000 in 0,2 M Sodium phosphate buffer (pH 6,5) and incubated at 4°C overnight. The next day, the plate was washed three times with 150 µl washing buffer and blocked with 150 µl Assay buffer for three

hours at RT. After three washing steps, 50 µl samples were applied undiluted to the ELISA plate. Additionally, an 8-rowed serial dilution of the recombinant IFN-α standard (100 U/ ml) was prepared with concentrations ranging from 5000 to 0 pg/ ml. Both, samples and standard row, were incubated for 16 - 48 hours at 4°C. After three washing steps, the plate was incubated with 50 µl of a polyclonal anti-mouse-IFN-α detection antibody made in rabbit (80 NU/ µl) diluted 1:1000 in assay buffer. Prior to the incubation with 50 µl of a HRP-conjugated secondary antibody, the ELISA plate was washed 10 times. The anti-rabbit- F(ab)2-Peroxidase made in donkey was diluted 1:10000 in assay buffer and applied for three hours in the dark at RT. After 10 washing steps, the plate was incubated with 50 µl substrate solution (BD OptEIA Substrate Reagent A and B) until the first five standard dilutions turned blue. The color reaction was stopped with 50 µl 2 M H_2SO_4 and the color intensity was measured with an ELISA reader at 450 and 570 nm.

2.2.4.2. Human IFN-α ELISA

To detect human IFN-α, the ELISA plate was incubated with diluted coating antibody to human IFN-alpha (final concentration 1 µg/ ml) in 1x PBS overnight at 4°C. To block unspecific binding sites, 50 µl assay buffer (1 x PBS with 0,5% BSA and 0,05 % Tween) were applied for one hour at RT. After three washing steps, 50 µl diluted samples (1:2 in assay buffer), 50 µl standard (highest concentration 500 pg/ ml) and 25 µl HRP (1:1000) conjugate were added simultaneously for two hours at RT. Subsequently, the plate was washed three times and the substrate (BD OptEIA Substrate Reagent A and B) was added. The color reaction was stopped with 2 M H_2SO_4 and color intensity was measured at 450 and 570 nm.

2.2.4.3. 8-OHG EIA ELISA

The amount of 8-Hydroxy-2-deoxy-guanosine (8-OHG) incorporated in DNA samples was quantified using the competitive 8-OHG EIA ELISA from Streß Marq Biosciences (Victoria). The kit is based on the principle that 8-OHG of a DNA sample competes with a tracer consisting of an 8-OHG-Acetylcholinesterase (AChE) conjugate for the binding to a limited 8-OHG antibody. Since the concentration of the tracer is kept constant, the amount of the tracer bound to the antibody is inversely proportional to the amount of 8-OHG being present in the DNA sample. The ELISA plate is coated with a polyclonal goat anti-mouse IgG antibody to which the 8-OHG-antibody complex binds. After washing away unbound reagents, Ellmann´s reagent is added that contains acetylthiocholine and 5,5'-Dithio-bis 2- nitrobenzoic acid. The acetylcholinesterase of the tracer hydrolyzes acetylthiocholine to thiocholine which then reacts with 5,5'-Dithio-bis-2-nitrobenzoic acid to 5-Thio-2-nitrobenzoic acid. This product has a yellow color and an absorbance maximum at 412 nm. The color intensity is proportional to the amount of ELISA plated- bound 8-OHG tracer and inversely proportional to the amount of free 8-OHG of the analyzed DNA sample.

According to the user manual, DNA samples were first digested using nuclease P1 to hydrolyze 3'-5' phosphodiester and monoester bonds. After dephosphorylation with alkaline phosphatase, 50 µl of the sample and a standard row starting with 3 ng/ ml were applied to the pre-coated ELISA plate. Additionally, 50 µl tracer and 50 µl monoclonal 8-OHG antibody were added. To measure non-specific binding (NSB), only 50 µl 8-OHG-Tracer and 100 µl buffer were added to two wells. To determine the maximal amount of tracer that can be bound by the antibody (B0), two wells were filled with 50 µl tracer, 50 µl monoclonal 8-OHG antibody and 50 µl buffer. In addition, two blank controls were made (Blk). After 20 hours at 4°C, the ELISA plate was washed five times and subsequently 200 µl Ellmann´s reagent was added. Regularly the absorption at 410 nm was measured, and as soon as the B_0 control minus background was between 0,3 and 1,0 the absorption of the samples was measured. For analysis, the absorption value of the Blk control was subtracted from the samples. Next, the NSB value was subtracted from the B_0 control (= corrected B_0) and the samples. Then the sample values were divided by the corrected B0 and multiplied by 100 to give the ratio of sample to B_0 control (% B/B_0). The data of the standard were linearized using a logit transformation (logit (B/B0) = ln [B/B0/(1 - B/B0)]). Logit (B/B0) data were plotted versus log concentrations and a linear regression fit was performed. The concentration of each sample was finally determined using the equation obtained from the standard curve plot.

2.2.5. Molecular Methods

2.2.5.1. Polymerase Chain Reaction

Polymerase Chain Reaction (PCR) is a method to amplify a piece of DNA. It relies on thermal cycles consisting of repeated heating and cooling to melt the DNA double strands and to allow enzymatic amplification. To target the DNA fragment of interest, short DNA oligonucleotides (primers) being complementary to the DNA sequence are used. The method is called chain reaction since the DNA generated in the previous cycle is used as a template for replication in the next one, allowing the DNA to be exponentially amplified by an enzyme called DNA polymerase. The first regular cycling event is a denaturation step in which the double stranded (ds) DNA is separated into single strands. To allow the annealing of the primers to their complementary sequence, the temperature is then lowered to ~50- 60°C. Subsequently, the temperature is raised to ~70°C so that the DNA polymerase can bind to the priming site and build up a new DNA strand in 5' to 3' direction, which is complementary to the DNA template strand. These temperature steps are usually repeated 20-40 times. After the last cycle, the reaction is kept at ~ 70°C for five minutes to make sure that all DNA strands are fully extended.

2.2.5.2. Generation Of Biotinylated GFP Via PCR

To pull down DNA-binding proteins, DNA encoding biotinylated green fluorescent protein (GFP, full length) was generated via PCR. For one 50 µl reaction 1 µl template (0.5 ng DNA), 1 µl forward primer (10 µM), 1 µl reverse primer (10 µM), 1 µl dNTPs (10 mM), 5 µl 5 x Taq buffer, 1.5 µl $MgCl_2$ (50 mM) and 0.2 µl Taq polymerase were mixed and filled up to 50 µl with H_2O (Ampuwa). The DNA was then amplified with a thermo cycler and the following program with 35 cycles:

94°C	05:00
94°C	00:30
60°C	00:30
72°C	01:00
72°C	10:00
8°C	--:--

Table 2: PCR program for the generation of biotinylated GFP (35 cycles)

2.2.5.3. Incorporation Of 8-OHG Into DNA

Different amounts of 8-OH-dGTP (TriLink, San Diego (USA) were introduced into an arbitrary DNA sequence e.g. GFP by PCR. Afterwards, the PCR products were purified with the InnuPrep PCR pure kit from Analytik Jena to rule out that free 8-OH-dGTP was carried over.

2.2.5.4. Purification Of PCR Products

PCR products were purified with the innuPREP PCR pure kit from Analytik Jena according to the user's manual. Shortly, binding buffer was added to the PCR product and the mixture was given onto a purification column on which the DNA binds to. After a washing step, the DNA was eluted in an appropriate amount of Ampuwa H_2O.For further concentrating the DNA, a precipitation with Ethanol and Sodiumacetate was done. For that, 2/3 volume 100 % Ethanol and 1/10 volume 3 M Sodiumacetate was added to the DNA. The mixture was incubated for five minutes at -80°C and subsequently centrifuged for 15 minutes with maximal speed at 4°C.The pellet was washed with 500 µl 70 % Ethanol and again centrifuged for five minutes. Finally, the pellet was dried at 37°C and taken up in Ampuwa H_2O.

2.2.5.5. RNA-Isolation From Cells

For RNA isolation, 1 -5 x 10^7 cells were lysed in 1 ml RNA Magic (BioBudget) for five minutes at RT. Afterwards, 200 µl Chloroform were added and the samples were vortexed for 10 seconds. After an incubation on ice for five minutes and centrifugation at 12.000 x g and 4°C for five minutes, the samples were separated into three phases. The upper aqueous phase contained the RNA and was transferred into a new tube. Next, an equal amount of Isopropanol was added and the samples were incubated on ice for 15 minutes. Centrifugation for 10 minutes at 4°C and maximal speed resulted in a RNA pellet, which was then washed twice with 70 % Ethanol. RNA

was dissolved in with 32 µL RNase free H_2O and digested with 4 µL DNaseI (1U/ µl) and 4 µL DNaseI 10 x Buffer (Invitrogen) for 15 minutes at 37°C.

2.2.5.6. cDNA Synthesis

For cDNA synthesis, RNA was reverse-transcribed with RevertAid Reverse Transcriptase (Thermo Scientific) and oligo-dT Primer. The use of anchored oligo (dT) 18 primers ensured that full-length cDNA was generated only from RNAs containing a poly-A tail. 1 µg of total RNA was incubated with 1 µl anchored- oligo (dT) 18 primer for 10 minutes at 70°C. 4 µL 5 x First Strand Buffer, 1 µL dNTP mix (10mM) and 1 µL Moloney Murine Leukemia Virus Reverse Transcriptase (MMLV-RT) were added and the whole reaction was incubated at 42°C for one hour. Afterwards, 80 µL H_2O were added and 2ul of the cDNA mix was used for a 10 µl RT-PCR reaction.

2.2.5.7. Quantitative Real Time PCR

Gene expression levels were measured using the my-Budget EvaGreen QPCR Mix II (Bio-Budget) on an Applied Biosystems ABI 7900 HT (Life Technologies). EvaGreen or SYBR green is a fluorescent dye that intercalates into dsDNA. Thus, the detected fluorescence increases proportionally to the amount of DNA. The C_t (cycle threshold) or C_p (crossing point) value describes the cycle when the fluorescence emitted from a sample exceeds the background threshold. The quantity of DNA ideally doubles with every PCR cycle during the exponential phase which allows the calculation of relative amounts of DNA, e.g. if the C_p values of two samples differ by 3, the amount of template DNA differs by 2^3 = 8 fold. However, often the efficiency of the chosen primer pair is not 100 %. Efficiency can be calculated with the help of a standard curve that results form a qPCR run with a cDNA dilution series. The logarithm of the input cDNA amount is plotted against the Ct values, which results in a linear regression curve with the slope –m. A slope of -3,32 results in an efficiency of 1 (100 %), meaning that the DNA doubles each PCR cycle. The efficiency is calculated with the following equation:

$$E = (10^{-1/-m} - 1) \times 100$$

To accurately compare gene expression independent of variations due to the preparation and quality of DNA between different samples, the gene of interest (GOI) was normalized to a housekeeping gene (beta- actin) of the same sample with delta Ct = Ct (GOI) – Ct (beta-actin). If samples were compared to an untreated control, data analysis was performed according to the Pfaffl model for relative quantification in RT-PCR, which considers the efficiency of each primer pair used:

$$\text{ratio} = (E_{\text{target}})^{\Delta \text{Ct target (control – treated)}} / (E_{\text{ref}})^{\Delta \text{Ct ref (control – treated)}}$$

2.2.5.8. *In-vitro* Transcription Of 3pRNA

5’ triphosphate double stranded RNA (3pRNA) is a synthetic ligand for RIG-I and was often used as positive control in stimulation experiments. The enzyme T7-RNA polymerase, which

synthesizes RNA in 5'- 3' direction, was used to transcribe 3pRNA. This enzyme needs a template with the complement sequence of the desired RNA and a ds T7 polymerase promoter. To generate this template, two ODNs were heated up to 70°C for five minutes and then slowly cooled to RT. Afterwards, the template was incubated with Klenow buffer, dNTPs and polymerase I for 30 minutes at 37°C. The Klenow reaction was stopped at 70°C for 10 minutes, and RNA synthesis was then performed with the help of the transcriptAid T7 high yield Transcription Kit (Thermo Scientific). Shortly, nucleotides, enzyme mix (recombinant T7 polymerase), the according buffer and DTT (Dithiothreitol) were added to the Klenow reaction and incubated overnight at 37°C. Afterwards, DNase I was used to digest the DNA template, and the 3pRNA was adjusted to 1 µg/ µl and stored at -80°C until use.

2.2.5.9. Isolation Of Genomic DNA

To extract total genomic DNA out of cells, 5 x 10^6 cells were washed with 1 x PBS and centrifuged for five minutes with 1200 rcf and 4°C. The cell pellet was then taken up in 500 µl Tail-Puffer plus 2,5 µl Proteinase K (20 µg/ µl) and incubated for at least two hours at 55°C and 800 rpm. Afterwards, 500 µl Phenol/Chloroform (mixed 1:1) were added and the samples were centrifuged for 10 minutes with 14000 x g at RT. The aqueous phase containing the DNA was transferred into a new tube and twice as much volume 100 % Ethanol was added. The mixture was centrifuged for two minutes with 14000 x g to pellet the DNA, which was then washed with 1 ml 70 % Ethanol and subsequently dried at 37°C before taking up in H_2O or PBS.

2.2.5.10. Determining the Concentration of Nucleic Acids

The concentration of nucleic acids was determined with the help of a Nanodrop 1000 Spectrophotometer which measures the optical density at λ = 260 nm, the absorption peak of nucleic acids. 47 µg/ ml DNA, respectively 40 µg/ ml RNA equate an OD_{260} of 1, meaning that the extinction coefficient of DNA is 47 and 40 for RNA. The values are inserted into the Beer-Lambert equation: c = A/(E x b) with c being the nucleic acid concentration, A the absorbance, e the extinction coefficient and b the path length. To get information about the purity of the samples, the Nanodrop measures additionally the optical density at λ = 280 nm, which is the absorption maximum of proteins. The ratio of OD260/OD280 equals 1,8 if the sample only contains DNA and 2,0 if only RNA is included. Values below 1,8 are a sign of contaminations with proteins.

2.2.6. Protein biochemistry

2.2.6.1. Polyacrylamide Gel Electrophoresis

Polyacrylamide gel electrophoresis is a method used for the separation of proteins according to their size. The principle behind this method is similar to that of an agarose gel electrophoresis.

The protein samples are mixed with sodium dodecyl sulfate (SDS), which denatures secondary and tertiary structures, and additionally applies a negative charge to each protein in proportion to its mass. Then, the samples are loaded onto a polyacrylamide gel and an electric field causes the movement of the negatively charged molecules towards the anode. Thereby, small molecules move faster than longer ones due to a smaller resistance of the gel. Thus, one can separate proteins according to their size. For tracking the progress of the proteins through the gel, a tracking dye is added which has a higher electrophoretic mobility. The gels are made up of acrylamide, bisacrylamide, SDS and Tris buffer (pH 8,8; respectively pH 6,8). A source of free radicals (APS) and a radical stabilizer (TEMED) initiate polymerization. This reaction leads to a gel since bisacrylamide can cross-link two polyacrylamide molecules. Changing the acrylamide concentration can vary the pore size. Generally, lower percentage gels are used to resolve high molecular weight proteins, while higher percentages are used for smaller proteins. For polyacrylamide gel electrophoresis the vertical electrophoresis system from C.B.S (80 x 85 x 0,75 mm) was used. The concentration of the collection gel was 3 % and its height approximately 2 cm. The separation gel had a concentration of 10-12 % and a height of approximately 6 cm. Samples were mixed 1:1 with 1 x Laemmli buffer, dynabeads used for pulldowns were eluted in 20 µl 1 x Laemmlli buffer. Heating for five minutes at 95°C denatured the proteins, and after cooling to RT, the samples were loaded in the pockets of the gel. For electrophoresis, 100 Volts (V) were applied for two hours.

2.2.6.2. Bacterial Expression Of TREX1 And cGAS

Primers for overexpression were designed such that they comprise the whole coding sequence (CDS) of the gene of interest. Additionally, the forward primer contained a Kozak sequence with the consensus gccRccAUGg, with R being a purine base and AUG the start codon. This sequence is recognized by the ribosome as the translational start site. If the protein to be overexpressed should contain a Flag-Tag the reverse primer did not comprise a stop codon, and the gene was cloned into a pET derivative with N-Terminal His6-Flag-Tag.

Molecular cloning of TREX1 and cGAS was performed by Thomas Zillinger. Shortly, the TREX1 open reading frame (ORF) was amplified from murine genomic DNA and cloned into a pET derivative with N-terminal His6-Tag and C-terminal FLAG-tag. For lentiviral expression, TREX1 was cloned into pLenti-EF1-MCS, kindly provided by Jonas Doerr (Institute of Reconstructive Neurobiology, University of Bonn). After positive verification by Sanger Sequencing (Seqlab, Göttingen, D), TREX1 protein expression was induced by Isopropyl-β-D-thiogalactopyranosid (IPTG) in *E. coli* and purified using Ni-NTA Agarose (Life Technologies, Darmstadt, D). The cGAS ORF was amplified from Open Biosystems Clone #BC145653 and cloned into a pET derivative with N-Terminal His6-Flag-Tag. Bacterial expression was performed as described for TREX1 and the eluted fraction was dialyzed against PBS before use.

2.2.6.3. Purification Of Proteins

The purification of overexpressed proteins was performed with the Ni-NTA purification system from Invitrogen. Therefore, IPTG (final concentration 0.1 mM) was used to induce the expression in the *E. coli* strain Rosetta (DE3). After three hours, the bacteria were washed with 0,9 % NaCl, taken up in 10 ml Binding Buffer **(**20 mM Tris-HCl pH 7.9, 500 mM NaCl, 2 mM Imidazole, Protease Inhibitor) and sonicated for four minutes. To remove cellular debris, the lysate was centrifuged for 10 minutes at max speed (>12000 x g) and 4°C. 1 ml of Ni--NTA resin was washed twice with Binding Buffer, taken up in 10 ml Binding Buffer and mixed with the cleared lysate. After one hour incubation under rotation at 4°C, the resin was washed twice with 8 ml of Wash Buffer **(**20 mM Tris-HCl pH 7.9, 500 mM NaCl, 20 mM Imidazole) and finally eluted with 2 ml Elution Buffer (20 mM Tris-HCl pH 7.9, 500 mM NaCl, 250 mM Imidazole). The purification procedure was analyzed with SDS-polyacrylamide gel electrophoresis (PAGE) and coomassie staining.

2.2.6.4. cGAS DNA Pulldown Assay

A pull-down assay is a method to identify interaction partners of a bait molecule. It can be compared to immunoprecipitation, even though the antibody is substituted by some other affinity system. In this case, biotinylated DNA was used to catch the DNA-binding protein cGAS in a cell free system. The DNA-protein complexes were fished out with the help of Streptavidin-coated Dynabeads.

1 µg of a biotinylated PCR product, either untreated or UV-C irradiated, was incubated for one hour at 4°C in 500 µl PBS, Proteinase inhibitor (Roche Complete Mini-EDTA free) and 0,5 % Bovine serum albumin (BSA) spiked with cGAS containing an N-terminal Flag-Tag extracted from bacteria (1:250). 10 µl Streptavidin Dynabeads MyOneT1 (Invitrogen) were then added to the mixture and further incubated for two hours at 4°C. After three washing steps with PBS, the eluted proteins were analyzed by Western blot. To determine the size of the isolated protein the PAGE Ruler Prestained Protein ladder from Piercenet was used.

2.2.6.5. Western Blot

Western blotting can be applied after a polyacrylamide gel electrophoresis to detect specific proteins from a heterogeneous sample. For this purpose, the proteins are transferred from the gel to a membrane (typically nylon, polyvinylidene difluoride or nitrocellulose). Thereby, the protein pattern is maintained. Protein binding is based upon hydrophobic interactions and charged interactions between the membrane and protein. Afterwards, the proteins can be detected by using antibodies linked to a reporter enzyme. When an appropriate substrate is added, the light of a colorimetric reaction causes an image on a photographic film.

In the Barchet laboratory, wet blots were performed. The membrane was put on top of the gel, and whatman papers were placed on top and underneath of that. The entire stack was then

placed in a buffer solution and by applying voltage vertically to the running direction of the gel the proteins moved out of the gel and onto the membrane. To prevent unspecific binding of the antibody, the membrane was incubated in a 0,5 % milk solution. The proteins in the solution occupy all places on the membrane where the proteins from the gel have not bound. Thus, the antibody can only bind to the binding sites of the specific target protein and not to unspecific binding sites of the membrane. After blocking, the proteins of interest were labeled with an antibody. Thereby, either a combination of a primary and secondary antibody-horseradish peroxidase (HRP) conjugate was used, or an antibody directly linked to HRP. For detection, Pierce's Enhanced Chemiluminescent (ECL) Western Blotting Substrate was added which is a luminal based chemiluminescent substrate for the detection of HRP enzyme activity. It produces luminescence in proportion to the amount of protein. A photographic film was then placed onto the membrane, and exposure to the light from the reaction generated an image of the antibody-labeled protein of interest.

2.2.6.6. SybrGreen-based DNase I, II And III Activity Assay

The protocol used was adapted from Brucet, Querol-Audı et al. (2007). 1 µg genomic DNA, respectively 2 µg of a 200 bp PCR product (GFP-200), were preincubated with SYBR Safe (Invitrogen) for 30 minutes at RT to allow the SYBR Green to incorporate into the DNA. The assay was performed in a 96-well plate in a final volume of 15 µl with 20 mM Tris-HCl, pH 7.5, 5 mM $MgCl_2$, 2 mM dithiothreitol (DTT), and 100 µg/ ml BSA for DNase I and III, or 80 mM sodium acetate buffer with 25 mM $MgCl_2$, pH 4.6 for DNase II. To start the reactions simultaneously, 1 unit DNase I (Sigma) or DNase II from bovine spleen (Sigma), respectively 1 µl of purified TREX1, were added to the wall of each well. After centrifugation, the degradation was real time followed with the Roche LightCycler® 480 Real-Time PCR System.

2.2.6.7. Fluorescence Activated Cell Sorting

Fluorescence activated cell sorting (FACS) is based on the labeling of specific cell surface molecules with antibodies that are fused to fluorescent dyes. Within the flow cytometer, the cell suspension enters a fast flowing liquid stream onto which a laser beam of a single wavelength is directed. Each cell that crosses the laser beam scatters the light ray and the fluorescent dyes are excited to emit light at different wavelengths. At the point where the cells pass the laser beam, a forward scatter (FSC), a side scatter (SSC) and several fluorescent detectors are located. The FSC correlates with the cell size and the SSC informs about the cell interior like nucleus dimension, the amount and type of cytoplasmic granules or the texture of the cell membrane.

To stain cells with fluorescently labeled antibodies at least 2 x 10^5 cells were first blocked with 10 % FCS in PBS (human cells) or anti-mouse CD16/CD32 (1:100 in FACS buffer) (murine cells) for 20 minutes at 4°C and then incubated with adequate antibody master mixes for 30

minutes at 4°C. Subsequently, cells were washed with FACS buffer and resuspended in 50 µL. FACS was executed with the BD LSR II flow cytometer, whereas cell sorting was performed with the BD FACSAriaTM III at the flow cytometry core facility in the institute of molecular medicine, Bonn.

FACS analysis was performed with the FACS DiVa Software, while the evaluation was done with the Flowjo Software. For discriminating cell populations from each other and to exclude cell debris, the FCS was plotted against the SSC and the population of interested was gated. For evaluation of single markers a histogram was made to get the percentage of cells being positive for a specific marker. Expression of multiple markers was investigated with dot plots using quadrant statistic by calculating the percentage of positive cells. To determine positive cells, stringent gating criteria were used and gates for positive cells were set with reference to the unstained control at the 1 % border.

2.2.6.8. Detection Of Cellular ROS And Superoxide Content In DNA

For the measurement of reactive oxygen species (ROS) and superoxide in UV irradiated cells, the Total ROS/Superoxide Detection Kit (Enzo Life Sciences, Lörrach) was used according to the manufacturer's protocol. After staining with the green fluorescent oxidative stress detection reagent and the orange fluorescent superoxide detection reagent, cells were immediately irradiated with different doses of UV light, then incubated for 30 minutes at 37°C and analyzed by FACS.

2.2.7. *In Vivo* Experiments

200 µg genomic DNA, either unmodified or UV irradiated, was administered i.v. and after four, six or eight hours blood was taken to analyze the serum type I IFN by ELISA. Additionally, splenocytes were individualized by incubation in Collagenase D for 10 minutes at 37°C followed by filtration with 150 µm gaze, and analyzed by FACS or RT-PCR. For the analysis of DNA uptaking cells, UV irradiated DNA was stained with Sytox Green (10 µM) for 15 minutes at RT before injection. Alternatively, mice were administered i.c. to the earlobes every third day with 10 µg untreated or UV irradiated genomic DNA, or with PBS (Mock). Ear thickness was determined 24 hours after the last injection.

3. Results

3.1. Increased ROS Levels After UV-A/-B/-C Irradiation Correlate With Enhanced Immune Stimulatory Properties Of DNA

UV irradiation can influence health in many ways. A certain level of UV-B exposure is required for vitamin D3 metabolism and calcium homeostasis. In addition, both UV-A and UV-B phototherapy are part of the treatment regimen of certain skin diseases, such as psoriasis, dermatitis and vitiligo. Nonetheless, prolonged UV exposure can result in sunburn and premature skin aging. Furthermore, it is also associated with several forms of skin cancer. These harmful effects of UV light are usually attributed to the suppression of immunity. However, under certain circumstances UV exposure can also lead to an activation of the immune system.

Previous experiments in the Barchet laboratory revealed that co-cultures of bone marrow derived dendritic cells (bmDCs) with UV irradiated cells lead to a reduced release of pro-inflammatory cytokines such as IL-6, IFN-α and IL12p40. In contrast to these co-culture experiments, stimulation of bmDCs with DNA isolated from UV irradiated cells resulted in an increased immune response compared to stimulation with DNA from untreated cells.

UV light can cause DNA damage both directly by photocrosslinking and the generation of DNA base dimers, and indirectly through the generation of Reactive Oxygen Species (ROS). To test whether cells show elevated ROS levels upon UV irradiation and whether this correlates with immune stimulation, RMA cells were incubated with a ROS detection reagent (Enzo Life Sciences) and exposed to different doses of UV-A, UV-B or UV-C light. After an incubation at 37°C for 30 minutes, the relative cellular ROS production was determined by flow cytometry. Simultaneously, DNA was isolated from the irradiated cells, complexed with the *Trans*IT-LT1 Transfection Reagent (Mirus) and used to stimulate murine bmDCs.

As depicted in **Figure 7 A**, a UV dose-dependent increase in cellular ROS was observed shortly after UV irradiation. Moreover, these increased ROS levels were closely correlated with the immune stimulatory property of the DNA, here shown by the induction of IFN-α secretion. Of note, IFN-α levels were increased irrespective of whether the cells were irradiated with UV-A, UV-B or UV-C light prior to DNA isolation (**Figure 7 B**).

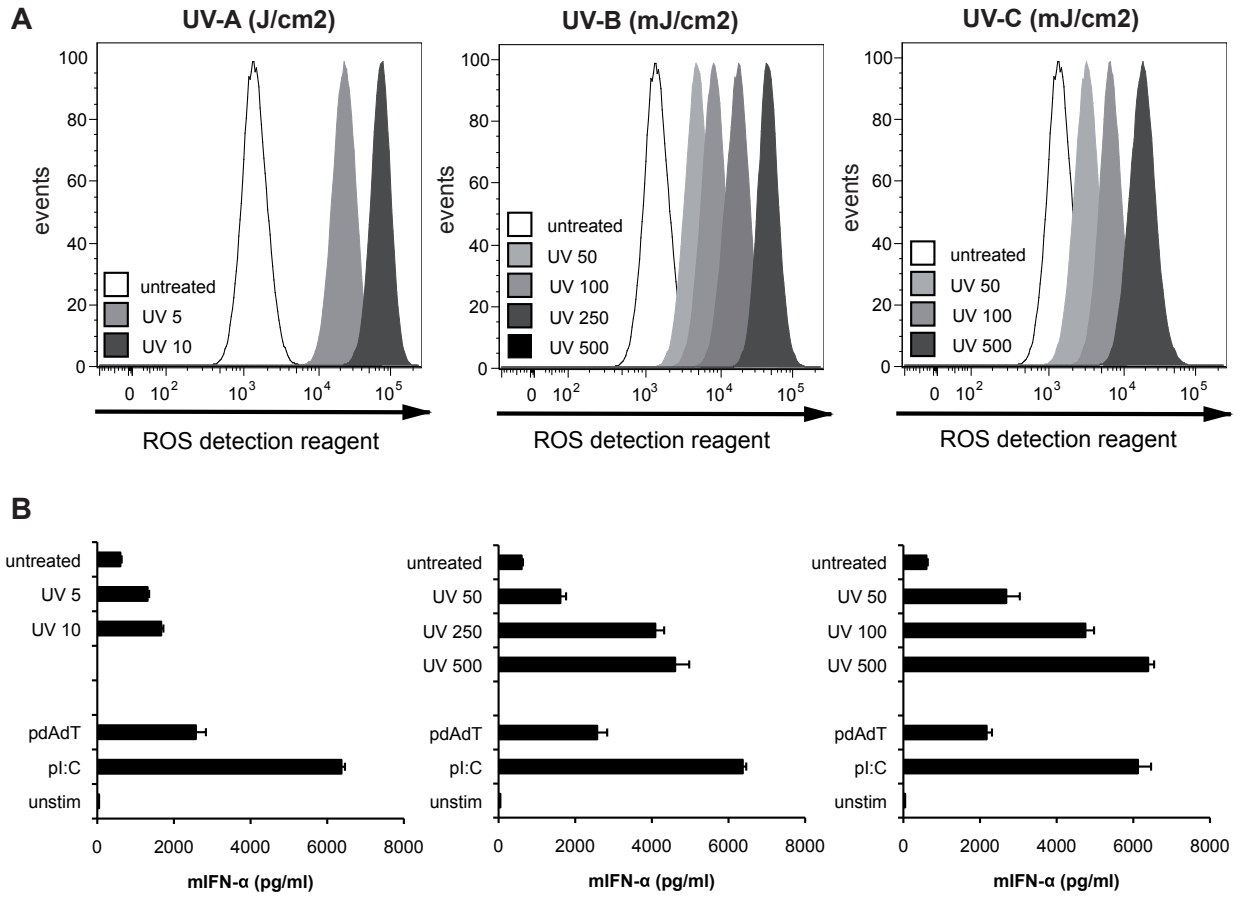

Figure 7: UV irradiation leads to increased intracellular ROS levels which correlate with increased DNA immunogenicity

RMA cells were incubated with a ROS detection reagent (Enzo Life Science) and exposed to UV-A, -B or -C light at the doses indicated. After 30 min, relative cellular ROS production was determined by flow cytometry. Data shown are representative of two independent experiments (A). 2 x 10^5 WT bmDCs were stimulated with 400 ng DNA derived from cells that were exposed to different UV-A, -B or -C light doses. Stimulations with 200 ng poly(I:C) and poly(dAdT) were used as positive controls. After 18-24 h, IFN-α was measured in the supernatants via ELISA. Data shown are representative of two independent experiments. Shown are means +SDM (B).

3.2. UV Irradiation Only Enhances The Immunogenic Potential Of DNA

It was initially observed that both RNA and DNA isolated from UV irradiated cells were more immunogenic than when isolated from untreated cells. To further test whether UV irradiation really increases the immunostimulatory potential of RNA, RMA cells were either left untreated or UV-C irradiated with the doses indicated. Subsequently, RNA was isolated and digested with either DNase I or RNase A. Murine bmDCs were stimulated with 400 ng RNA complexed with transit LT1 (Mirus), a transfection reagent that delivers nucleic acids predominantly to the cytosol. After 18 hours, mIFN-α was measured in the supernatants via ELISA. As shown in **Figure 8 A**, stimulation with RNA that was not DNase I treated led to a substantial amount of type I IFN, which increased further when cells were irradiated with UV light prior to RNA isolation. However, in the RNA samples digested with DNase I, the type I IFN response was completely abrogated. In contrast, RNase A treatment had no significant influence on the type I

IFN response in comparison with the undigested RNA samples. These results were also observed when DNA isolated from untreated or UV irradiated cells was digested with either DNase I or RNase A (**Figure 8 B**). Thus, one can conclude that UV irradiation only enhances the stimulatory potential of DNA, but not of RNA. The enhanced activity observed after RNA isolation was due to contaminating DNA, and could be eliminated by treating RNA isolations with RNase free DNase I.

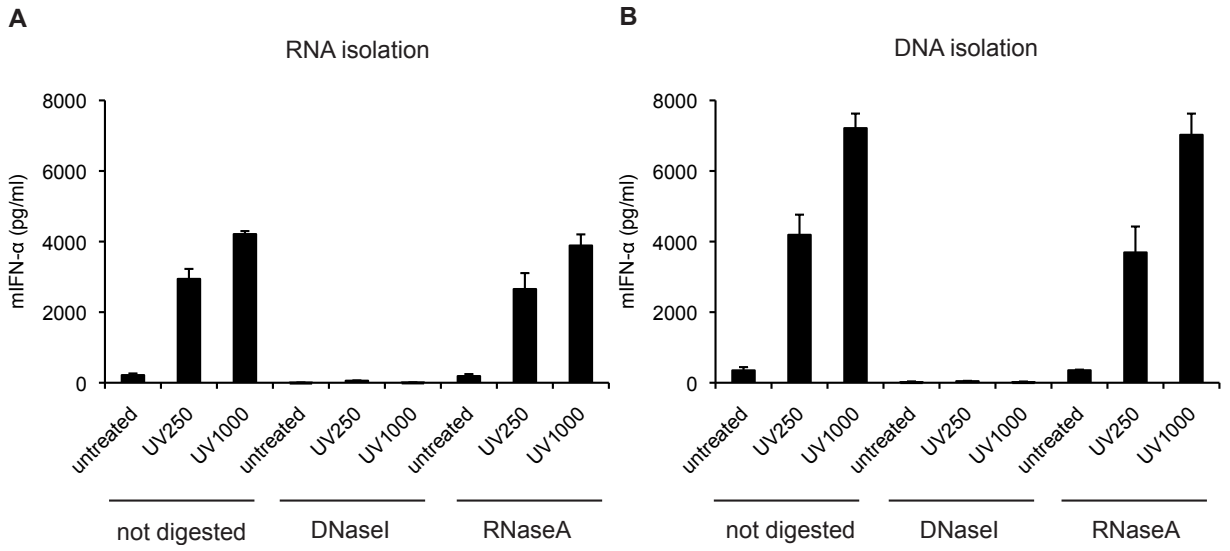

Figure 8: RNA or DNA samples from UV irradiated cells lose their immunostimulatory capacity after DNase I treatment

RNA (A) or DNA (B) was isolated from either untreated or UV irradiated RMA cells and digested with DNase I or RNase A for 30 min at 37°C. 2 x 10^5 bmDCs were stimulated with 400 ng RNA/ DNA complexed with TransIT-LT1 (Mirus). 18 h later, IFN-α was measured in the supernatants via ELISA. This figure is representative of three independent experiments. Shown are means +SDM.

3.3. DNA Double-strand Breaks Are Not The Reason For The Increased Immunogenicity Of Cell-free UV Irradiated DNA

Previous experiments in the Barchet laboratory revealed that not only DNA isolated from UV irradiated cells, but also DNA that was directly UV irradiated in a cell-free system is more immunogenic than unmodified DNA. Thus, DNA fragmentation as part of the apoptotic process could be ruled out to play a role in the immunogenicity of UV-DNA. However, UV light can induce double-strand breakage either directly by the absorption of UV photons by DNA, or indirectly during nucleotide excision repair following UV damage (Sancar et al., 2004).

In the case of direct DNA irradiation, repair mechanisms that account for the majority of double-strand breaks occurring after UV exposure must not be considered. However, those double-strand breaks that are caused by a direct energy absorption could theoretically enhance the immunogenicity of UV irradiated DNA, since moderate fragmentation may facilitate the uptake of genomic DNA into immune cells.

To verify if the observed differences in the immunostimulatory potential of untreated and UV irradiated DNA are dependent on the length of the transfected DNA strand, untreated and UV-C

irradiated genomic DNA were loaded onto an agarose gel (**Figure 9 A**). There was no difference between these two DNA samples visible. However, to make sure that smaller fragment size of UV-DNA has nothing to do with the observed immunogenicity, the restriction enzymes EcoRI and EcoRV were used to generate DNA fragments with an average length of 2000 base pairs (bp). Stimulation with the fragmented DNA did indeed lead to slightly higher type I IFN levels compared to uncut DNA. However, stimulation with the fragmented genomic DNA was not comparable to stimulation with UV irradiated DNA, and the relative increase in stimulation by UV irradiation remained unchanged. Thus, a differential uptake of shorter DNA fragments generated via double-strand breaks could be excluded as cause for the enhanced recognition of UV-damaged DNA (**Figure 9 B**).

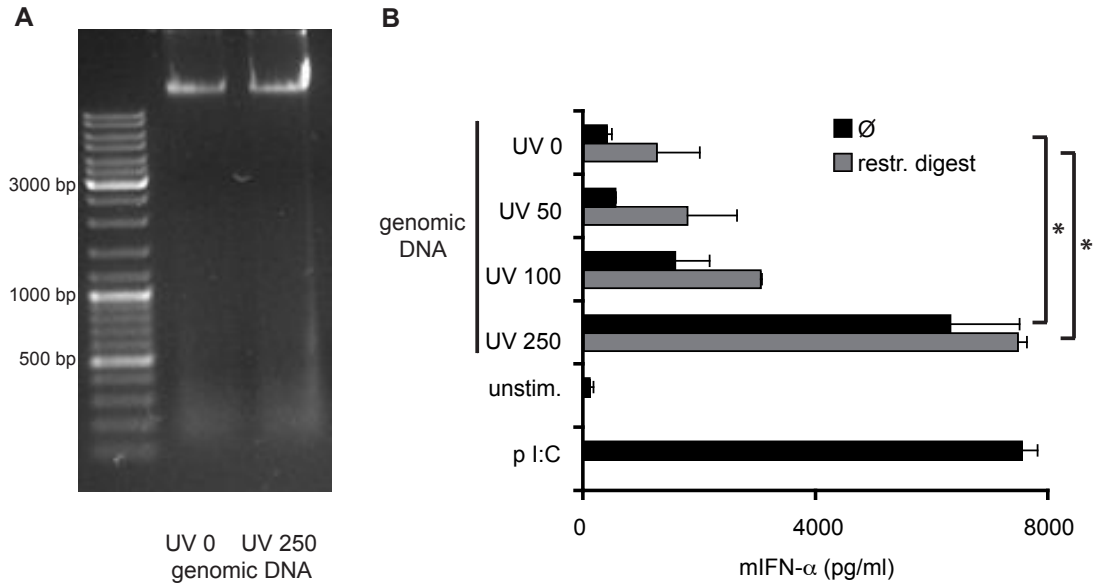

Figure 9: DNA fractionation is not the reason for the immunogenicity of UV irradiated DNA

Genomic DNA from RMA cells was isolated and either left untreated or UV-C irradiated with 250 mJ/ cm^2. Subsequently 500 ng were loaded on a 1% agarose gel (A). Genomic DNA from RMA cells was either left untreated or fragmented with the restriction enzymes EcoRI and EcoRV for 16 h at 37°C. After UV-C irradiation at the doses indicated, the DNA was used to transfect murine bmDCs, and IFN-α was measured in the culture supernatants 18 h later via ELISA. This figure is representative of three independent experiment, shown are means +SDM; * $P < 0.05$ (Student's t-test). (B).

3.4. UV Irradiated DNA Induces A Prolonged Upregulation Of Type I IFN

To further characterize the enhanced recognition of UV irradiated DNA, the kinetics of type I IFN production following UV-DNA stimulation was analyzed. Following stimulation with either unmodified or UV irradiated DNA, supernatants were collected four, five, six, seven, eight or 24 hours after stimulation. IFN-α levels were quantified using ELISA, and detectable levels of the pro-inflammatory cytokine could be observed as soon as five hours after stimulation. Six hours after stimulation, a significant difference in the response to unmodified and UV irradiated DNA was measurable (**Figure 10 A**). These results indicate a fast upregulation and secretion of IFN-α in response to oxidatively modified DNA. Next, the time kinetics were analyzed by real-time

quantitative polymerase chain reaction (RT-PCR) following *in vitro* stimulation of bmDCs with unmodified and UV irradiated DNA. As shown in **figure 10 B**, IFN-α induction was observed within the first two hours after stimulation. For unmodified DNA, maximum transcript accumulation was obtained three hours after stimulation, followed by a rapid decrease in expression. In contrast, the response to UV irradiated DNA was several times greater than the response to unmodified DNA and reached its maximum after four hours of stimulation, followed by a moderate downregulation up to baseline expression levels. These results showed that cells react to UV irradiated DNA with cytokine expression that is not only increased but also prolonged, suggesting that oxidatively damaged DNA might remain in the cytosol for a longer duration than unmodified DNA.

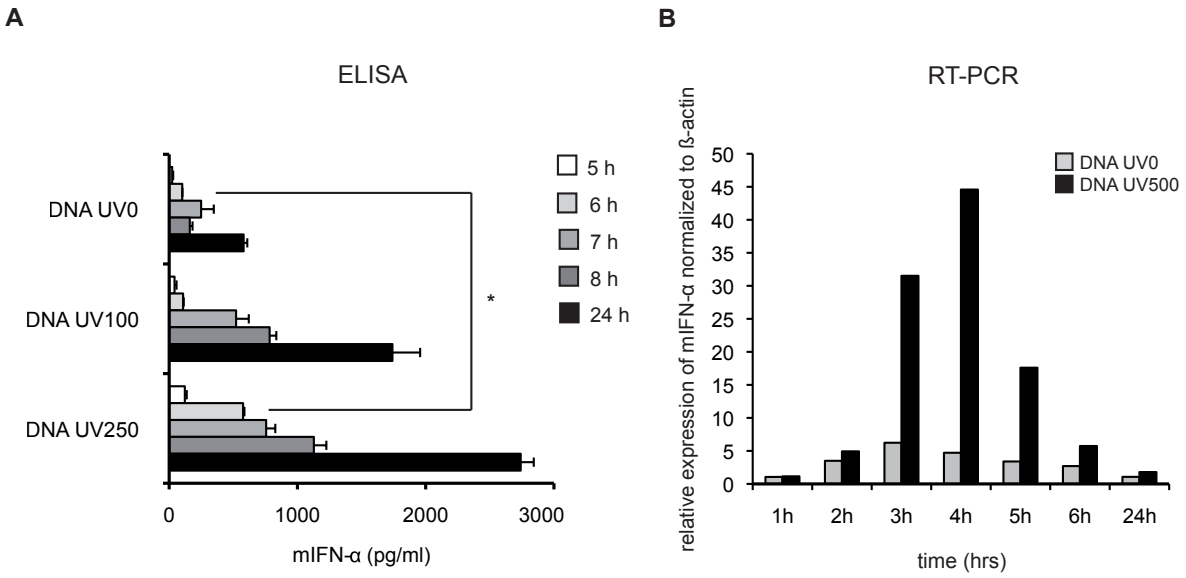

Figure 10: The kinetics of the type I IFN response to unmodified and UV irradiated DNA

2 x 10 ^{5} bmDCs were stimulated with 400 ng genomic DNA that was either left untreated or UV irradiated with the doses indicated and secretion of mIFN-α was quantified in the culture supernatants at the indicated time points after stimulation. Shown are means +SDM; * $P < 0.05$ (Student's t-test). (A). Alternatively, RNA was reverse transcribed after 1–6 and 24 h, and subsequently analyzed by qPCR (B). The data are representative of three independent experiments.

3.5. DNA Stimulus And UV Damage Signal Can Be Separated Temporally And Spatially

Our initial observation took place before the identification of cGAS as the cytosolic DNA-receptor upstream of STING. Since it was then unknown how cytosolic DNA is recognized in general, it could not be excluded that a second distinct pathway might participate in UV-DNA recognition. To analyze whether a second synergistic pathway might be involved in the immune response to UV-DNA, co-transfection experiments were carried out with unmodified genomic DNA and an UV irradiated dsDNA oligonucleotide composed of the repetitive base triplets ATA / TAT, which is only weakly immunogenic by itself. Furthermore, it was analyzed whether an enhanced type I IFN response could still be observed if the UV irradiated oligonucleotide was first added two, four or six hours after the stimulation with genomic DNA (**Figure 11**). As expected, stimulation

with the unmodified as well as with the UV irradiated ATA oligonucleotide only induced low levels of IFN-α, while upon stimulation with genomic DNA substantial levels of IFN-α could be measured in the supernatant. Genomic DNA in combination with the unmodified oligonucleotide caused only a weak increase in type I IFN levels in comparison to stimulation with genomic DNA alone. However, genomic DNA together with the UV irradiated oligonucleotide led to significantly higher IFN-α levels. This was also true if the oligonucleotide was added to the cells two or four hours after genomic DNA stimulation. Even if the UV irradiated oligonucleotide was added six hours after genomic DNA stimulation, type I IFN levels were still increased, although to lesser extent. These results suggested that possibly two pathways could be interacting, one for DNA recognition and the other being specific for DNA base modifications.

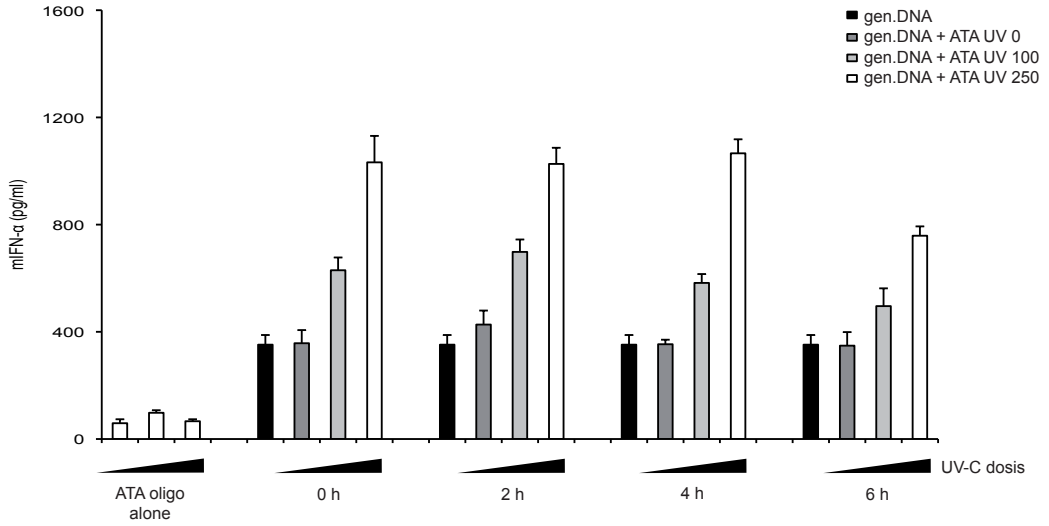

Figure 11: Co-stimulation with genomic DNA and an UV irradiated double stranded oligonucleotide induces enhanced IFN-α production in murine bmDCs

Murine bmDCs were co-transfected with genomic DNA and a 54 bp ds ATA-oligonucleotide that was either left untreated or UV-C irradiated with 100 or 250 mJ/cm^2. The ATA oligonucleotide was either added directly to the genomic DNA or added to the cells 2, 4, or 6 h after the cells were stimulated with genomic DNA. Stimulation with genomic DNA, the untreated or UV irradiated ATA oligonucleotide alone was carried out as a control. All nucleic acids were complexed with TransIt-LT (Mirus). 18 h later, IFN-α was measured in the supernatant via ELISA. The data shown are representative of four independent experiments. Shown are means +SDM.

3.6. Using Inhibitors That Target Different Signal Transducers Or Regulators To Identify Signal Pathways Involved In The Enhanced Recognition of UV-DNA

In order to identify a potential second pathway involved in the response to UV irradiated DNA, the influence of different inhibitors prior to DNA stimulation was tested. Previous experiments in the Barchet laboratory had already excluded a role for phosphoinositid-3 kinase (PI3K), protein kinase C (PKC), spleen tyrosine kinase (Syk), Vav1 guanine nucleotide exchange factor, janus kinase 3 (JAK3), nuclear factor of activated T cells (NFAT), nuclear factor 'kappa-light-chain-enhancer' of activated B-cells (NFkB) and Signal Transducer or Activator of Transcription 5 (Stat5) in the improved recognition of UV-DNA. However, promising results were observed when the well-established mitogen-activated protein kinase (MAPK) p38 inhibitor SB202190 (Sigma)

was applied prior to DNA stimulation in bmDCs. Preincubation with low doses of SB202190, led to a reduced IFN response to UV irradiated DNA, while cytokine production was unhindered upon stimulation with unmodified DNA or poly(I:C) (data not shown). These results indicated that p38 might have a specific involvement in the cytosolic recognition of UV irradiated DNA. However, in human monocytes no effect for SB202190 could be observed. Thus, a second p38 inhibitor (SB203580, Sigma) was tested and experiments with the initially used p38 inhibitor, SB202190, were repeated. As shown in **figure 12 A and B**, a role for p38 in the improved recognition of UV irradiated DNA could not be confirmed since p38 inhibition globally reduced the type I IFN response. With increasing inhibitor concentrations the induction of IFN-α following DNA, UV-DNA and poly(I:C) stimulation was inhibited due to toxicity of the inhibitors which decreased cell viability (assessed with cell titer blue, data not shown).

UV induced DNA damage can be repaired by a variety of intracellular DNA repair mechanisms. However, the involvement of DNA-dependent protein kinase (DNA-PK) involved in base excision repair (BER), or ataxia-telangiectasia mutated kinase (ATM), a key mediator of DNA damage response (DDR), in the immune sensing had already been excluded by previous experiments performed within the Barchet group (data not shown). To investigate whether other proteins involved in DNA damage repair might be important for the recognition of UV-DNA, different inhibitors of polymerase 1 (PARP-1), a protein involved in non-homologous end joining (NHEJ), were tested (**Figure 12 C**). In this experiments, the highest inhibitor concentrations not leading to decreased cell viability were used (tested by cell titer blue assay). There was however no indication for an involvement of PARP-1 in enhanced immune sensing of UV irradiated DNA.

Next, the nucleotide exchange repair (NER) mechanism was blocked in the stimulated cells prior to DNA transfection. Specifically, xeroderma pigmentosum A (XPA), which is part of the NER complex, was inhibited by titrated doses of X80. As depicted in **Figure 12 D**, there was no specific inhibition of IFN-α secretion in response to UV-DNA visible, instead the DNA response was unchanged, while the immune reaction to poly(I:C) was slightly reduced with high inhibitor concentrations. These results suggested that NER, or at least XPA, is not involved in the recognition of UV-DNA. In addition, p53 was blocked with two different inhibitors (**Figure 12 E and F**). Nutlin-3 had no effect on the immune response to UV-DNA, while there was a specific reduction of the type I IFN secretion in response to UV irradiated DNA visible at low inhibitor concentrations of Pifithrin-mu. However, higher doses of this inhibitor did not further decrease IFN-α levels. Taken together, the involvement of DNA damage repair proteins in enhanced immune sensing of UV-DNA could be excluded.

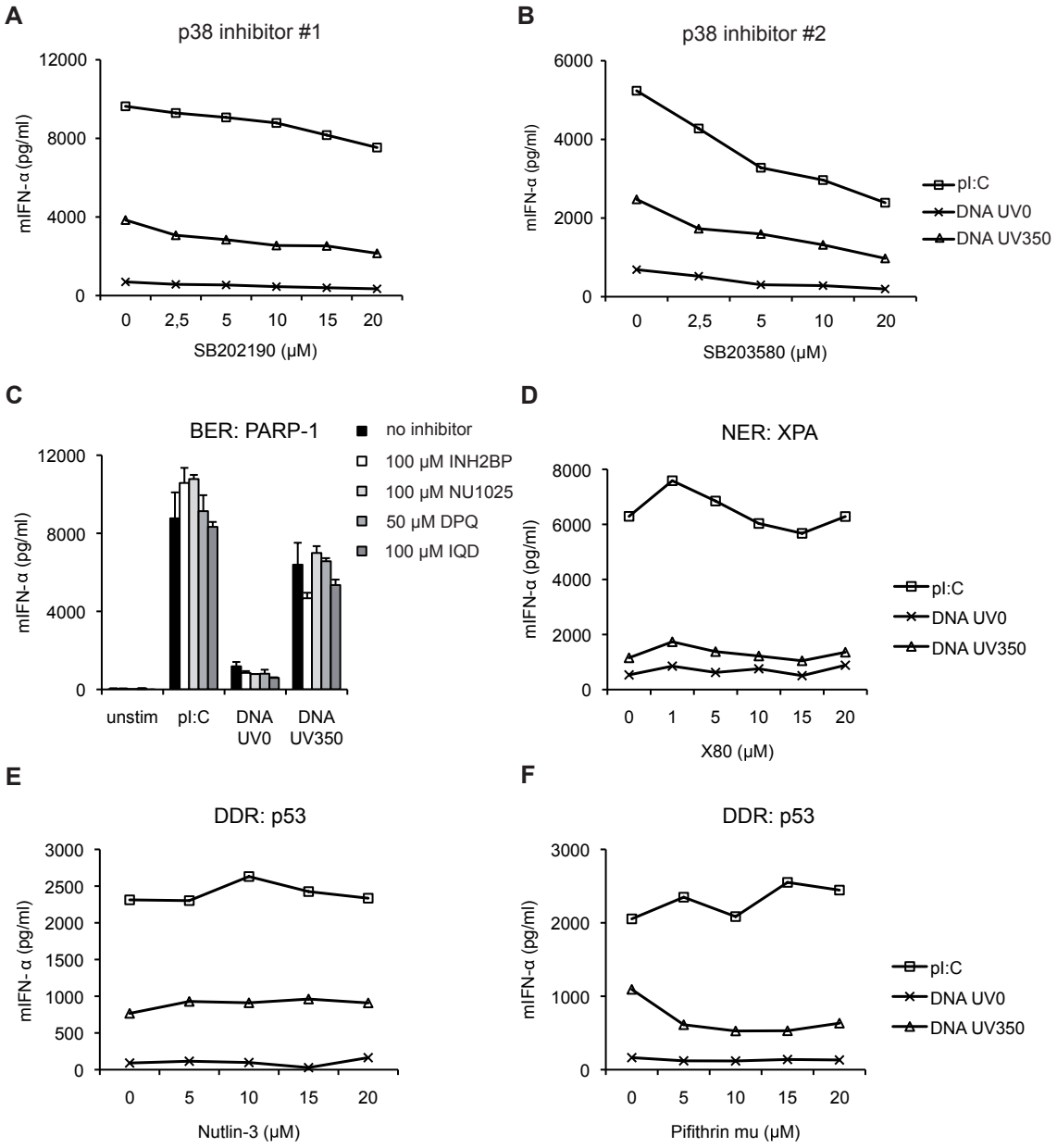

Figure 12: Blocking of p38 or different DNA damage signaling pathways does not impair the immune detection of UV irradiated DNA

Murine bmDCs were pre-treated with the p38 inhibitors SB202190 (A) and SB203580 (B) or different inhibitors blocking key proteins involved in base excision repair (C), nucleotide excision repair (D) or DNA damage repair (E and F). After 1h, cells were washed and subsequently stimulated with unmodified or UV irradiated genomic DNA. After 18 h, mIFN-α was measured in the supernatants via ELISA. Stimulation with poly(I:C) served as control. These data are representative of three independent experiments.

3.7. The Cytosolic DNA Receptor cGAS Recognizes Unmodified And UV Irradiated DNA In Equal Measure

Knockdown experiments in the Barchet laboratory demonstrated that UV-DNA is recognized by the cytosolic DNA receptor cyclic GMP-AMP (cGAMP) synthase (cGAS). Upon DNA binding, cGAS produces the second messenger cGAMP, which then binds to STING and activates the STING-TBK1-IRF3 signaling axis, finally resulting in the production of type I IFNs (Wu et al.,

2013; Sun et al., 2013). Since knocking down cGAS abolished the pro-inflammatory response to both untreated and UV irradiated DNA (data not shown), another hypothesis to explain the enhanced immunostimulatory activity of UV irradiated DNA was that the cytosolic receptor cGAS might have a higher affinity for UV-DNA compared to unmodified DNA. To test this, a pulldown experiment with cGAS and equal amounts of either untreated or UV irradiated DNA was performed *in vitro.* Biotinylated PCR products served as DNA probe and were incubated for one hour with recombinant Flag-tagged cGAS. Subsequently, the PCR products were recaptured using Streptavidin-coated magnetic Dynabeads and cGAS binding was visualized by anti-Flag western blot. As shown in **Figure 13**, no binding differences of cGAS to unmodified and UV irradiated DNA was observed. Thus, a higher binding affinity of cGAS for UV-DNA could be excluded as a reason for the enhanced recognition of UV irradiated DNA.

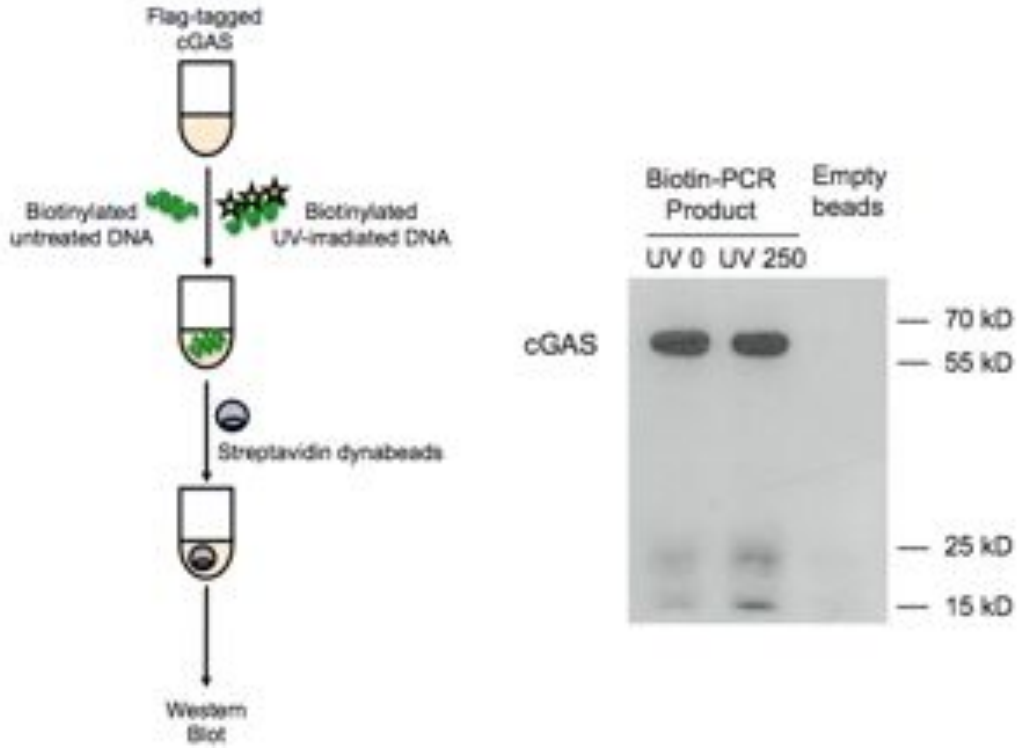

Figure 13: Comparable cGAS affinity of unmodified and UV irradiated DNA

Biotinylated PCR products were either left untreated or UV-C irradiated with 250 mJ/cm^2, and subsequently incubated for 1 h with recombinant cGAS-Flag. DNA was recaptured using Streptavidin-coated magnetic Dynabeads T1 for 2 h. cGAS binding to beads without DNA served as specificity control. cGAS was visualized by anti-Flag western blot analysis. Pulldown was performed three times.

3.8. Oxidative Modifications Protect DNA From TREX1-mediated Degradation

Another possibility for the enhanced activation of cGAS by UV-DNA is that UV exposure might induce modifications, which protect the DNA from degradation. There are three major deoxyribonucleases (DNases) known to catalyze the hydrolytic cleavage of phosphodiester linkages in the DNA backbone and thus degrade extranuclear DNA in different cellular compartments: DNAse I, which is found extracellularly; DNase II, which works best at acidic pH and is present in lysosomes; and DNase III (also known as TREX1) that is located in the cytosol.

DNase I and II are endonucleases that cleave anywhere along the DNA chain, while DNase III/ TREX1 belongs to the group of exonucleases that cleave only residues at the ends of DNA molecules.

To test whether these DNases have difficulties degrading UV-DNA, genomic DNA that was either left untreated or UV irradiated, was digested *in vitro* with recombinant DNase I, II and III (**Figure 14**). To visualize the activity of the different DNases, DNA was stained with SybrGreen, which allowed following DNA degradation via corresponding fluorescence decay in real time. While the endonucleases DNase I and DNase II both demonstrated no significant difference in their ability to degrade unmodified and UV irradiated DNA (**Figure 14 A and B**), degradation of UV-DNA by the cytosolic exonuclease TREX1 was less efficient than degradation of unmodified DNA (**Figure 14 C**). These results were of particular interest, since UV irradiated DNA is recognized in the cytosol where also TREX1 is predominantly located. Previous experiments in the Barchet laboratory demonstrated that the incorporation of the oxidized base 8-hydroxy guanosine (8-OHG) was sufficient to increase the immune response of myeloid cells to PCR products (data not shown). To analyze whether the presence of 8-OHG is adequate to protect DNA from degradation by TREX1, PCR products containing 10% 8-OHG were analyzed for resistance to TREX1-mediated degradation (**Figure 14 D**). Incorporation of 8-OHG protected the PCR products from TREX1-mediated degradation, suggesting that the oxidized base is indeed sufficient to shield DNA from destruction.

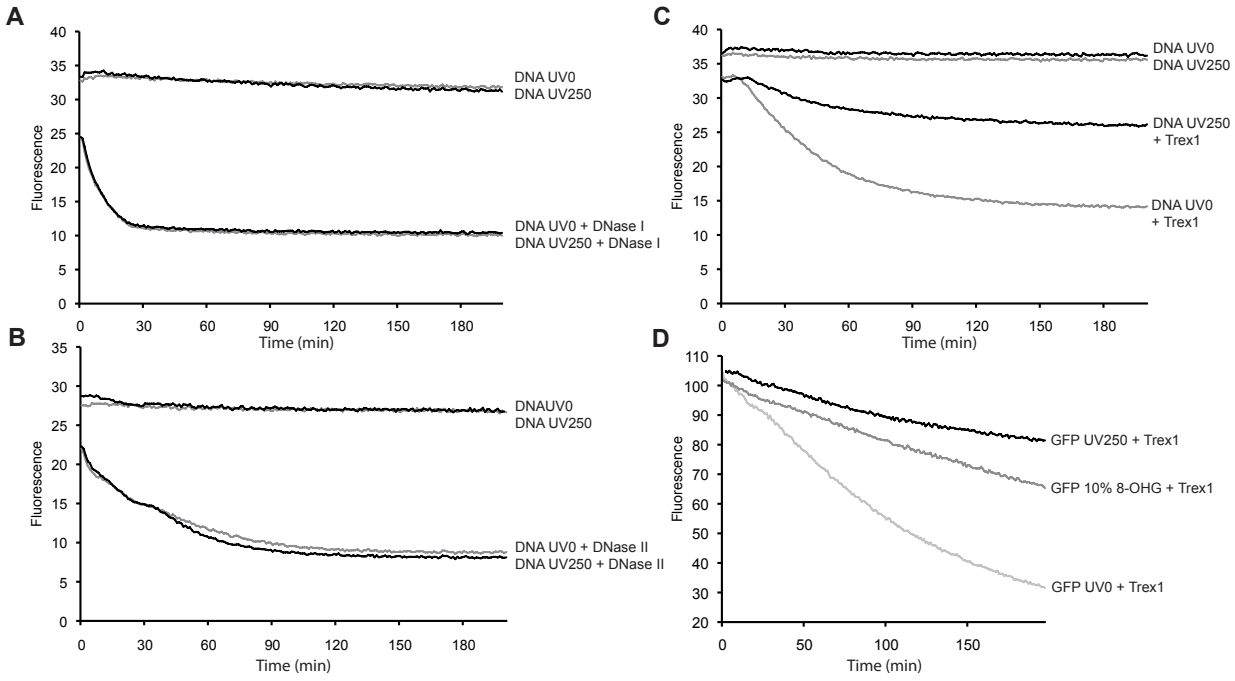

Figure 14: Unmodified and oxidized DNA is degraded similarly by DNase I and DNase II, but differentially by TREX1

Recombinant DNase I (A), DNase II (B) or TREX1 (C and D) was added to genomic DNA (A, B and C) or PCR products (D) that were either left unmodified (UV 0), UV damaged (UV 250; A, B and C) or contained 10 % 8-OHG (D). DNA degradation was monitored over time as vanishing SYBR Green signal. The data shown are representative of three independent experiments.

3.9. TREX1 Knockout Cells React To All Types Of DNA With High Amounts Of Type I IFN

The role of the exonuclease TREX1 is to digest cytosolic DNA in order to prevent an inappropriate immune response. To confirm that oxidative DNA modifications conferring resistance to TREX1-mediated degradation are responsible for elevated immune responses upon UV-DNA stimulation, bmDCs generated from the bone marrow of TREX1-deficient mice were stimulated with UV irradiated or ROS damaged genomic DNA (**Figure 15 A**) or PCR products (**Figure 15 B**). Murine bmDCs that did not express TREX1 demonstrated a high responsiveness to all sorts of the DNA tested, irrespective of whether these DNAs were unmodified or oxidatively damaged. In contrast, WT bmDCs with functional TREX1 responded with low amounts of IFN-α to unmodified DNA but retained their high level of responsiveness to oxidized DNA. Likewise, could be demonstrated that lentiviral overexpression of TREX1 in the mouse leukemic monocyte/ macrophage cell line RAW 264.7 restored increased responsiveness to oxidized DNA as compared to unmodified DNA (data not shown). Taken together, these results suggest that oxidative modifications shelter DNA from degradation and that modified self-DNA can cause cytosolic immune activation even in the presence of TREX1.

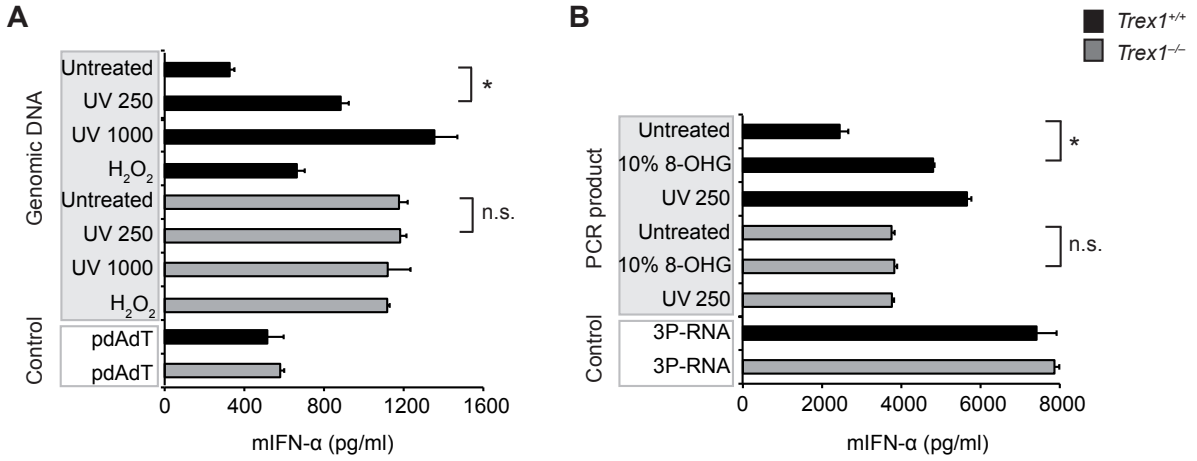

Figure 15: TREX1-deficient bmDCs do not differentiate between unmodified and oxidized DNA

WT and TREX1-deficient bmDCs were stimulated with either unmodified and oxidized genomic DNA (A) or with unmodified or oxidized PCR products (B). Stimulations with pdAdT or 3pRNA were used as positive controls. After 18-24 h, secretion of mouse FN-α in the supernatants was quantified via ELISA. These data are representative of four independent experiments. Shown are means +SDM; * $P < 0.05$ (Student's t-test).

3.10. Ear Swelling Reactions Of Different Knockout Mice To UV-DNA

To investigate the inflammatory response to UV-DNA *in vivo,* unmodified or UV irradiated DNA were repeatedly injected into the ears of WT mice. 24 hours after the last intracutaneous (i.c.) administration, ear thickness was determined as measure of inflammation. The injection of unmodified DNA induced only marginal ear swelling, whereas a significant increase in ear thickness was observed after injection of UV-DNA (**Figure 16**). *In vitro*, it was shown that UV-DNA is recognized by a TLR9-independent and cGAS/STING-dependent pathway (data not shown). Thus, the same ear swelling assay was also carried out in TLR9- or STING-deficient

mice (golden ticket mutation). TLR9-deficient mice displayed similar ear swelling reactions as WT mice (**Figure 16 A**), while STING-deficient mice showed a reduced ear swelling in response to injections of both unmodified and UV damaged DNA (**Figure 16 B**). These results showed that also *in vivo* STING dependent signaling mediated the enhanced recognition of UV-DNA. Additionally, the same ear swelling experiment was also carried out in TREX1-deficient mice. As expected, an equally potent ear swelling reaction to both unmodified and UV-DNA could be observed in TREX1-deficient mice (**Figure 16 C**), demonstrating that in the absence of TREX1 accumulating DNA induces a strong immune response.

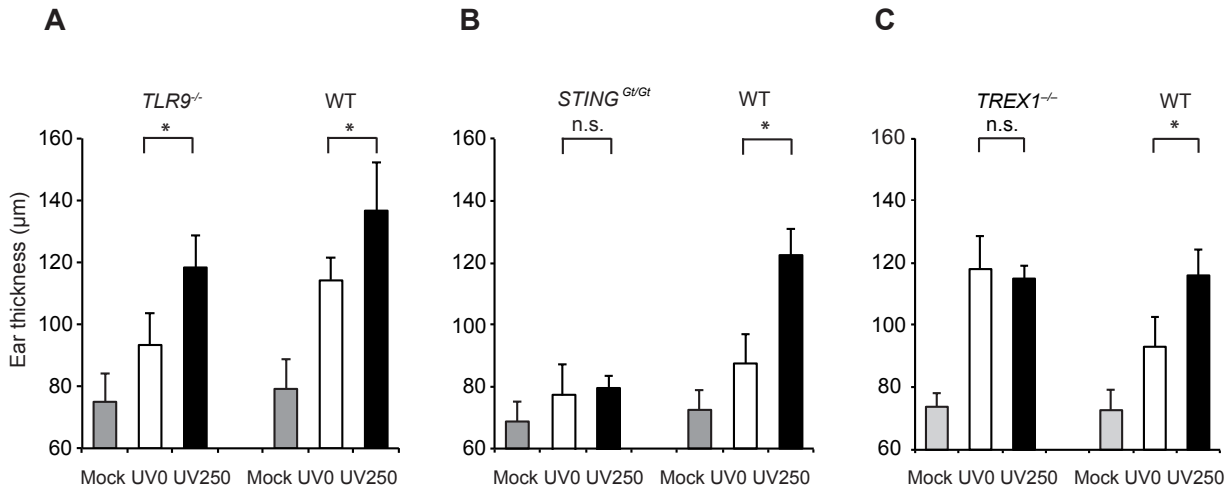

Figure 16: The ear swelling response to UV-DNA in WT, TLR9-, STING- and TREX1- deficient mice
10 µg untreated or UV irradiated DNA were administered i.c. to the earlobes of WT, TLR $9^{-/-}$, $STING^{(gt/gt)}$ and $TREX1^{-/-}$ mice every third day for a period of one week. 24 h after the last i.c. injection, ear thickness was determined using a caliper (each group n=4). Shown are means +SDM; * $P < 0.05$ (Student's t-test).

3.11. ROS Also Increase The Immune Response To Pathogenic DNA

After determining the mechanism behind the increased immune response to oxidatively modified DNA, we wished to address in which physiological situations this phenomenon might be important. ROS is not only produced after UV exposure, but can also be actively generated by cells to kill pathogens. Phagocytic cells such as macrophages create hydrogen peroxide in phagosomes, and neutrophils release both peroxide and hypochlorite to damage microbes in their direct vicinity. During a respiratory or oxidative burst, up to four nanomoles of oxygen are converted to ROS per 10^6 cells each minute (Segal and Coade, 1978). Professional phagocytes make use of an enzyme called NADPH oxidase, which catalyzes the reaction of oxygen and Nicotinamide adenine dinucleotide phosphate (NADPH) to hyperoxide anions (O_2^-). Hyperoxid anions are highly reactive and can be processed to a series of other ROS, such as hydrogen peroxide (H_2O_2) generated by the enzyme superoxide dismutase (SOD). H_2O_2 can easily penetrate cell membranes and can be transformed into highly reactive hydroxyl radicals (·OH), which attack a multiplicity of molecules, such as lipids, proteins or DNA. In addition, another enzyme called myeloperoxidase can further process H_2O_2 and chloride ions into hypochlorous

acid (HOCl), which is even more reactive with a wide variety of biomolecules (Albrich et al., 1981).

To study the impact of oxidative damage on immune sensing of microbial DNA, bacterial DNA isolated from *E. coli, and* viral DNA isolated from the dsDNA viruses HSV-1 and adenovirus were incubated with different micromolar concentrations of hydrogen peroxide (H_2O_2) or hypochlorous acid (HOCl). In addition, pathogen DNA was also UV-C irradiated with 100 mJ/cm^2. After precipitation to remove free ROS, pathogen DNAs were transfected into murine bmDCs. ROS exposure as well as UV irradiation further increased cytosolic DNA recognition of both bacterial and viral DNA (**Figure 17**). Thus, ROS might be used in two ways to fight microbes: on the one hand pathogens are directly damaged and eventually killed by the oxidation of their biomolecules, and on the other hand ROS can tag microbial DNA for detection by either the same phagocyte that produced ROS in the first place or by surrounding immune cells that come to fight the infection.

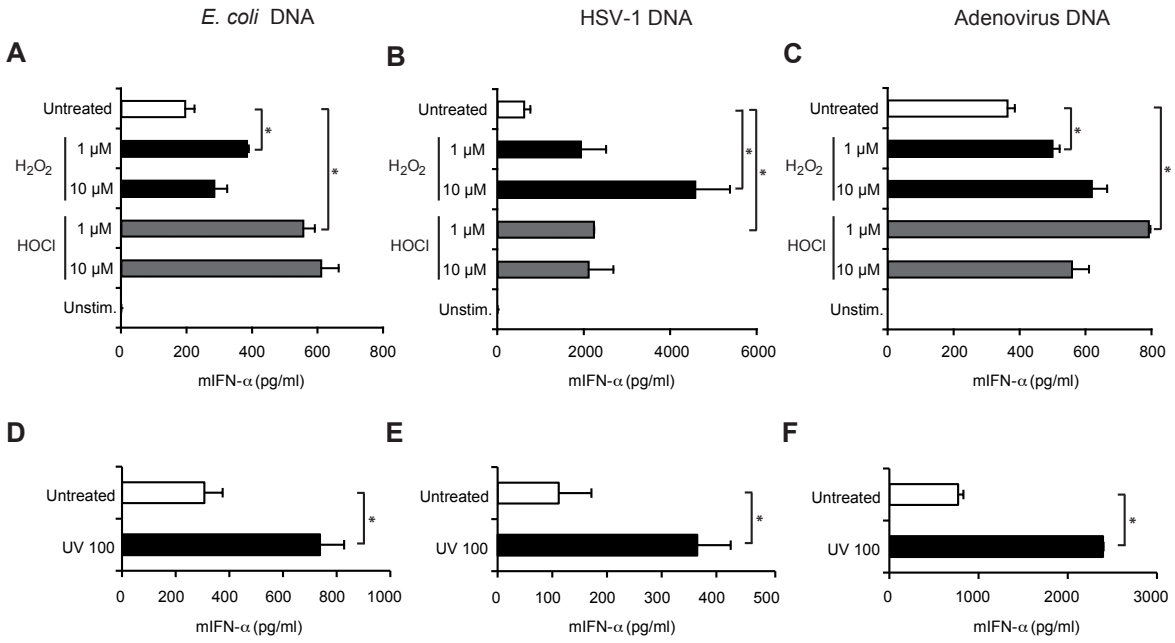

Figure 17: Oxidative damage of pathogenic DNA enhances cytosolic recognition by bmDCs

Bacterial genomic DNA from *E. coli* (A/ D), and viral genomic DNA from HSV-1 (B/ E) or adenovirus (C/ F) were oxidatively damaged with hydrogen peroxide (H_2O_2) or hypochlorite (HOCl), or alternatively UV-C irradiated with 100 mJ/cm^2. After precipitation to remove ROS, DNAs were transfected into murine bmDCs. IFN-α secretion of bmDCs was measured in the supernatants after 18-24 h. These data are representative of three independent experiments, shown are means +SDM; * $P < 0.05$ (Student's t-test).

3.12. Neutrophil Extracellular Trap - DNA Induces A Stronger Immune Response Than Genomic Neutrophil DNA

Recently, ROS were also found to play an important role in another mechanism to fight pathogens, namely the formation of neutrophil extracellular traps (NETs). NETs are composed of DNA, histones and many granular proteins, and are released to trap and kill invading pathogens at the site of infection (Brinkman et al., 2004). Since this defense mechanism was shown to be

dependent on ROS (Fuchs et al., 2007), it was of interest whether NET-DNA might also cause an increased type I IFN response in comparison to genomic DNA isolated from neutrophils. Experimentally, the release of NETs can be triggered by the addition of phorbol 12-myristate 13-acetate (PMA) to primary neutrophils or neutrophil-like cell lines. To investigate the kinetics of NET-DNA release, human neutrophils were treated with PMA for one, two or three hours. Subsequently, SytoxGreen, a nucleic acid stain that cannot penetrate the cell membranes of living cells, was added to allow the analysis of NET-DNA release. After the addition of PMA, neutrophils became adherent within 30 minutes, but for the majority of the cells it took more than one hour before the cell membrane ruptured and DNA was expelled in the form of NETs. As shown in **Figure 18 A**, there was a time dependent increase of extracellular NET-DNA visible, and after three hours nearly all neutrophils had released their DNA in form of NETs. These results were also confirmed with NET-DNA isolated from murine neutrophils (data not shown). However, murine neutrophils generated NETs more slowly and less efficiently. This difference could be attributable to differences in maturity of the cells being used, since murine neutrophils were isolated from bone marrow, while the source for human neutrophils was peripheral blood.

Remijsen and co-workers have recently shown that NET formation needs superoxide generation, and that inhibition of NADPH oxidase activity prevents the release of NETs and instead leads to neutrophil cell death by apoptosis (Remijsen et al., 2011). To investigate whether the released NET-DNA harbors oxidative modifications and thus constitutes a potential immune trigger, human neutrophil DNA isolated following stimulation with PMA (hNETs) was compared to neutrophil DNA without prior PMA stimulation. As shown in **Figure 18 B,** the more cells which had undergone NETosis, the higher the amounts of type I IFN which was induced following stimulation with neutrophil DNA in bmDCs.

ROS are highly reactive with DNA, and oxidation of guanine to 8-hydroxy-2-deoxy guanine (8-OHG) is considered a hallmark of oxidative DNA damage (Wiseman and Halliwell, 1996). Thus, the amount of 8-OHG in neutrophil genomic DNA and NET-DNA was analyzed. The 8-OHG content increased with duration of NETosis (**Figure 18 C**) and correlated with the induction of increased type I IFN levels in myeloid cells after DNA stimulation. These results indicate that NETs may have a dual function: they may not only bind and kill pathogens but also render self-DNA more immune stimulatory and induce an enhanced type I IFN response.

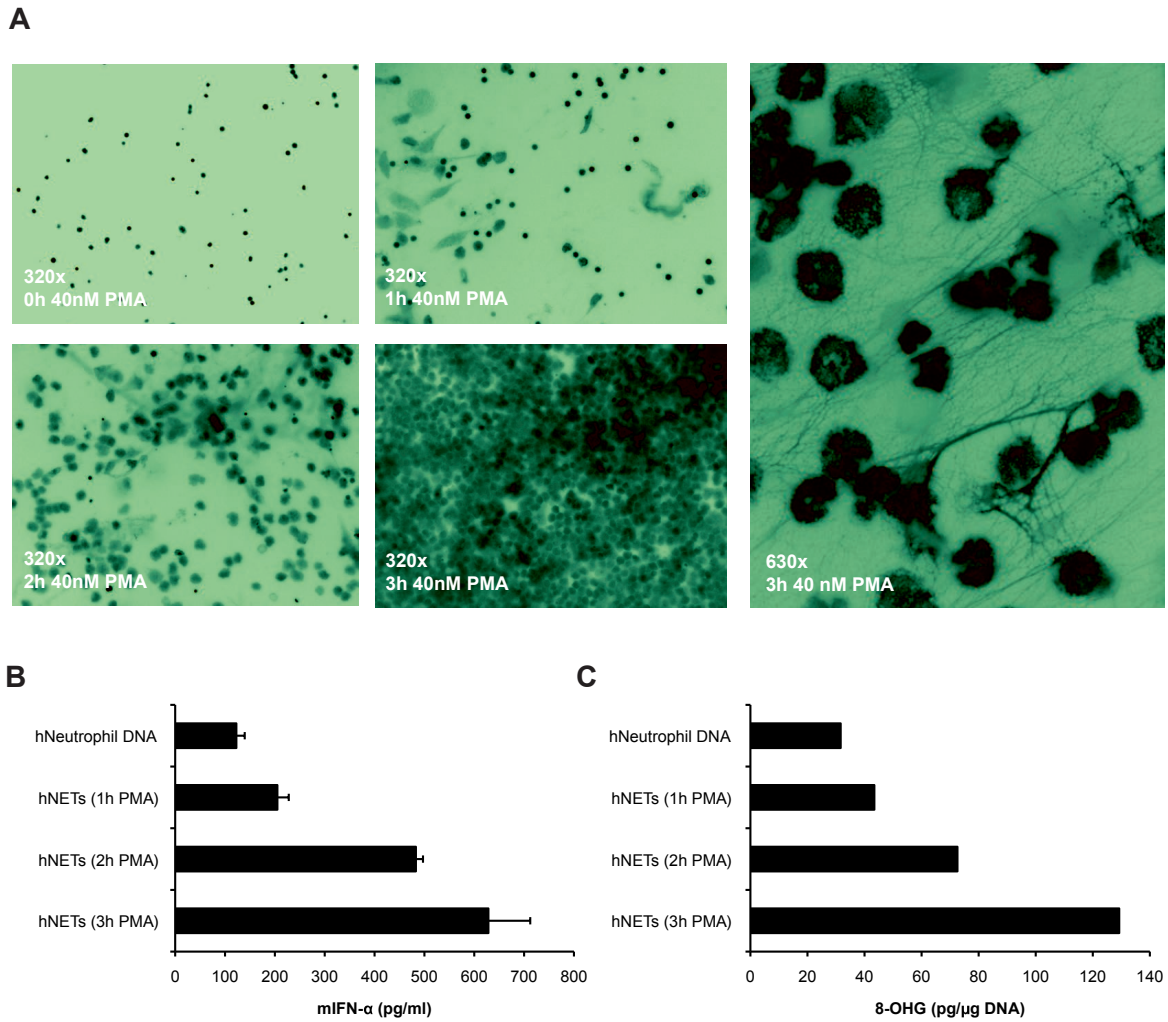

Figure 18: ROS damage enhances cytosolic recognition of self-DNA in the form of neutrophil extracellular traps

Human neutrophils were purified from whole blood and exposed to 40 nM PMA for 1 2 or 3 h (hNETs). Neutrophils without PMA treatment were used as control (hNeutrophil DNA). 5 x 10^6 neutrophils were plated on cover slips in 24-wells and imaged using a fluorescent microscope. Extracellular DNA was stained with SytoxGreen (A). Isolated genomic DNA from neutrophils and NET-DNA was transfected using *Trans*IT-LT1 Transfection Reagent (Mirus) into murine bmDCs. After 18-24 h, secretion of mIFN-α was quantified via ELISA. The data shown are representative of three independent experiments. Shown are means +SDM. (B). The relative content of 8-OHG in human neutrophil and NET-DNA was determined with an 8-OHG ELISA. The data shown are representative of two independent experiments (C).

3.13. High Amounts Of Oxidized DNA Alone Are Sufficient To Trigger A Type I IFN Response In Human Monocytes

Neutrophils can release large amounts of NETs at the site of infection, but it is not clear whether the presence of oxidized DNA alone can induce an immune response without some sort of "uptake facilitator" either physiological or artificial to bring DNA into the cells. To this end, human monocytes were incubated with high doses of protein-free self-DNA isolated from cells previously treated with either hydrogen peroxide or hypochlorite. As shown in the upper panel of **Figure 19**, only oxidatively damaged DNA was able to induce a type I IFN response without an

additional uptake agent, while unaltered DNA did not lead to detectable IFN levels. These results indicated that DNA uptake facilitators are not mandatory if the oxidized DNA is present at very high local amounts.

However, it is unlikely that high levels of protein-free extracellular DNA exist *in vivo*. NETs for example consist not only of DNA, but do also contain histones and granular proteins, including antimicrobial peptides (Brinkmann et al., 2004). The antimicrobial peptide LL37, which is present in NETs, is able to transfer extracellular plasmid DNA to the nucleus of mammalian cells (Sandgren et al., 2004). Furthermore, it can transport extracellular DNA into endosomal compartments of pDCs, and thus leads to an activation of TLR9 and the production of type I IFNs (Lande et al., 2007). Recently, it was also demonstrated that LL37 promotes cytosolic delivery of nucleic acids in non-pDCs such as monocytes (Chamilos et al., 2012). Thus, it was speculated about LL37 being able to further enhance the response to naked oxidized DNA. To test this hypothesis, high doses of untreated or oxidized DNA were incubated with LL37 and then added to human monocytes. As depicted in the lower panel of **Figure 19**, the immune response to oxidized DNA was increased when the DNA was complexed with LL37 prior to monocyte stimulation. Thus, oxidized self-DNA is sufficient to trigger the cytosolic DNA sensing pathway at high local concentrations, but in combination with natural cationic peptides such as LL37 lower DNA concentrations are sufficient to induce a potent immune response.

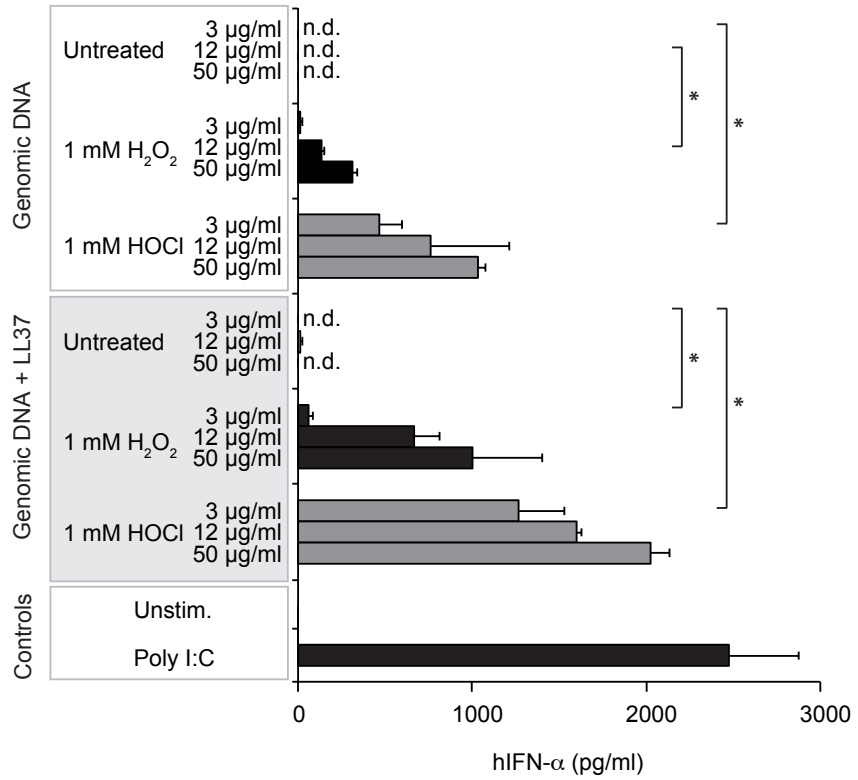

Figure 19: The antimicrobial peptide LL37 further enhances the immune response to oxidized DNA

Protein-free genomic DNA isolated from hydrogen peroxide- or hypochlorite-treated RMA cells alone, or complexed with LL37, was added to human monocytes. 18-24 h later, secretion of hIFN-α was quantified in the culture supernatants via ELISA. The data shown are representative of three independent experiments and given as means +SDM; * $P < 0.05$ (Student's t-test).

3.14. NETing Neutrophils Induce A Type I IFN Response In Co-cultures With Myeloid Cells

Since both the presence of high local amounts of oxidized DNA complexed with LL37 and the transfection of NET-DNA led to an enhanced type I IFN response, it was of interest to investigate whether NETing neutrophils can also induce IFN-α secretion in co-cultures with myeloid cells. Murine neutrophils were co-cultured with FLt3L DCs, bmDCs and a macrophage cell line derived from mice with 129 background respectively, and NETosis was induced with 40 nM PMA. After 18 hours, the supernatants were analyzed for the presence of mIFN-α. As depicted in **Figure 20**, higher levels of IFN were measured when myeloid cells were co-cultured with neutrophils in the presence of PMA, further supporting that NET-DNA can boost the type I IFN response.

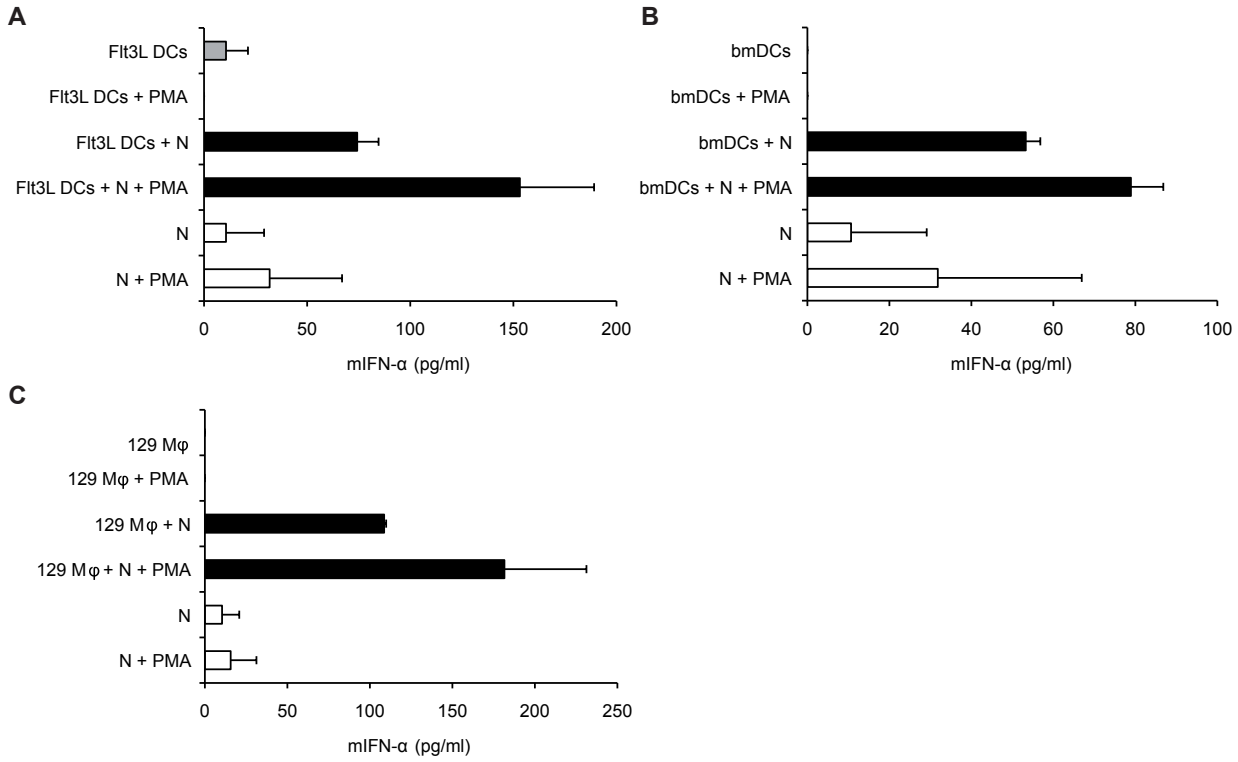

Figure 20: NETing neutrophils induce higher IFN-α levels in co-cultures with DCs or macrophages

1 x 10^5 Flt3L DCs, bmDCs or 129 Macrophages (129 Mϕ) were co-cultured with 1 x 10^5 murine neutrophils (N). NETosis was induced with 40 nM PMA for 3 h. 18 h later, secretion of mIFN-α was quantified in the culture supernatants via ELISA. Shown are means +SDM.

3.15. Effects Of DNA Modifications By Chemotherapeutic Agents

DNA cannot only be damaged by ROS but also by many other mutagens such as x-rays, toxins or chemicals. To test whether also other DNA modifications lead to an increased immunostimulatory capacity of DNA, RMA cells were incubated in the presence of five different chemotherapeutic agents that are known to interact with DNA: Cisplatin, Melphalan, Dactinomycin, Idarubicin and Etoposide.

Cisplatin (*cis*-$PtCl_2(NH_3)_2$) belongs to the class of platinum-containing anti-cancer drugs and causes crosslinking of DNA. Following administration, one of the chloride atoms is displaced by water, allowing the platinum atom to bind to DNA bases, preferentially to guanine. Crosslinking

then occurs via the removal of the other chloride by another DNA base and can result in either intra-strand adducts or inter-strand crosslinks (Johnson et al., 1989). Melphalan belongs to the class of nitrogen mustard alkylating agents and adds an alkyl group (C_nH_{2n+1}) to the DNA bases. It causes the linkage between DNA strands and thus blocks DNA replication and RNA synthesis in a manner similar to Cisplatin (Kohn, 1981). Dactinomycin, also known as actinomycin-D, is an antibiotic isolated from *Streptomyces* bacteria. It binds to DNA at the transcription initiation complex and thus interferes with RNA elongation (Golderg et al, 1962; Sentenac et al. 1968). Idarubicin or 4-demethoxydaunorubicin belongs to the group of anthracyclines. Like Doxorubicin and other anthracyclines, it intercalates between DNA base pairs and prevents replication. Moreover, it interferes with the enzyme topoisomerase II so that the DNA cannot be uncoiled for transcription. The inhibition of the topoisomerase II complex might also lead to DNA-cleavage and prevention of its repair (Jensen et al., 1993). Furthermore, it was shown that Idarubicin damages DNA through a mechanism that involves its redox cycling with P450 reductase to ROS (Celik and Arinç, 2008). Etoposide is a member of the topoisomerase inhibitor drug class, which does not intercalate with DNA. It forms a ternary complex with DNA and topoisomerase II, and thus, prevents re-ligation of the DNA strands, leading to DNA strand breaks (Pommier et al., 2010).

To investigate the influence of these chemotherapeutic agents on the stimulatory capacity of DNA, RMA cells were incubated with these substances for 24 hours. Subsequently, genomic DNA was isolated for stimulation of murine bmDCs. As shown in **Figure 21**, DNA isolated from cells that were treated with the crosslinking agents Cisplatin or Melphalan, as well as with the intercalating agents Dactinomycin and Idarubicin, induced higher IFN-α levels compared to DNA isolated from untreated cells. The DNA strand-breaking agent Etoposide did however not lead to an enhanced immune recognition of the DNA, which was expected since it has been previously shown that moderate DNA strand fragmentation does not dramatically change the immunogenicity of genomic DNA (**Figure 9**). To investigate whether a direct treatment of DNA with the described chemotherapeutic agents also has a comparable effect, genomic DNA isolated from untreated RMA cells was incubated with Cisplatin, Melphalan, Dactinomycin, Idarubicin or Etoposide for four hours at 37°C. Subsequently, the DNA was precipitated and then used to stimulate murine bmDCs. With the exception of Etoposide, cell-free treated DNA did also induced higher IFN-α levels (**Figure 22)**. These results suggested that next to oxidative damage also other DNA modifications such as alkylation or intercalation could enhance the immunostimulatory capacity of DNA.

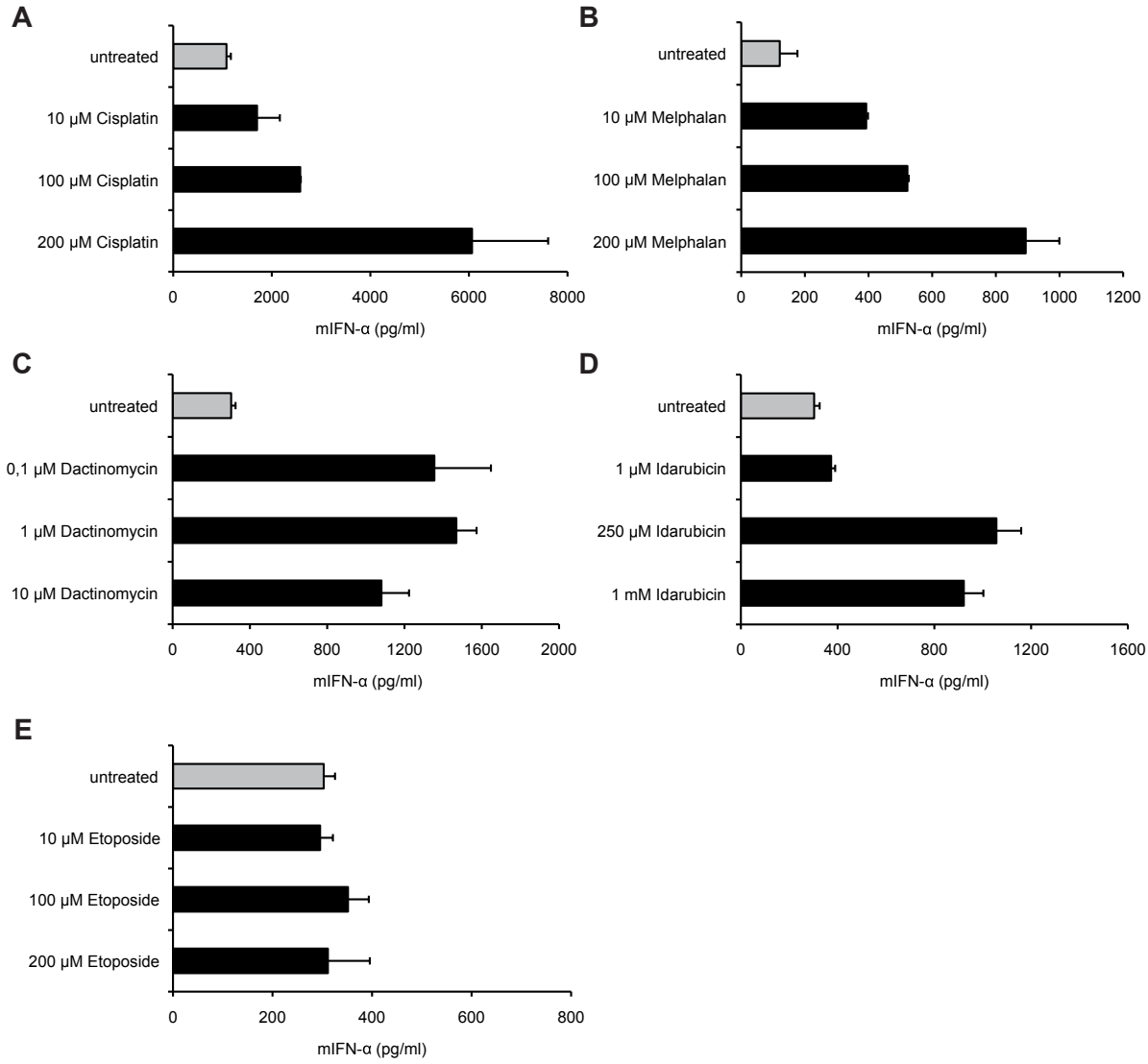

Figure 21: Treatment of RMA cells with alkylating or intercalating chemotherapeutic agents increases the immunostimulatory capacity of their DNA

RMA cells were incubated with the alkylating agents Cisplatin (A) and Melphalan (B), or with the intercalating agents Dactinomycin (C) and Idarubicin (D), or with the DNA strand break-inducing Etoposide (E) for 4 h at 37°C. Subsequently, genomic DNA was isolated and used for stimulation of murine bmDCs. 18-24 h later, IFN-α was measured in the supernatant via ELISA. The data shown are representative of three independent experiments and given as means +SDM.

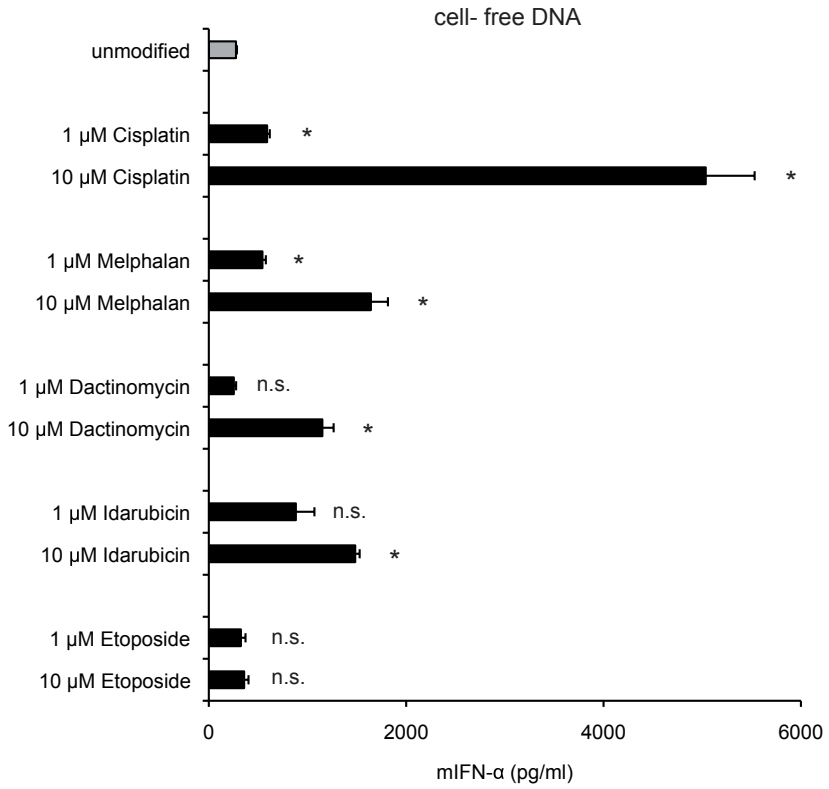

Figure 22: Cell-free treatment of DNA with alkylating or intercalating chemotherapeutic agents does also increase its immunogenicity

Genomic DNA was isolated from untreated RMA cells and then incubated with Cisplatin, Melphalan, Dactinomycin, Idarubicin, or Etoposide for 4 h at 37°C. Subsequently, DNA was purified and then used for stimulation of murine bmDCs. After 18-24 h, IFN-α was measured in the supernatant via ELISA. These data are representative of two independent experiment, shown are means +SDM; * $P < 0.05$ (Student's t-test).

3.16. Oxidized DNA Can Induce Lupus-like Skin Lesions

Lupus erythematosus (LE) is an autoimmune disease, which is characterized by anti-DNA autoantibodies and a type I IFN signature. In addition, mutations in the TREX1 gene are associated with LE and correlate with disease severity (Lee-Kirsch et al., 2007). However, impaired activity of TREX1 is only found in 3 % of LE patients. Interestingly, symptoms of UV-phototoxicity after exposure to sunlight can be frequently observed in LE patients with functional TREX1, and it has been postulated that extracellular DNA accumulates in cutaneous LE lesions due to defects in phagocytic or enzymatic DNA clearance (Kuechle and Elkon, 2007).

To investigate the immune mechanism triggering the formation of lesions in UV light exposed skin regions of LE patients, 10 µg of unmodified or UV-damaged DNA were repeatedly injected in the ears of lupus prone MRL/lpr mice over three weeks. Injection of UV-DNA led to local skin lesions (**Figure 23 A**) and massive ear swelling (**Figure 23 B**), while the response to unmodified DNA was comparatively weak. Furthermore, typical histological features of skin lesions in human LE such as lymphocyte infiltrate, hydropic degeneration of the basal epidermal layer and colloid bodies, were observed in the ears of MRL/lpr mice that were treated with UV irradiated DNA (data not shown). Importantly, this phenotype could only be observed in MRL/lpr mice that were

at least 18 weeks old and had already developed lupus-like symptoms. These results indicate that the recognition of UV damaged DNA might play an important role in the development of lupus lesions in sun-exposed skin areas.

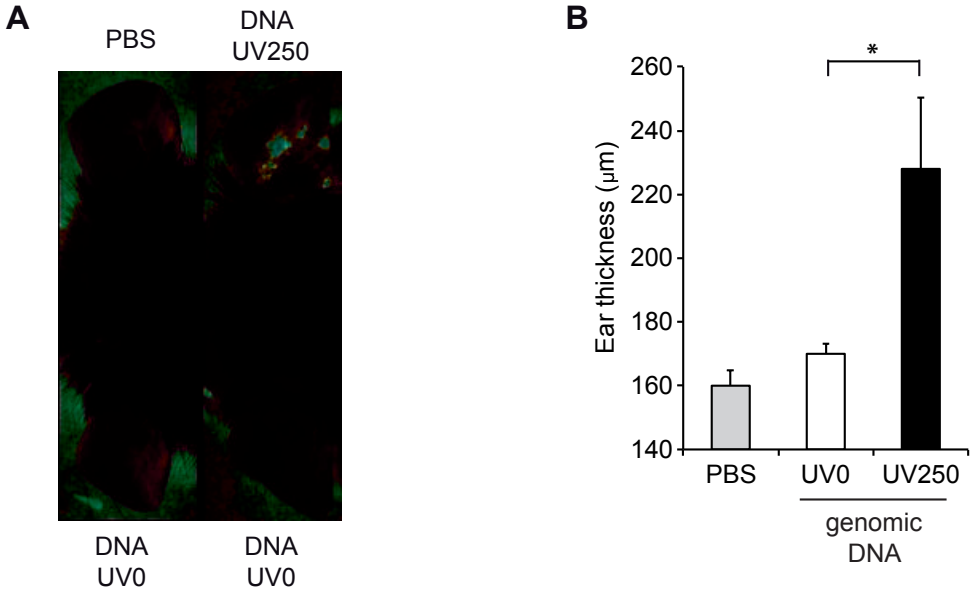

Figure 23: Ear injection of UV irradiated DNA induces lupus-like skin lesions in MRL/lpr mice

10 µg untreated or UV irradiated DNA were administered i.c. to the earlobes of MRL/lpr mice every third day. After 21 days, mice were monitored for lupus-like skin lesions (A). 24 h after the last DNA injection ear thickness was determined using a caliper. Shown are means +SDM; * $P < 0.05$ (Student's t-test). (B).

3.17. Oxidized DNA Plays A Role In The Pathogenesis Of Lupus Erythematosus

Lupus patients are often positive for a variety of serum autoantibodies, including antinuclear and anti-dsDNA autoantibodies that have been shown to promote the uptake of self nucleic acids (Boulé et al., 2004; Vallin et al., 1999). To analyze the role of oxidatively damaged DNA in the systemic form of lupus, uncomplexed unmodified or UV-DNA was administered i.v. to either WT (C57BL/6) or lupus-prone MRL/lpr mice and blood was analyzed for the presence of serum IFN-α. WT mice did not respond to any form of uncomplexed DNA (**Figure 24 A**). However, they did produce low levels of type I IFN in response to oxidized DNA that was complexed with the transfection reagent Dotap prior to i.v. administration, while no serum IFN-α was measured after the injection of Dotap-complexed unmodified DNA (data not shown). By contrast, MRL/lpr mice reacted with low levels of serum type I IFN to the injection of naked unmodified DNA, and showed a significant induction of IFN-α in response to naked UV-DNA (**Figure 24 B**). These results suggest that extracellular DNA is indeed a trigger for elevated pro-inflammatory immune responses in a lupus-prone environment and that oxidative DNA damage further exacerbates this process.

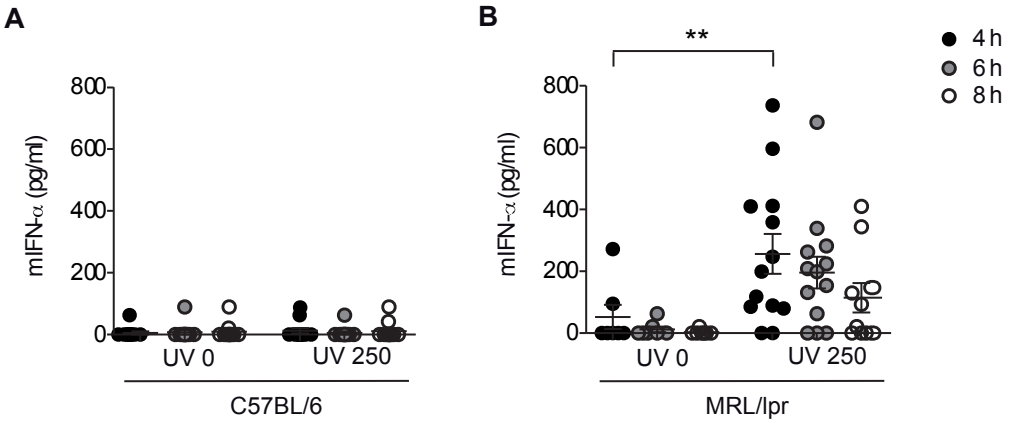

Figure 24: The lupus prone MRL/lpr mouse responds to naked oxidized DNA

200 µg of naked uncomplexed genomic DNA, that was either left untreated or UV irradiated, was i.v. administered to C57BL/6J (A) and MRL/lpr (B) mice. After 4, 6 and 8 h serum IFN-α was quantified via ELISA. Shown are means +SDM; ** $P < 0.01$ (Student's t-test).

3.18. CD11b$^+$ CD11c$^-$ Cells Constitute The Largest Fraction Of IFN-producing Cells Demonstrating DNA Uptake

To identify cell types that might be responsible for the type I IFN production in response to oxidized DNA *in vivo*, UV-DNA was stained with SytoxGreen and then administered i.v. to MRL/lpr and C57BL/6 mice. After one hour, splenocytes were harvested for analysis since one of the spleen's functions is to collect antigens from blood. Alternatively, one could have taken lymph nodes for investigation; however, cell isolation would probably have not been so lucrative. After cell separation with Collagenase D and DNase I, splenocytes were visualized in a SytoxGreen (FITC) vs. PE dot plot (**Figure 25 A**). Roughly 1 % of the analyzed splenocytes were SytoxGreen-positive in both C57BL/6 and MRL/lpr mice (**Figure 25 B**).

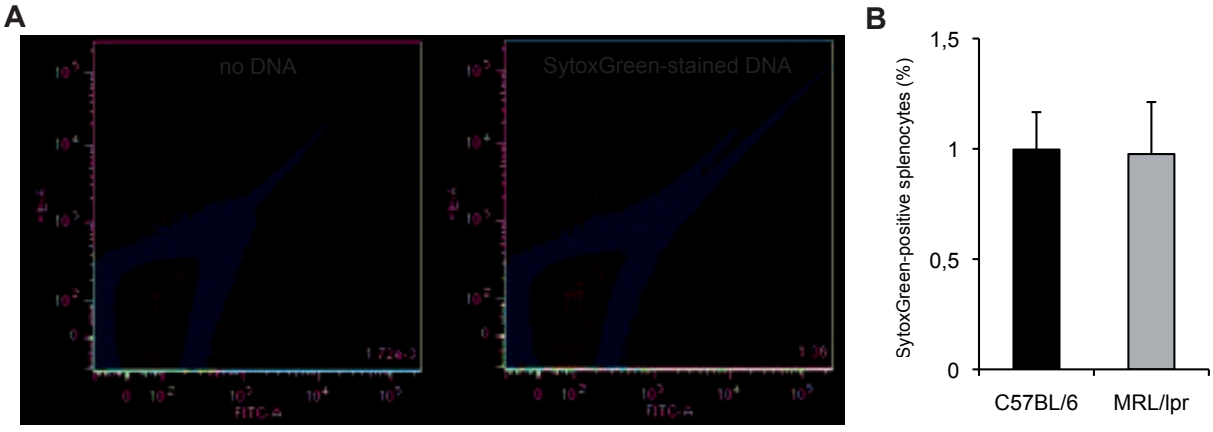

Figure 25: Uptake of SytoxGreen-stained oxidized DNA in WT and MRL/lpr splenocytes

200 µg SytoxGreen-labeled UV-DNA was administered i.v. to C57BL/6 and MRL/lpr mice. After 1 h, splenocytes were analyzed by FACS. SytoxGreen-positive cells were defined in a SytoxGreen (FITC) vs. PE plot to exclude autofluorescence. The gate was drawn with regard to an untreated mouse (A). Quantification of SytoxGreen-positive splenocytes in C57BL/6 (n = 5) and MRL/lpr mice (n=6). These data are representative of five independent experiments; shown are means +SDM (B).

Type I IFNs can be produced by almost any cell type in the body (Trinchieri, 2010). However, phagocytic cells such as DCs and monocytes/macrophages are probably the most interesting cells being able to produce type I IFN in response to foreign DNA. DCs and monocytes/macrophages are known to express moderate to high levels of CD11b and/or CD11c (**Figure 26**). Therefore, further analysis of DNA uptaking cells was focused on splenocytes that expressed either one or both of these markers.

SytoxGreen-positive splenocytes that expressed CD11c but no CD11b were found to a similar extent in both C57BL/6 and MRL/lpr mice. However, the combination of CD11b and CD11c was expressed on 8 % of the MRL/lpr SytoxGreen-positive splenocytes, but only on 2 % of the C57BL/6 SytoxGreen-positive splenocytes. The discrepancy was even larger for CD11b-positive cells that did not express CD11c, as these cells made up 8 % of the SytoxGreen-positive splenocytes in C57BL/6 mice, but 41 % in MRL/lpr mice (**Figure 27 A)**. Interestingly, there was no significant difference in the total number of CD11b-positive splenocytes in C57BL/6 and MRL/lpr mice (**Figure 27 B)**.

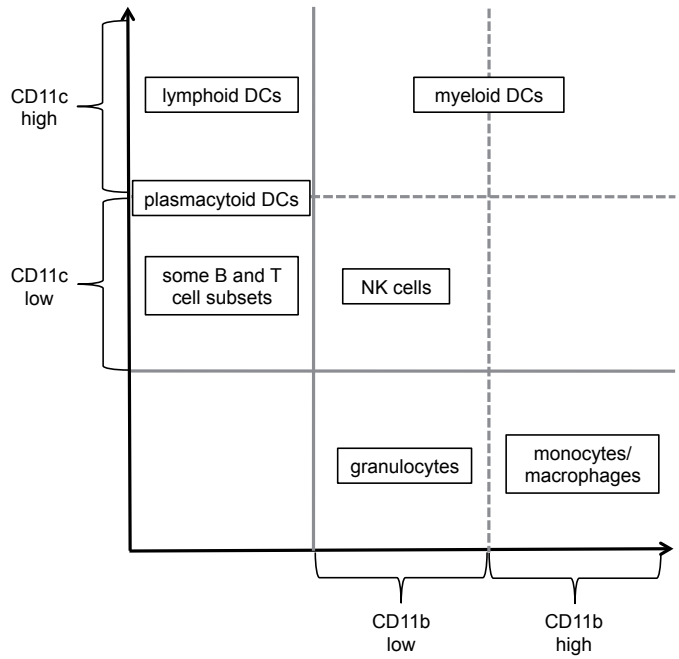

Figure 26: CD11b and/ or CD11c expression on murine cell types

In mice, CD11b is highly expressed on monocytes/macrophages and to a lower extent on granulocytes, NK cells, and myeloid DCs. Murine CD11c is highly expressed on conventional DCs (lymphoid and myeloid), at moderate levels on plasmacytoid DCs and weakly expressed on NK cells and some B and T cell subsets. This figure was drawn according to information provided by Miltenyi Biotec.

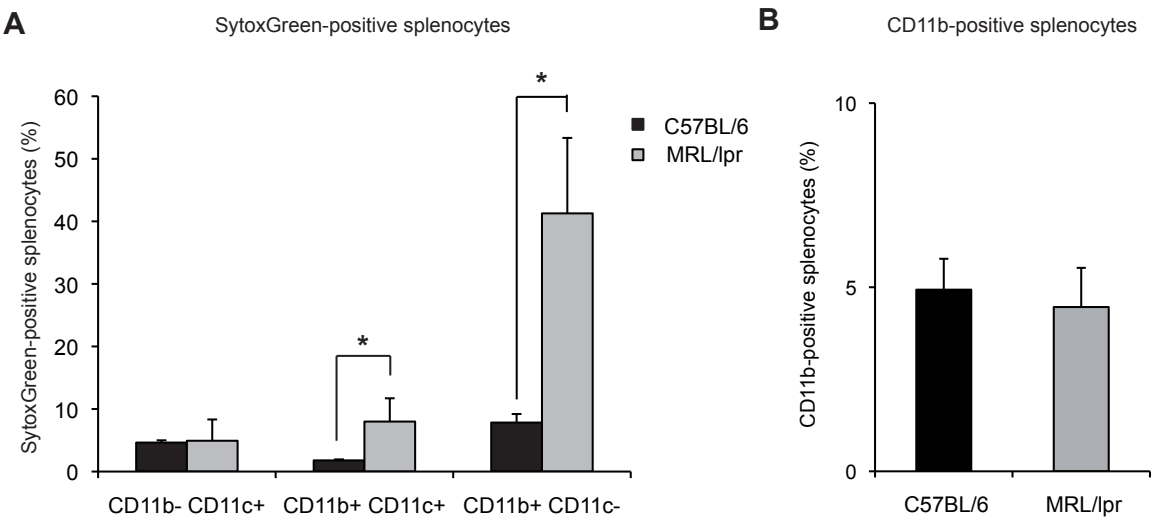

Figure 27: UV-DNA uptake by CD11b- and/or CD11c- positive splenocytes

200 µg SytoxGreen-labeled UV irradiated DNA was administered i.v. to C57BL/6 and MRL/lpr mice. After 1 h, SytoxGreen-positive splenocytes were analyzed for the expression of CD11b and/or CD11c (A). Total splenocytes were analyzed for the expression of CD11b (B). These data are representative of five independent experiments, shown are means +SDM; * $P < 0.05$ (Student's t-test).

To better characterize the CD11b and/or CD11c positive cells, the proportion of CD8-DCs, plasmacytoid DCs (pDCs), CD4-DCs, conventional DCs (cDCs), F4/80-monocytes/macrophages and CD11bLy6C-positive cells were analyzed (**Table 3**). CD8-DCs made up a larger portion of the SytoxGreen-positive cells in C57BL/6 mice, while CD4-DCs and pDCs represented only a very small percentage of the SytoxGreen-positive cells in both mice strains. Conventional DCs as well as F4/80-positive monocytes/macrophages made up larger portions of the SytoxGreen-positive cells in MRL/lpr mice compared to C57BL/6. Interestingly, the combination of CD11b and Ly6C, which is mostly expressed by monocytes/macrophages, was found on 6 % of the SytoxGreen-positive cells in C57BL/6 mice, but on 26 % in MRL/lpr mice. Taken together, these results suggest that in particular $CD11b^{+}Ly6C^{+}$ cells take up large amounts of injected UV-DNA in MRL/lpr mice.

Cell population	Cell surface markers	Reference for cell surface markers	SytoxGreen-positive splenocytes (%) C57BL/6 vs. MRL/lpr
CD8-DCs	CD11b- CD11c+ CD8+	Vremec et al., 2000	2,6 vs. 0,6
CD4-DCs	CD11b+ CD11c+ CD4+	Vremec et al., 2000	0,8 vs. 0,6
pDCs	CD11b- CD11c int B220+	Asselin-Paturel et al., 2001	1,6 vs. 1,3
cDCs	CD11b+ CD11c+ CD4- CD8-	Vremec and Shortman, 1997	0,6 vs. 6,2
F4/80-monocytes/ macrophages	CD11b+ CD11c- F4/80 +	Austyn and Gordon, 1981	2,5 vs. 3,4
monocytes/macrophages and granulocytes	CD11b+ Ly6C+	Geismann et al., 2003	6,0 vs. 26,1

Table 3: Percentages of SytoxGreen-positive cells

3.19. CD11b^{+}Ly6C^{low}F4/80^{+} Cells Contribute To The Type I IFN Response To Oxidized DNA *In Vivo*

To identify cells that produce type I IFN in response to UV-DNA *in vivo*, UV irradiated DNA was administered i.v. to three MRL/lpr mice, while two MRL/lpr mice were left untreated as negative control. Four hours after DNA injection, splenocytes were collected to analyze the levels of IFN-α mRNA. Commonly, pDCs are known as professional IFN producing cells, which are able to release large amount of type I IFN in a very short period of time (Siegal et al., 1999; Cella et al., 1999). However, over the years it was demonstrated that pDCs seem not necessarily required for the response to certain viruses (Delale et al., 2005; Geburts vanKessell et al, 2008; Jewell et al., 2007). Furthermore, pDC depletion experiments suggest that also other cell types produce IFN-α in SLE (Blanco et al., 2001). Thus, the focus of the IFN-α mRNA analysis was set on those cells that were shown to take up large amounts of UV-DNA: cDCs and monocytes/ macrophages.

Splenocytes were separated by FACS sorting into four fractions. One sorting fraction contained cDCs (CD11c^{high}, visualized in yellow), and CD11b-positive cells were further separated into i) Ly6C^{low}F4/80^{+} (visualized in turquoise), ii) Ly6C^{high}F4/80^{+} (visualized in red) and iii) Ly6C^{low}F4/80^{-} (visualized in light yellow) subpopulations (**Figure 28 A**). RNA was isolated from the separated cells and reverse transcribed into cDNA. Subsequently, IFN-α4 mRNA levels were measured by RT-PCR, normalized to ß-actin expression and compared to MRL/lpr mice that got no DNA injected. RT-PCR analysis revealed that IFN-α4 mRNA was highest upregulated in the CD11b^{+}CD11c^{-}Ly6C^{low}F4/80^{+} cell population (**Figure 28 B**). The combination of CD11b, Ly6C and F4/80 can be expressed by both monocytes and macrophages. Thus, these markers alone are not sufficient to discriminate between these two cells types. However, their appearance in the FCS vs. SSC plot pointed to macrophages rather than monocytes (large granular cells, visualized in turquoise). Thus, these sorting experiments with subsequent RT-PCR analysis revealed that in the lupus-prone MRL/lpr mice Ly6C^{low}F4/80-positive macrophages largely contribute to the type I IFN response to UV-DNA injection.

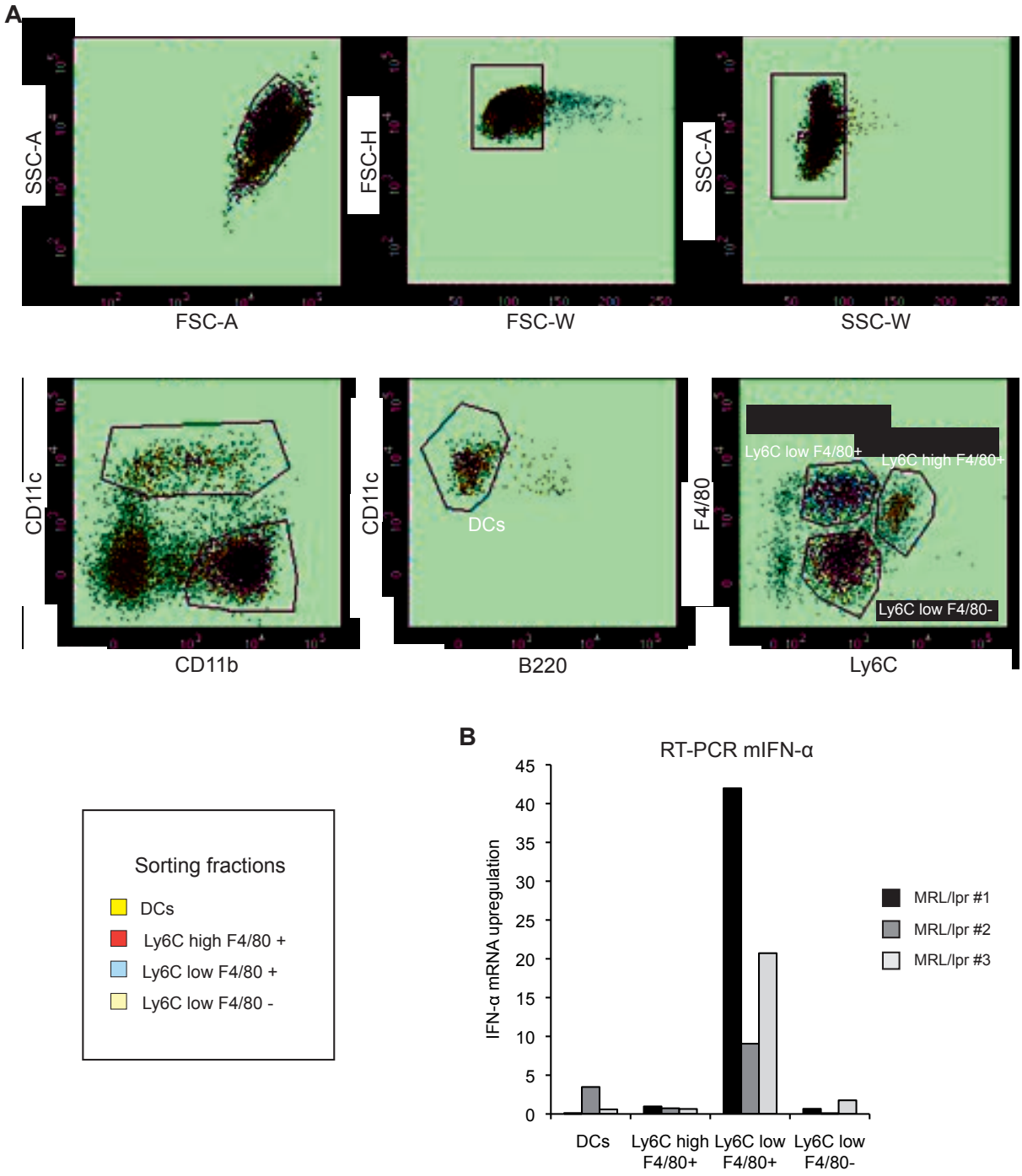

Figure 28: In MRL/lpr mice, Ly6C^{low} F4/80-positive splenocytes mostly upregulate mIFN-α in response to i.v. administration of naked UV-DNA

250 µg UV irradiated genomic DNA was administered i.v. to MRL/lpr mice. After 4 h, splenocytes were harvested and separated into four cell populations: A DC fraction containing no pDCs (i), CD11b^{+} CD11c^{-} Ly6C ^{low} F4/80^{+} cells (ii), CD11b^{+} CD11c^{-} Ly6C ^{low} F4/80^{-} cells (iii) and CD11b^{+} CD11c^{-} Ly6C ^{high} F4/80^{+} cells (iv) (A). Upregulation of mIFN-α4 mRNA was analyzed by RT-PCR, normalized to ß-actin and compared to untreated MRL/lpr mice (B).

4. Discussion

4.1. UV Irradiation Causes ROS-dependent DNA Damage That Leads To Enhanced Immunogenicity

UV radiation is present in sunlight and has many both beneficial and deleterious effects on organisms. Its energetic potential induces chemical reactions such as the conversion of 7-dehydrocholesterol to vitamin D_3. Nonetheless, uncontrolled UV exposure can also damage the integrity of the skin both macroscopically and through the impairment of intracellular biomolecules such as nucleic acids (NAs) and proteins (Maverakis et al., 2010).

Previous experiments in the Barchet laboratory revealed that stimulation of myeloid cells with NAs isolated from UV irradiated cells resulted in an increased immune response when compared to stimulation with NAs from untreated cells. Although initial results indicated that the phenomenon applied to transfections with both DNA and RNA, in the current work, careful analysis revealed that RNA samples still contained traces of DNA, and that the observed phenomenon applied only to DNA but not to RNA.

Before the discovery of intracellular DNA receptors, metazoan DNA was considered immunogenically inert due to a low frequency of non-methylated CpG motifs. These motifs are required to activate endosomal TLR9 and are frequent in viral or bacterial but not metazoan DNA (Wagner, 1999; Bird, 2002; Krieg, 2002). However many subsequent publications have described that vertebrate DNA also can become immunogenic when introduced into the cytoplasm. In 1999, double-stranded (ds) DNA was shown to increase the expression of genes necessary for antigen processing and presentation (Suzuki et al., 1999). Later, the same group reported that high amounts of genomic DNA released from dying cells are sufficient to induce antigen presenting cell (APC) maturation (Ishii et al., 2001). Moreover, it was described that mammalian DNA in complex with cytofection agents stimulated DCs to secrete substantial amounts of type I IFN, TNF-α and IL12p70 (Martin and Elkon, 2006; Boulé et al., 2004), which were induced by the TBK1 kinase-mediated activation of the transcription factor IRF3 (Ishii et al., 2005; Stetson and Medzhitov, 2006).

These publications described a TLR9-independent activation of the immune system by self-DNA and initiated the quest for the cytosolic DNA receptor. In 2008, stimulator of interferon genes (STING)/mediator of IRF3 activation (MITA) was identified to be critical to the cytosolic DNA signaling pathway, since ablation of STING/MITA inhibited non-CpG DNA triggered expression of type I IFNs (Ishikawa and Barber, 2008; Zhong et al., 2008; Ishikawa et al., 2009), although it was unclear if this molecule was acting concomitantly with or downstream to the cytosolic DNA receptor. However, the receptor acting upstream of STING was also later identified: cyclic-GMP-AMP (cGAMP) synthase (cGAS). In response to DNA binding, cGAS synthesizes the second messenger cGAMP, which then activates the STING pathway (Sun et al., 2013; Wu et al., 2013; Gao et al., 2013).

In our experiments, silencing of cGAS or its signal transducing adaptor protein STING/ MITA resulted in a complete abrogation of the UV-DNA response (data not shown). Likewise, the concept that the internalization of self-DNA is important for cell activation is in line with our data, since a type I IFN response could only be measured if genomic DNA from untreated cells was complexed with transfection reagents. However, high concentrations of naked UV-DNA were adequate to induce an immune response in myeloid cells, suggesting that the traces of DNA that are taken in without transfection reagent are sufficient to activate cGAS when the DNA was UV irradiated beforehand.

Since UV irradiation can cause indirect DNA damage through the generation of intracellular reactive oxygen species (ROS) (Halliwell and Aruoma, 1991; Davis, 1987; Wise and Naylor, 1987; McKersie and Leshem, 1994; Imlay and Linn, 1998), it was tested whether cells produce ROS after exposure to UV-A, UV-B, or UV-C light. An UV-dose dependent increase in ROS was observed regardless of the type of UV light used, and it was in fact the ROS levels rather than the UV source that correlated with the enhanced immunogenicity of DNA from UV irradiated cells. This correlation strongly suggested that ROS-mediated DNA modifications were the reason for an enhanced immune recognition of UV irradiated DNA. In keeping with these results, elevated levels of 8-hydroxy-2'-desoxy-guanosine (8-OHG), a hallmark of oxidative DNA damage (Kasai et al., 1984; Floyd et al., 1988; Kasai, 1997), were found in UV-DNA, and the incorporation of 8-OHG was sufficient to increase the immunogenicity of a PCR product. Moreover, the treatment of cells or cell-free DNA with different ROS such as hydrogen peroxide (H_2O_2) or hypochlorite (HOCl) could mimic the immunostimulatory effect that was achieved with UV irradiation. These data demonstrated that oxidative damage of DNA was indeed central to the observed effect of UV treatment.

4.2. UV Irradiated DNA Becomes Resistant To TREX1-mediated Degradation

To find out how cells distinguish between untreated and UV-DNA, various proteins involved in signal transduction, regulation, transcriptional activation and DNA damage repair were inhibited prior to UV-DNA stimulation. However, none of the proteins analyzed seemed to be important for an enhanced immune sensing of UV-DNA. Additionally, since it was demonstrated that UV irradiated DNA is recognized by the cGAS/STING pathway (data not shown), the binding affinity of UV-DNA for cGAS was carefully investigated. Of note, a higher affinity binding of DNA from UV irradiated cells to cGAS could be excluded to play a role in the observed UV-dependent phenomenon. Since we noticed not only an increased but also a prolonged cytokine response after UV-DNA stimulation, it was hypothesized that DNA from UV irradiated cells might somehow be protected from degradation which would increase the availability within the cytosol and allow an extended stimulation of cGAS. There are three major DNases that degrade extranuclear DNA in different subcellular compartments: i) DNase I is an endonuclease, which is found in most body fluids (Laskowski, 1971; Lacks, 1981, Takeshita et al., 1997; Napirei et al., 2004). ii)

DNase II is an endonuclease that is present in lysosomes where it degrades DNA from phagocytized pathogens and apoptotic debris (Krieser et al., 2002). Iii) DNase III, also known as TREX1, is a 3'-5' exonuclease that is localized in the cytosol (Atianand and Fitzgerald, 2013).

To test if UV-induced DNA modifications might protect DNA from degradation, genomic DNA that was either left untreated or UV irradiated, was digested *in vitro* with the three DNases. DNase I and DNase II degraded both DNAs in equal measure, while TREX1 was unable to degrade UV-DNA compared to unmodified DNA. This finding can be explained by DNase I and II being endonucleases that attack DNA within the molecule, while TREX1 is a 3'-5' exonuclease that can only degrade DNA from one end and is detained from degradation as soon as it encounters an obstruction.

To further evaluate the role of oxidative DNA modifications conferring resistance to TREX1-mediated degradation, bmDCs from TREX1-deficient mice were stimulated with UV irradiated or ROS damaged DNA. Cells that did not express TREX1 showed high responsiveness to both unmodified and oxidatively damaged DNA. In contrast, wild type (WT) bmDCs with functional TREX1 reacted to the same unmodified DNA with lower amounts of IFN-α and to oxidized DNA with an enhanced cytokine response.

Importantly, the interplay of cGAS/STING and TREX1 could also be confirmed *in vivo* with repeated i.c. injections of unmodified and UV-DNA in the ears of WT, TLR9$^{-/-}$, STING$^{gt/gt}$ and TREX1$^{-/-}$ mice. Both WT and TLR9-deficient mice displayed an enhanced ear swelling to UV irradiated DNA in comparison to unmodified DNA, while STING-deficient mice (golden ticket mutation) reacted with a reduced ear swelling and TREX1-deficient mice with an equally potent ear swelling reaction to both forms of DNA. Importantly, these results confirmed that *in vivo*, oxidized DNA is also protected from TREX1-mediated degradation and that this process may allow an accumulation of cGAS ligands in the cytosol, triggering the activation of the cGAS/STING-signaling pathway (**Figure 29).**

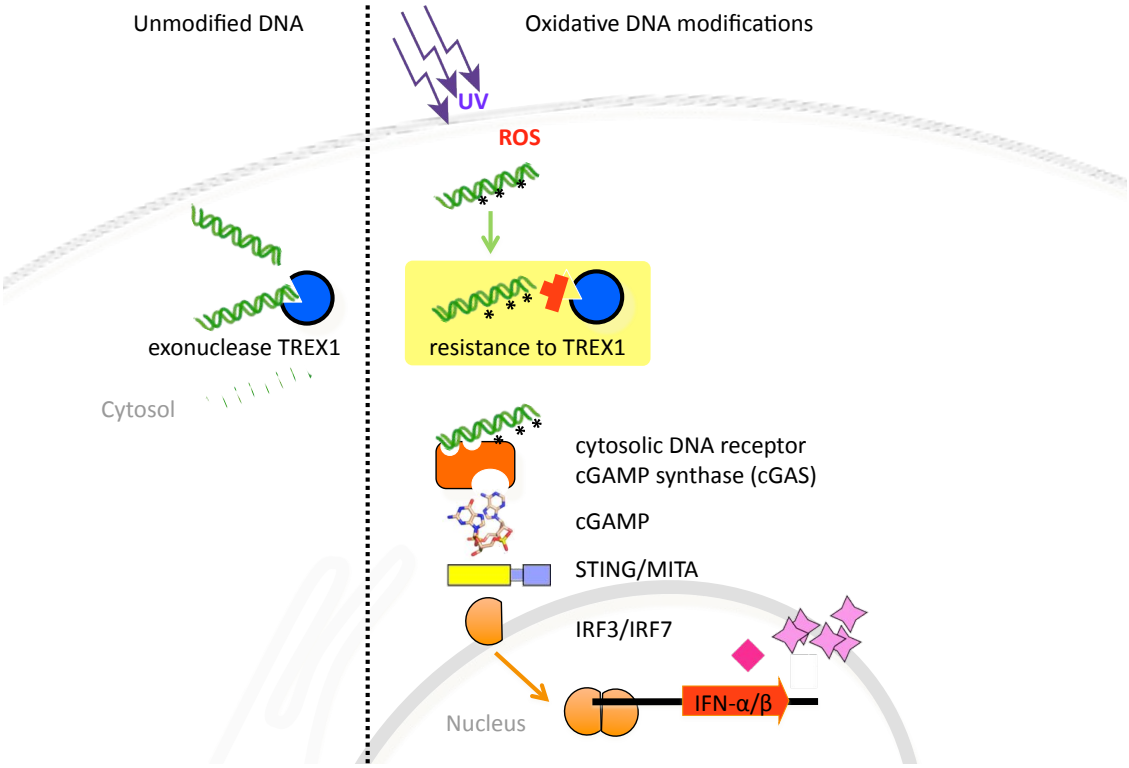

Figure 29: Oxidative damage of DNA confers resistance to TREX1 degradation and potentiates cGAS-STING-dependent immune sensing

Upon entering the cellular cytosol, unmodified DNA is degraded by the exonuclease TREX1, which limits potential immune activation (left panel). However, oxidatively modified DNA becomes largely resistant to TREX1-mediated degradation and can accumulate in the cytosol where it engages the cytosolic DNA receptor cGAS (right panel).

Strikingly, stimulation with UV-DNA leads to effects that are similar to those observed in people with defective DNase(s). Given that a dysfunction of DNase I, II or III can lead to the accumulation of innate immune ligands, it is unsurprising that all three are associated with autoimmune diseases. Defects in DNase I cause the accumulation of extracellular DNA released by dying cells (Yoshida et al., 2005), which is highly immunogenic and was shown to cause a lupus-like syndrome in DNAse I-deficient mice (Napirei et al, 2000). Moreover, mutations in the DNase I gene have been found in systemic lupus erythematosus (SLE) patients (Yasutomo et al., 2001), which are characterized by anti-dsDNA autoantibodies and a type I IFN signature.

Although no human diseases have been linked to a deficiency in this enzyme, human DNase II polymorphisms have been associated with increased risk of renal disorder among SLE patients (Shin et al., 2005). In DNase II–deficient mice, undigested DNA induces fatal levels of type I IFNs (Krieser et al., 2002). However, lethality does not occur in DNaseII/STING-double knockout mice (Kawane et al., 2006; Ahn et al., 2012), indicating that in DNaseII-deficient mice DNA escapes from lysosomes and ends up in the cytosol where it triggers the cytosolic DNA signaling pathway.

STING has also been shown to rescue *TREX1*$^{-/-}$ mice (Gall et al., 2012), which otherwise accumulate endogenous DNA substrates that trigger a lethal, type I IFN-dependent autoimmune

disease (Morita et al., 2004; Stetson et al., 2008). Loss-of-function mutations in the human *TREX1* gene cause Aicardi-Goutières syndrome (AGS), a severe autoimmune disease that mimics the features of congenital viral infection, including elevated type I IFN levels (Crow et al., 2006). Moreover, TREX1 mutations have also been associated with SLE and familial chilblain lupus (FCL), a rare cutaneous form of SLE (Rice et al., 2007; Lee-Kirsch et al., 2007; Kavanagh et al., 2008; Crow and Rehwinkel, 2009; deVries et al., 2010), both of which are also associated with elevated type I IFN levels.

Importantly, TREX1 was identified as an essential negative regulator of the interferon-stimulatory DNA (ISD) response (Stetson et al., 2008), which is significantly upregulated in response to different pro-inflammatory cytokines, including type I IFNs (Xu et al., 2012), and limits excessive activation of cGAS/STING by cytosolic DNA. This feedback regulation allows immune recognition of cytosolic DNA at first but also limits the immune response to prevent autoimmunity. Our data suggest that oxidation might be a DNA modification contributing to the specific recognition of cytosolic DNA in the case of danger, allowing UV-DNA to avoid the safeguard usually provided by functional TREX1.

4.3. The Physiological Role Of Enhanced Immune Recognition Of Oxidized DNA

In the last years it has been shown that pattern recognition receptors (PRRs) do not only recognize pathogen-associated molecular patterns (PAMPs) but also altered self-molecules. These endogenous molecules, known as damage-associated molecular patterns (DAMPs), allow the host to distinguish between viable and damaged or dying cells (Matzinger, 2002). One example is the recognition of oxidized 1-palmitoyl-2-arachidonyl-sn-glyero-3-phosphocholine (OxPAPC), which was shown to activate alveolar macrophages via TLR4 (Imai et al., 2008). Another example includes the binding of oxidatively modified Low Density Lipoprotein (OxLDL) to CD36, which triggers a TLR4/TLR6-dependent inflammatory response in macrophages (Stewart et al., 2010). We hypothesize that oxidized self-DNA might also function as DAMP and envision three scenarios how oxidized self-DNA might become available in the cytosol (**Figure 30**): Neutrophils provoked into undergoing oxidative burst release oxidized DNA in the form of neutrophil extracellular traps (NETs), which may be taken up by phagocytes (ii). Self-DNA released from dying cells may signal immunogenic forms of cell death (iii). Similarly, oxidation damaged mitochondrial (mt) DNA may be released from rupturing mitochondria during necrosis and apoptosis (iv). In addition, lysosomal ROS may transform pathogen DNA into an even more potent PAMP (i).

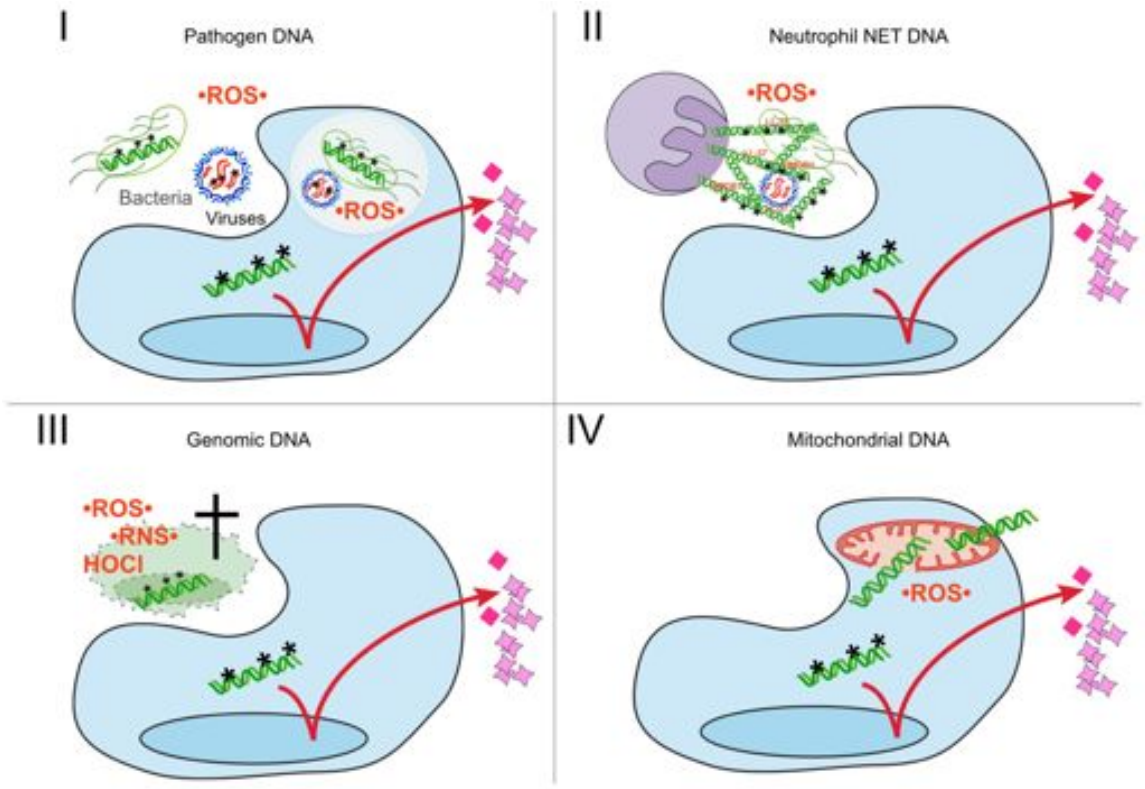

Figure 30: Scenarios how oxidized DNA might become available in the cytosol

Phagocytes make use of reactive oxygen species (ROS) to damage and kill pathogens in their close vicinity or within phagosomes. Pathogen DNA might therefore be labeled for immune recognition (I). Neutrophils release their genomic DNA in a ROS-dependent manner to enclose pathogens within neutrophil extracellular traps (NETs). NET DNA might improve the recognition of the associated pathogens (II). Oxidized genomic DNA might be released and recognized as damage associated molecular pattern (DAMP) to indicate 'dangerous' forms of cell death (III). Upon contact with pathogens or during apoptosis mitochondrial DNA might be released to promote cytosolic immune activation of adjacent cells (IV). ROS = reactive oxygen species, RNS = reactive nitrogen species, HOCl = hypochlorous acid

Pathogen DNA

ROS can be actively generated by phagocytes to kill pathogens (Sbarra and Karnovsky, 1959; Hampton et al., 1998). During an oxidative burst microbes are damaged and eventually killed by the oxidation of their biomolecules. In this process, also microbial DNA comes into contact with the released ROS. Thus, it is possible that ROS are not only used to kill pathogens within the phagolysosome but also to tag microbial DNA for detection in the cytosol in case of an escape from the phagolysosomal compartment. Since ROS in the form of hydrogen peroxide (H_2O_2) or hypochlorite (HOCl) are also released by neutrophils to damage microbes in their direct vicinity, oxidation would serve as a label for pathogen DNA not only for an intrinsic, but also for an extrinsic detection by surrounding immune cells. This scenario was modeled by the stimulation of bmDCs with pathogen DNA that was beforehand incubated with H_2O_2 or HOCl. ROS exposure increased cytosolic recognition of both bacterial and viral DNA in a dose-dependent manner. Additionally, the response of macrophages to H_2O_2-treated *E. coli* was also investigated. However, there was no difference in the secreted type I IFN levels in response to

untreated or oxidatively damaged bacteria observed (data not shown). This might be explained by the fact that most bacteria utilize catalases or dismutases to minimize ROS damage. It therefore remains to be determined to what degree DNA of different pathogenic bacteria will de facto incur oxidative damage in the course of infections of the host. To ascertain whether oxidative modifications of pathogen DNA really contribute to the antibacterial innate immune response further investigation is needed. One possibility would be the incubation of macrophages with superoxide dismutase-deficient *E. coli* or alternatively the usage of ROS-deficient macrophages. Furthermore, it would be interesting to recover intact bacteria from phagolysosomes to assess the oxidative state of bacterial genomic DNA directly.

Another important aspect that needs to be resolved is whether and in what circumstances oxidized pathogen DNA may end up in the cytosol of a target cell. Pathogen DNA could be oxidized extrinsically or intrinsically within the phagolysosome, yet the oxidized DNA must then somehow get into the cytosol. However, pathogens have developed numerous mechanisms to escape the endosomal pathway. Enveloped viruses for example use their viral envelope to fuse with the lipid bilayer and non-enveloped viruses as well as bacteria either lyse the vesicular membrane or generate a pore through which the viral genome or the bacteria, respectively, is released into the cytosol (Meier et al., 2003; Hogle et al., 2002; Mandall and Lee, 2002; Parente et al., 1988). Thus, it could be very interesting to track the route of pathogen DNA for example with the help of intercalating dyes in order to analyze under which circumstances oxidized pathogen DNA is recognized in the cytosol of a host cell.

Neutrophil NET-DNA

In 2004, a novel mechanism utilized by neutrophils to fight pathogens was described by Brinkman et al. Their study demonstrated that neutrophils release net-like DNA structures, called neutrophil extracellular traps (NETs), to capture pathogens in their surroundings (Brinkman et al., 2004). NETs are composed of a meshwork of chromatin fibers that are decorated with granule-derived antimicrobial peptides and enzymes such as neutrophil elastase and myeloperoxidase (MPO).

Experimentally, the release of NETs can be triggered by the addition of phorbol 12-myristate 13-acetate (PMA), which is a potent activator of protein kinase C (PKC). There is evidence that the induction of NETs by PMA depends on active nicotine amide adenine dinucleotide phosphate (NADPH) oxidase, since NET formation could be suppressed by a NADPH oxidase inhibitor (Fuchs et al., 2006) and were not observed in NADPH oxidase knockout mice (Ermert et al., 2009). We investigated the immunogenicity of NET-DNA that was released by neutrophils following PMA treatment. Murine bmDCs as well as human monocytes reacted to NET-DNA with an enhanced type I IFN response, which could be correlated with an increased concentration of the oxidatively damaged DNA base 8-OHG.

It was demonstrated that neutrophils can release large amounts of NETs, but it is not clear whether the presence of oxidized DNA alone can induce an immune response without some sort of “uptake facilitator”. Thus, it was analyzed whether the presence of oxidized DNA alone can provoke an immune response in cells taking up the DNA. A robust type I IFN response was achieved when human monocytes were incubated with micrograms/ml of oxidatively damaged DNA, while unaltered DNA without transfection reagent did not lead to detectable IFN levels. These data supported that high local amounts of oxidized DNA are sufficient to induce an immune response. Interestingly, the antimicrobial peptides LL37, which is present in NETs and has recently been shown to promote endosomal as well as cytosolic delivery of nucleic acids (Lande et al., 2007; Hurtado and Peh, 2010; Chamilos et al., 2012), was able to amplify the response to oxidized DNA. Thus, NET-DNA might function as endogenous adjuvant that further boosts the response to the associated pathogens.

To investigate whether NETing neutrophils can also induce IFN-α secretion in co-cultures with myeloid cells, murine neutrophils were incubated with FLt3L DCs, bmDCs or a 129-macrophages. As expected, the presence of the NETosis-inducing stimulus PMA led to higher type I IFN levels compared to co-cultures without PMA. However, the amounts of IFN-α that could be measured were quite low. Three possible explanations for these low IFN levels are: i) The myeloid cells chosen for experimentation are not the cell type that is most responsive, ii) PMA might itself inhibit IFN signaling (Petricoin et al., 1996; Du et al., 2005), iii) NET-DNA might bind to the plastic of the 96-well plate and can in this state not be taken up by the myeloid cells. To analyze if the low IFN-α levels were due to poor IFN production in general, the co-culture experiment was repeated with human monocytes that we previously found to respond well to high local amounts of oxidized DNA. However, in human co-cultures as well only low levels of IFN-α were measured in the supernatant (data not shown), indicating that probably not the cell type but the co-culture scenario must be optimized in a way that the uptake of NET-DNA is better facilitated.

Next, the effect of PMA on IFN-α secretion was tested in bmDCs that were stimulated with genomic unmodified or UV irradiated DNA complexed with the transfection reagent TransIT-LT1 (Mirus). The presence of PMA did indeed reduce the immune response to both unmodified and oxidized DNA, but IFN secretion was not completely inhibited (data not shown). The PKC activator PMA causes the dephosphorylation of the tyrosine kinase Tyk2 and can thus inhibit the Jak/ STAT signaling pathway downstream of the IFN receptor (Petricoin et al, 1996; Du et al, 2005). To test if one can rescue the type I IFN response to PMA-induced NETing neutrophils, the co-culture experiments were repeated in bmDCs and Flt3L-DCs that were treated for one hour with the PKC inhibitor Go6983 before stimulation. However, preincubation with increasing inhibitor concentrations did not lead to an improved IFN response (data not shown). In the future, it would be interesting to investigate co-cultures with other NETosis inducing stimuli that do not interfere with IFN-signaling.

To circumvent the interaction of NET-DNA with the plastic walls of the culture plate, co-culture experiments were repeated in a hanging drop culture system, originally developed for protein crystallization. However, this alternative culture system also did not enhance the type I IFN response (data not shown). Thus, while we were able to show that NET-DNA, released after PMA treatment, is able to directly induce an IFN response in myeloid cells, it is possible that we did not find the right parameters for a robust *in vitro* co-culture assay. It is nevertheless attractive to suggest that in the presence of infection neutrophils are able to transform their self-DNA into a DAMP to further boost an immune response to the associated pathogens.

There is increasing evidence that different pathways of NET-formation exist. Depending on the inducing stimulus, lytic as well as non-lytic mechanisms make use of either nuclear or mitochondrial DNA to form NETs (Yipp and Kubes, 2013). So far, we cannot clearly say whether each NET-DNA would become more immunogenic due to ROS-induced modifications. Even though it has been shown that PMA is not able to induce NETs in the absence of oxidants or a functional NADPH oxidase (Bianchi et al., 2009; Patel et al., 2010; Remijsen et al., 2011b; Palmer et al., 2012; Keshari et al., 2013), there are other data suggesting that some stimuli such as *S.aureus* or Aspergillus induce NETs independently of ROS (Pilsczek et al., 2010; Byrd et al., 2013). Fittingly, 3-hydroxy 3-methylglutaryl coenzyme A (HMG-CoA) reductase inhibitors, which are used to lower cholesterol in humans, block the oxidative burst, but cause an enhanced release of NETs in response to staphylococci (Chow et al., 2010). Thus, it would be interesting to further evaluate which stimuli promote the generation of immunogenic oxidatively modified NET-DNA.

Genomic DNA

Pathogens have developed different mechanisms to disarm ROS and thereby prevent oxidative damage to their DNA. Thus, cells that expel their own oxidized DNA as a danger signal may represent a host strategy to enhance the immune response to an associated pathogen. The release of nuclear DNA in the form of extracellular traps (ETs) is not exclusively found to be used by neutrophils but has also been reported to be utilized by mast cells (von Kockritz-Blickwede et al., 2008). Typically, mast cell ETs (MCETs) are released in response to the same stimuli that also trigger NET release from neutrophils. Additionally, they were reported to contain the same components as NETs, namely DNA, nuclear histones and the antimicrobial cathelicidin LL37. Digestion of the DNA within MCETs by DNase abolished the extracellular bacterial killing effect (von Kockritz-Blickwede et al., 2008). Importantly, MCETs seem also to be generated by a ROS-dependent cell death mechanism, since the NADPH oxidase inhibitor DPI prevented MCET formation. Experiments with dihydrorhodamine 123 further demonstrated that ROS production was dependent of the cytosolic rather than mitochondrial oxidase activity (von Kockritz-Blickwede et al., 2008). The formation of ETs has also been described playing a role in host defense when used by monocytes and macrophages in response to certain pathogens.

E.coli and *K.pneumoniae* induced monocyte ETs within one hour postexposure, while *S.aureus, H.somni*, *M.haemolytica* and PMA were shown to cause nuclear DNA release from primary macrophages and macrophage cell lines (Webster et al., 2010; Chow et al., 2010; Aulik et al., 2012; Hellenbrand et al., 2013).

It is unknown why only some pathogens cause the release of ETs and what the overall contribution to antimicrobial defense by ETs is. Some pathogens such as *S.pyogenes* can form clumps in order to escape phagocytic killing, since the clumps are too big to be phagocytosed **(**Dinkla et al., 2003). Thus, it is conceivable that ETs might support killing of large pathogen clumps by delivering ROS and antimicrobial peptides that dissolve these structures and at the same time by providing oxidized self-DNA for the uptake by surrounding phagocytes, which are subsequently activated by the cytosolic DNA recognition pathway and in turn clear the dissolved bacterial clumps and recruit more immune cells to the site of infection.

Mitochondrial DNA

A few years ago, Yousefi et al. broadened the understanding of extracellular trap formation when they observed both that the released DNA can also be of mitochondrial (mt) origin and ET formation must not necessarily lead to the death of the ET expelling cell. In their studies, eosinophils and neutrophils were primed with IL-5/ IFN-gamma or with GM-CSF/ C5a, respectively. Subsequent stimulation with LPS resulted in a rapid release of mt DNA. Similar to ETs containing nuclear DNA, the structures composed of mt DNA and granule proteins were able to bind and kill bacteria both *in vitro* and *in vivo* (Yousefi et al., 2008; Yousefi et al., 2009). Release of mt DNA by viable cells would have the advantage that the cells can still fulfill other functions like phagocytosis or the production of cytokines. Moreover, mt DNA is particularly prone to accumulate oxidative damage due to the immediate vicinity of the ROS producing respiratory chain in the mitochondrial inner membrane. In preliminary experiments, the immunostimulatory capacity of mt DNA was directly compared to that of nuclear DNA and as expected, stimulation with mt DNA induced higher type I IFN levels compared to nuclear DNA (data not shown). Thus, mt DNA seems to be predestinated to be part of ETs and to function as DAMP that can activate the innate immune system.

In 2004, Collins and colleagues showed that the intra-articular injection of mt DNA induced arthritis, while nuclear DNA did not. Since mt DNA contains unmethylated CpG motifs, they next investigated whether unmethylated CpG motifs or oxidative DNA modifications were required for inflammation. Oligonucleotides (ODNs) that lacked CpG motifs but contained a single 8-OHG residue were immunogenic, while the same ODNs with CpG motif and without the oxidized base did not induce inflammation (Collins et al., 2004). However, a few years later, Yoshida and his group made contradictory observations. Using footpad swelling as readout for rheumatoid inflammation, they only observed a significant increase in inflammation when a CpG-bearing ODN was injected in combination with an 8-OHG-bearing nonCpG-ODN, but not for footpad

treatment with CpG or 8-OHG ODNs alone (Yoshida et al., 2011). Recently, also another group published that oxidative modifications enhance the immunostimulatory effects of extracellular mtDNA on TLR9 bearing pDCs (Pazmandi et al., 2014). Pazmandi and colleagues could show that the exposure to oxidatively modified mt DNA led to a significant higher upregulation of CD86, CD83 and HLA-DQ on the cell surface of primary human pDCs when compared to native mt DNA. Furthermore, these cells secreted significant amounts of TNF-α and IL-8 in response to oxidized mt DNA. Interestingly, simultaneous administration of a TLR9 antagonist abrogated the effects of both native and oxidized mt DNAs on human pDCs. The results by Yoshida and Pazmandi suggested that oxidatively damaged DNA alone is not able to induce an immune response although it could enhance the CpG-dependent activation of TLR9.

In contrast to Yoshida and Pazmandi and in line with Collins study, we observed that oxidatively damaged DNA alone was sufficient to induce an inflammatory response. The participation of TLR9 in the enhanced recognition of oxidized DNA was excluded by stimulation of bone marrow (bm) cells and bmDCs derived from TLR9-deficient mice, which reacted to UV irradiated DNA in a manner similar to WT cells (data not shown). In line with these results, an increased immune response to oxidatively damaged DNA was also observed in human monocytes, which do not express TLR9.

It is not only conceivable that mt DNA is released in the extracellular space in the form of ETs, but it might be also possible that mt DNA is directly delivered into the cytosol where it then activates the cGAS/STING pathway. Very recently, it was shown that cells release mt DNA during Bax/Bak-dependent apoptosis. This mt DNA is recognized by the cGAS/STING pathway and can lead to type I IFN production. However, apoptotic caspases normally block this pathway to protect the host from unnecessary inflammation (White et al., 2014; Rongvaux et al., 2014). Moreover, West et al. described that herpes virus infections cause mitochondrial instability and thus promote the escape of mt DNA into the cytosol, where it engages the cGAS/ STING-signaling pathway to potentiate type I interferon responses and enhance the expression of interferon-stimulated genes (West et al., 2015). The authors did however not comment on the oxidative status of the mt DNA.

Under normal circumstances, mt DNA is organized as circular ds DNA and thus not accessible for TREX1, but in case of mitochondrial stress it might get released in a fragmented form and then oxidative modifications would ensure that it stays long enough in the cytosol for a potent activation of the cGAS/STING signaling pathway. Thus, it would be interesting to analyze mitochondria ROS production during the course of an infection and to track the intra- and extracellular location of mt DNA as well as its integrity.

4.4. Not Only DNA Oxidation Enhances The DNA-induced Immune Response

DNA cannot only be damaged by UV irradiation or ROS exposure but also by many other mutagens such as chemotherapeutic agents that directly interact with DNA. To test whether other DNA modifications in addition to oxidation also lead to an increased immunostimulatory capacity of DNA, cells were treated with Cisplatin, Melphalan, Dactinomycin, Idarubicin or Etoposide prior to DNA isolation. Cisplatin and Melphalan are DNA alkylating agents and cause either intra-strand adducts or inter-strand crosslinks (Johnson et al., 1989; Kohn, 1981). In contrast, Dactinomycin and Idarubicin belong to the group of DNA intercalating agents, which prevent transcription and replication (Golderg et al., 1962; Sentenac et al., 1968; Jensen et al., 1993). Etoposide is a member of the topoisomerase inhibitor drug class, which does not intercalate into DNA but causes DNA strand breaks (Pommier et al., 2010).

Stimulation of murine bmDCs with DNA isolated from cells that were treated with DNA alkylating or intercalating agents induced higher IFN-α levels compared to DNA from untreated cells. Etoposide was however unable to enhance the immunogenicity of the DNA. Similar results were obtained when cell-free DNA was directly treated with the described chemotherapeutic agents, showing that next to oxidative damage also other DNA modifications like alkylation or intercalation can enhance the immunostimulatory capacity of DNA. To date, there are no reports on chemotherapeutic agents directly changing the immunostimulatory potential of DNA. Nonetheless, there are indications that chemotherapeutic agents can influence the type I IFN signaling pathway.

In 2001, Melphalan was shown to induce IFN-ß expression in mice. Even though the precise signaling pathway was not revealed, the authors suggested that ROS are involved in the transcriptional regulation of Melphalan-induced IFN-β gene expression. Melphalan-induced accumulation of IFN-β mRNA could be mimicked with H_2O_2 and was prevented with the antioxidant *N*-acetyl-L-cysteine (Jovasevic, V.M. and Mokyr, 2001). Thus, it might be possible that the enhanced immunogenicity of DNA from Melphalan-treated cells is not or not only due to DNA intercalation but indirectly emerges from an upregulation of ROS, which then oxidatively damage the DNA. To evaluate which kind of DNA modification is eventual responsible for the observed immunogenicity, an analysis by mass spectrometry of DNA from Melphalan-treated cells would be necessary. In 2012, a cell-based high-throughput screening (HTS) assay identified Idarubicin as an enhancer of STAT1-dependent interferon stimulated gene (ISG) expression. However, this effect was shown to be independent of IFN production or IFN–IFN-receptor interaction, suggesting that Idarubicin works distal to ligand-receptor binding. In the same assay, Etoposide was shown as a control to not influence IFN-stimulated response element (ISRE) activity (Patel et al., 2012). Very recently the group of Barber published that Cisplatin and Etoposide induce nuclear DNA leakage into the cytosol that then intrinsically activates STING- dependent cytokine production (Ahn et al., 2014). However, the authors did not comment on the constitution of the nuclear DNA.

4.5. The Role Of Oxidized DNA In The Pathogenesis Of Lupus Erythematosus

Continuous activation of nucleic acid receptors is usually prevented by the physiological subcellular compartmentalization of the sensors (Barton and Kagan, 2009) as well as by several nucleases that degrade nucleic acids and thus deplete the respective ligands. However, in autoimmune diseases such as systemic lupus erythematosus (SLE) and psoriasis, a chronic activation of nucleic acid receptors has been described (Barrat et al., 2005; Hari et al., 2010). Importantly, impairment in TREX1 activity is also strongly associated with autoimmunity (Stetson et al., 2008). There are at least 15 different mutations in TREX1 which have been associated with Aicardi-Goutières syndrome (AGS), a severe inflammatory neurodevelopmental disorder (Crow et al., 2006). Several groups have highlighted the phenotypic overlap of AGS with lupus (Crow et al., 2003; Dale et al., 2000; Aicardi and Goutières, 2000; Rasmussen et al., 2005; De Laet et al., 2005). Thus, TREX1 mutations were also analyzed in lupus patients. Familial Chilblain Lupus (FCL) is a rare, inherited form of cutaneous lupus in which autosomal dominant mutations in TREX1 that decrease exonuclease activity have been described (Lee-Kirsch et al., 2006; Rice et al., 2007a/b). In addition, heterozygous mutations in TREX1 have also been found in ~3 % of SLE patients (Lee-Kirsch et al., 2007). These mutations are more diverse compared to FCL; some disrupt exonuclease activity, others result in altered intracellular localization (Rasmussen et al., 2005; Lee-Kirsch et al., 2007). However, in 97 % of lupus patients TREX1 is functional (Lee-Kirsch et al., 2007), and the majority of these patients react to UV exposure with the development of skin lesions. Since UV-exposure could theoretically cause inflammation in a variety of ways, the specific role of UV-DNA in UV-induced inflammation was investigated by injecting unmodified or UV irradiated DNA repeatedly in the ears of lupus prone MRL/lpr mice. After three weeks, massive ear swelling and local skin lesions could be observed in the ears that had been exposed to UV-DNA. These results demonstrate the specific inflammatory potential of UV irradiated DNA *in vivo* as well as its role in the development of cutaneous lupus in an accepted lupus mouse model.

Anti-dsDNA autoantibodies are a characteristic of SLE and are also found in MRL/*lpr* mice (Pisetsky et al. 1982). Since they can facilitate the uptake of DNA into cells, it was analyzed whether MRL/lpr mice are in general more susceptible to DNA. Unmodified or UV-DNA was administered i.v. to either WT or lupus-prone MRL/lpr mice and several hours later serum type I IFN levels were determined. C57BL/6 mice that were used as WT control, did not respond to any form of DNA, whereas MRL/lpr mice reacted lightly to unmodified and heavily to UV-DNA. These findings demonstrate that UV-DNA is a very potent inflammatory stimulus in a lupus-like environment and in combination with the *in vitro* resistance to TREX1 degradation demonstrated for UV-DNA, these data allow the conclusion that in lupus patients UV-DNA leads to effects that are similar to TREX1 deficiency as exemplarily shown by the administration of unmodified DNA causing a massive ear swelling in TREX1-deficient mice.

One plausible explanation for UV phototoxicity in lupus patients would be that UV exposure leads to the death of keratinocytes, which are not efficiently cleared by phagocytes (Herrmann et al., 1998; Baumann et al., 2002; Kuhn et al., 2006). These keratinocytes would then release a variety of inflammatory mediators and display autoantigens such as oxidized self-DNA. This DNA could be taken up by surrounding immune cells and potently activate the cGAS/STING-signaling pathway, contributing to an inflammatory micromilieu that finally leads to formation of skin lesions.

According to Baccala and colleagues, the development of SLE can be divided into two phases (Baccala et al., 2007). At the cellular level, the initial phase is characterized by DCs that take up apoptotic cell debris and associated nucleic acids. These then start to produce type I IFNs in a TLR7/9- independent fashion. In turn, lymphoid and myeloid DCs differentiate into self-antigen presenting cells (self-APCs), which induce the activation of autoreactive T and B cells. In contrast, the subsequent amplification phase is mainly dependent on pDCs that take up immune complexes consisting of autoantibodies and endogenous RNA or DNA. The antibody/FcR-mediated uptake targets the nucleic acids into endosomes, where they induce a TLR7/9-dependent production of type I IFN (Barrat et al., 2005). According to this two-phase paradigm of autoimmunity, our finding that oxidatively damaged DNA causes a TLR9-independent induction of IFN via the cGAS/STING-signaling pathway might be especially important in the understanding of the dynamics of initial disease development as well as that of acute relapses or disease flares.

Since type I IFN has already been shown to play an important role in the pathogenesis of SLE, different treatments targeting IFN-α have emerged over the years. Treatment strategies involve antibodies against IFN-α or its receptor, as well as approaches that specifically target pDCs or the signaling downstream of TLR7/9 in pDCs (Kirou and Ckrouzman, 2013). In the light of our results, it might also be clinically advantageous to block cGAS and/or STING, although this would also require careful consideration of the suppressive effects such a treatment may have on anti-viral immunity. However, when compared to treatments directly targeting IFN-α signaling, blocking the cGAS/STING pathway would have the advantage that MAVS-dependent signaling downstream of the critical cytosolic RNA receptors RIG-I and MDA-5 would remain intact, thus preserving immunity against important viral threats such as influenza.

4.6. Identification Of IFN Producing Cells In The MRL/lpr Mouse Model

Plasmacytoid DCs (pDCs) are known as professional IFN producing cells and have been shown to contribute to the IFN signature in lupus patients (Vallin et al., 1999; Bennet et al., 2003; Sisirak et al., 2014; Rowland et al., 2014). However, they respond to DNA via a TLR9-dependent pathway (Brawand et al., 2002; Lund et al., 2003; Barrat et al., 2005; Means et al, 2005; Guiducci et al., 2009) and our data clearly exclude a role for TLR9 in the enhanced recognition of UV-DNA. Furthermore, depletion experiments showed that not only pDCs, but also other cell

types might contribute to type I IFN levels in SLE (Blanco et al., 2001). Thus, we set out to identify cell types other than pDCs that are responsible for the uptake and response to oxidatively damaged DNA *in vivo*. In MRL/lpr mice, $CD11b^{+}Ly6C^{low}F4/80^{+}$cells internalized large amounts of untransfected UV-DNA and showed the highest upregulation of IFN-α mRNA among cDCs and monocytes/macrophages. Although the combination of these cell surface markers can be expressed by both monocytes and macrophages, the morphology of the cells in the FCS vs. SSC plot pointed to macrophages (large granular cells) rather than monocytes.

Murine spleen macrophages can be divided into five different subsets based on their localization and surface marker signature: marginal zone, metallophilic, red pulp, white pulp and from blood immigrated monocyte-derived macrophages. Marginal zone, metallophilic and white pulp macrophages are F4/80-negative, whereas red pulp and monocyte-derived macrophages were shown to express F4/80 (Davies et al, 2013). Thus, the identified IFN-producing cells must belong to either red pulp or monocyte-derived macrophages. Red pulp macrophages are defined as $CD11b^{low}F4/80^{high}$ and monocyte-derived macrophages as $Ly6C^{low}F4/80^{+}$. Since the IFN-producing cells expressed high levels of CD11b and medium amounts of F4/80, they likely derive from blood immigrated monocyte-derived macrophages. This conclusion is in line with the classical M1/M2 division of macrophages: monocyte-derived macrophages characteristically produce IFN-α as part of their pro-inflammatory cytokine profile, whereas tissue-resident macrophages such as red pulp macrophages are thought to belong to the anti-inflammatory M2 subtype (Mantovani *et al.*, 2004). Nevertheless, these cells need to be further characterized to allow a specific treatment of the UV-DNA response in lupus patients. Conceivable therapeutic treatments include the inhibition of inflammatory M1 macrophages and simultaneous promotion of M2 macrophages. Promising are anti-TNF treatments as well as PPARγ agonists that stimulate M2a expansion and mildened murine lupus nephritis (Venegas-Pont *et al.*, 2009; Zhao *et al.*, 2009; Lefèvre *et al.*, 2010).

Our results suggest that the two-phase paradigm of autoimmunity suggested by Baccala and colleagues (Baccala et al., 2007) should to be amended. While Baccala et al. ascribed the type I IFN signature in lupus to specific DC subsets, DCs did not contribute much of the type I IFN observed in response to UV-DNA, at least in the MRL/lpr lupus model. However, there are also indications that the cell types involved may vary between different lupus models. Lee and colleagues investigated the pristane-induced lupus model and demonstrated that pristane treatment induced an accumulation of immature $Ly6C^{high}$ monocytes, which were identified as major source of IFN-I in this lupus model. Ly6C-positive monocytes can differentiate into both macrophages and DCs depending on the environmental signal they receive. However, Lee et al. also excluded a substantial role for DCs in this lupus model, as only monocyte depletion led to a decreased expression of IFN and ISGs, whereas systemic ablation of DCs had little effect (Lee et al., 2008). Taken altogether, lupus remains a very complex disease with many different cell types being involved in its initiation and conduction. It appears reasonable that in genetically

different forms of SLE also distinct cell types contribute to the sustained overproduction of IFN-α/β, with varying contributions depending on the disease trigger.

4.7. Final Summary And Outlook

When DNA accumulates in the cytosol, it activates the cGAS/STING pathway, leading to type I IFN production. The compartmentalization of cGAS to the cytosol and the presence of several nucleases, in particular TREX1, that degrade DNA in this compartment contribute to preventing the erroneous recognition of self-DNA. However, here we provided evidence that DNA modifications can transform self-DNA into a damage-associated molecular pattern (DAMP) that becomes resistant to degradation by the cytosolic exonuclease TREX1, allowing the activation of cGAS by endogenous DNA.

Oxidative modifications of self-DNA occurred due to antimicrobial ROS production or upon physical damage such as the absorption of UV light. In future studies, it will be important to investigate in which physiological and pathophysiological conditions oxidized self-DNAs are released. Likewise, it should be studied whether only phagocytes are able to take up the modified DNA from the extracellular space, and in which situations oxidized DNA is intrinsically released into the cytosol. Similar to what has been observed with self-DNA, exposure to ROS also increased the immunogenicity of pathogen DNA. It therefore needs to be determined whether there are instances in which the DNA of infectious microbes becomes oxidatively tagged during an infection and whether these modifications contribute to the innate immune detection via the cGAS/STING-signaling pathway.

5. Literature

Ablasser, A., Bauernfeind, F., Hartmann, G., …, and Hornung, V. (2009). RIG-I-dependent sensing of poly(dA:dT) through the induction of an RNA polymerase III-transcribed RNA intermediate. Nat Immunol *10*, 1065-1072.

Ablasser, A., Goldeck, M., Cavlar, T., ..., and Hornung, V. (2013). cGAS produces a 2'-5'-linked cyclic dinucleotide second messenger that activates STING. Nature *498*, 380-384.

Adolf, G.R. (1995). Human interferon omega--a review. Mult Scler *1 Suppl 1*, S44-47.

Aicardi, J., and Goutières, F. (2000). Systemic lupus erythematosus or Aicardi-Goutières syndrome? Neuropediatrics *31*, 113.

Ahn, J., Gutman, D., Saijo, S. and Barber, G.N. (2012). STING manifests self-DNA dependent inflammatory disease. Proc Natl Acad Sci USA 109 (47), 19386-19391.

Ahn, J. ,Xia, T. , Konno, H., Konno, K., ... and Barber, G.N. (2014). Inflammation-driven carcinogenesis is mediated through STING. Nature Communications 5:5166, DOI: 10.1038

Aksoy, E., Zouain, C.S., Vanhoutte, F., …, and Trottein, F. (2005). Double-stranded RNAs from the helminth parasite Schistosoma activate TLR3 in dendritic cells. J Biol Chem *280*, 277-283.

Albrich, J. M., McCarthy, C. A. and J. K. Hurst (1981). Biological reactivity of hypochlorous aicd: Implications for microbicidal mechanisms of leukocyte myeloperoxidase. *Proc. Natl. Acad. Sci.* 78 (1): 210–214

Alexopoulou, L., Desnues, B., and Demaria, O. (2012). [Toll-like receptor 8: the awkward TLR]. Med Sci (Paris) *28*, 96-102.

Alexopoulou, L., Holt, A.C., Medzhitov, R., and Flavell, R.A. (2001). Recognition of double-stranded RNA and activation of NF-kappaB by Toll-like receptor 3. Nature *413*, 732-738.

Andrejeva, J., Childs, K.S., Young, D.F., …, and Randall, R.E. (2004). The V proteins of paramyxoviruses bind the IFN-inducible RNA helicase, mda-5, and inhibit its activation of the IFN-beta promoter. Proc Natl Acad Sci U S A *101*, 17264-17269.

Andrews, B.S., Eisenberg, R.A., Theofilopoulos, A.N., …, and Dixon, F.J. (1978). Spontaneous murine lupus-like syndromes. Clinical and immunopathological manifestations in several strains. J. Exp. Med. 148, 1198-1215

Asselin-Paturel C, Boonstra A, Dalod M., …, and Trinchieri, G. (2001). Mouse type I IFN-producing cells are immature APCs with plasmacytoid morphology. Nat. Immunol.; 2: 1144–50

Atianand, M.K. and Fitzgerald, K.A.(2013). Molecular basis of DNA recognition in the immune system. J Immunol. 190(5):1911-8

Aulik, N.A., Hellenbrand, K.M. and Czuprynski, C.J. (2012). Mannheimia haemolytica and its leukotoxin cause macrophage extracellular trap formation by bovine macrophages. Infect Immun 80:1923–1933

Austyn, J. M., and Gordon, S. (1981). F4/80, a monoclonal antibody directed specifically against the mouse macrophage. Eur. J. Immunol. *11: 805*

Baccala, R., Hoebe, K., Kono, D.H., ..., and Theofilopoulos, A.N. (2007). TLR-dependent and TLR-independent pathways of type I interferon induction in systemic autoimmunity. Nat Med *13*, 543-551.

Balomenos, D., Rumold, R. and Theofilopoulos, A.N. (1998), Interferon is required for lupus-like disease and lymphoaccumulation in MRL-lpr mice. J Clin Invest 101 (2), 364- 371

Banáth, J.P. and Olive, P.L. (2003). Expression of phosphorylated histone H2AX as a surrogate of cell killing by drugs that create DNA double-strand breaks. Cancer Res 63, 4347-4350

Barker, J.R., Koestler, B.J., Carpenter, V.K., ..., and Valdivia, R.H. (2013). STING-dependent recognition of cyclic di-AMP mediates type I interferon responses during Chlamydia trachomatis infection. MBio *4*, e00018-00013.

Barrat, F.J., Meeker, T., Gregorio, J., ..., and Coffman, R.L. (2005). Nucleic acids of mammalian origin can act as endogenous ligands for Toll-like receptors and may promote systemic lupus erythematosus. J Exp Med *202*, 1131-1139.

Barton, G.M and Kagan, J.C. (2009). A cell biological view of Toll-like receptor function: regulation through compartmentalization. *Nature Reviews Immunology* 9, 535-542

Barton, G.M., Kagan, J.C., and Medzhitov, R. (2006). Intracellular localization of Toll-like receptor 9 prevents recognition of self DNA but facilitates access to viral DNA. Nat Immunol *7*, 49-56.

Batista, L.F., Kaina, B., Meneghini, R., and Menck, C.F. (2009). How DNA lesions are turned into powerful killing structures: insights from UV-induced apoptosis. Mutat Res *681*, 197-208.

Baum, R.; Sharma, S.; Carpenter, S., ... and Gravallese, E.M. (2014). Cutting Edge: AIM2 and Endosomal TLRs differentially Regulate Arthritis and Autoantibody Production in DNaseII-deficient Mice. J Immunol 194 (3): 873-877

Baumann, I., Kolowos, W., Voll, R.E., ..., and Herrmann, M. (2002). Impaired uptake of apoptotic cells into tingible body macrophages in germinal centers of patients with systemic lupus erythematosus. *Arthritis Rheum. 46(1):191-201.*

Bebenek, K., Matsuda, T., Masutani, C., ..., and Kunkel, T.A. (2001). Proofreading of DNA polymerase eta-dependent replication errors. J Biol Chem *276*, 2317-2320.

Beitner, H. (1988). Immediate pigment-darkening reaction. Photodermatol *5*, 96-100.

Bennett, L., Palucka, A.K., Arce, E., ... and Pascual, V. (2003). Interferon and granulopoiesis signatures in systemic lupus erythematosus blood. *J Exp Med* 197(6):711-723

Bhattacharya, S., HuangFu, W.-C., Dong, G., ..., and Fuchs, S.Y. (2013). Anti-tumorigenic effects of Type 1 interferon are subdued by integrated stress responses. *Oncogene* **32**, 4214–4221

Bianchi, M., Hakkim, A., Brinkmann, V., …, and Reichernbach, J. (2009). Restoration of NET formation by gene therapy in CGD controls aspergillosis. Blood 114(13):2619-2622.

Bird, A.P. (1986). CpG-rich islands and the function of DNA methylation. Nature *321*, 209-213.

Blanco, P., Palucka, A.K., Gill, M., ..., and Banchereau J. (2001). Induction of dendritic cell differentiation by IFN-alpha in systemic lupus erythematosus. *Science*, 294:1540-1543.)

Boulé, M.W., Broughton, C., Mackay, F., ..., and Rifkin, I.R. (2004). Toll-like receptor 9-dependent and -independent dendritic cell activation by chromatin-immunoglobulin G complexes. J Exp Med *199*, 1631-1640.

Box, H.C., Dawidzik, J.B., and Budzinski, E.E. (2001). Free radical-induced double lesions in DNA. Free Radic Biol Med *31*, 856-868.

Brash, D.E., Rudolph, J.A., Simon, J.A., ..., and Pontén, J. (1991). A role for sunlight in skin cancer: UV-induced p53 mutations in squamous cell carcinoma. Proc Natl Acad Sci U S A *88*, 10124-10128.

Brawand, P., Fitzpatrick, D.R., Greenfield, B.W., …, and De Smedt, T. (2002). Murine plasmacytoid pre-dendritic cells generated from flt3 ligand-supplemented bone marrow cultures are immature APCs. J. Immunol. 169:6711–6719.

Brucet, M., Querol-Audí, J., Serra, M., …, and Celada, A. (2007). Structure of the dimeric exonuclease TREX1 in complex with DNA displays a proline-rich binding site for WW Domains. J Biol Chem *282*, 14547-14557.

Brzostek-Racine, S., Gordon, C., Van Scoy, S., and Reich, N.C. (2011). The DNA damage response induces IFN. J Immunol *187*, 5336-5345.

Burdette, D.L., Monroe, K.M., Sotelo-Troha, K., …, and Vance, R.E. (2011). STING is a direct innate immune sensor of cyclic di-GMP. Nature *478*, 515-518.

Burnham, T.K., Neblett, T.R., and Fine, G. (1963). The application of the fluorescent antibody technic to the investigation of lupus erythematosus and various dermatoses. J Invest Dermatol *41*, 451-456.

Byrd, A.S., O'Brien, X.M., Johnson, C.M., ..., and Reichner, J.S. (2013). An Extracellular Matrix- Based Mechanism of Rapid Neutrophil Extracellular Trap Formation in Response to Candida albicans. J Immunol 190(8):4136-4148.

Bürckstümmer, T., Baumann, C., Blüml, S., ..., and Superti-Furga, G. (2009). An orthogonal proteomic-genomic screen identifies AIM2 as a cytoplasmic DNA sensor for the inflammasome. Nat Immunol *10*, 266-272.

Carey, M. (1998). The enhanceosome and transcriptional synergy. Cell *92*, 5-8.

Carvalho, A., De Luca, A., Bozza, S., …, and Romani, L. (2012). TLR3 essentially promotes protective class I-restricted memory CD8$^+$ T-cell responses to Aspergillus fumigatus in hematopoietic transplanted patients. Blood *119*, 967-977.

Celik, H. and Arinç, E. (2008). Bioreduction of idarubicin and formation of ROS responsible for DNA cleavage by NADPH-cytochrome P450 reductase and its potential role in the antitumor effect. J Pharm Pharm Sci.11(4), 68-82.

Cella, M., Jarrossay, D., Facchetti, F., …, and Colonna, M.(1999). Plasmacytoid monocytes migrate to inflamed lymph nodes and produce large amounts of type I interferon. Nat. Med.;5:919–923

Chamilos, G., Gregorio, J., Meller, S., ..., and Gilliet, M. (2012). Cytosolic sensing of extracellular self-DNA transported into monocytes by the antimicrobial peptide LL37. Blood *120*, 3699-3707.

Chiu, Y.H., Macmillan, J.B., and Chen, Z.J. (2009). RNA polymerase III detects cytosolic DNA and induces type I interferons through the RIG-I pathway. Cell *138*, 576-591.

Chow, O.A., von Kockritz-Blickwede, M., Bright, A.T., …, and Nizet, V.(2010). Statins enhance formation of phagocyte extracellular traps. Cell Host Microbe. 8(5):445-454.

Civril, F., Deimling, T., de Oliveira Mann, C.C., ..., and Hopfner, K.P. (2013). Structural mechanism of cytosolic DNA sensing by cGAS. Nature *498*, 332-337.

Clark, W.H., Reed, R.J., and Mihm, M.C. (1973). Lupus erythematosus. Histopathology of cutaneous lesions. Hum Pathol *4*, 157-163.

Collins, L.V., Hajizadeh, S., Holme, E., ..., and Tarkowski, A. (2004). Endogenously oxidized mitochondrial DNA induces *in vivo* and *in vitro* inflammatory responses. *J Leukoc Biol* **75**: 995–1000.

Conrad, B. (2003). Potential mechanisms of interferon-alpha induced autoimmunity. Autoimmunity *36*, 519-523.

Conrady, C.D., Zheng, M., Fitzgerald, K.A., ..., and Carr, D.J. (2012). Resistance to HSV-1 infection in the epithelium resides with the novel innate sensor, IFI-16. Mucosal Immunol *5*, 173-183.

Cook, J.S. (1970). Photoreactivation in animal cells. Photophysiology *5*, 191-233.
Coscoy, L., and Raulet, D.H. (2007). DNA mismanagement leads to immune system oversight. Cell *131*, 836-838.

Crow, Y.J., Black, D.N., Ali, M., ..., and Lebon, P. (2003). Cree encephalitis is allelic with Aicardi-Goutiéres syndrome: implications for the pathogenesis of disorders of interferon alpha metabolism. J Med Genet *40*, 183-187.

Crow, Y.J., Hayward, B.E., Parmar, R., …, and Lindahl, T. (2006). Mutations in the gene encoding the 3'-5' DNA exonuclease TREX1 cause Aicardi-Goutières syndrome at the AGS1 locus. Nat Genet *38*, 917-920.

Crow, Y.J. and Rehwinkel, J. (2009). Aicardi-Goutieres syndrome and related phenotypes: linking nucleic acid metabolism with autoimmunity. Hum Mol Genet. 18(R2):R130-6.

Crowson, A.N., and Magro, C.M. (2009). Cutaneous histopathology of lupus erythematosus. Diagn Histopathol *15*, 28.

Dale, R.C., Tang, S.P., Heckmatt, J.Z., and Tatnall, F.M. (2000). Familial systemic lupus erythematosus and congenital infection-like syndrome. Neuropediatrics *31*, 155-158.

Daniels, F., Brophy, D., and Lobitz, W.C. (1961). Histochemical responses of human skin following ultraviolet irradiation. J Invest Dermatol *37*, 351-357.

Davies, L.C., Jenkins, S.J., Allem, J.E. and Taylor, P.R. (2013). Tissue-resident macrophages. Nature Immuno 14, 986-995

De Laet, C., Goyens, P., Christophe, C., ..., and Dan, B. (2005). Phenotypic overlap between infantile systemic lupus erythematosus and Aicardi-Goutières syndrome. Neuropediatrics *36*, 399-402.

Delale T., Paquin A., Asselin-Paturel C., …, and Brière, F. (2005). MyD88-dependent and -independent murine cytomegalovirus sensing for IFN-α release and initiation of immune responses in vivo. J. Immunol. 175: 6723–6732

de Veer, M.J., Holko, M., Frevel, M., ..., and Williams, B.R. (2001). Functional classification of interferon-stimulated genes identified using microarrays. J Leukoc Biol *69*, 912-920.

de Vries, B., Steup-Beekman, G.M., Haan, J., ..., and Ferrari, M.D. (2010). TREX1 gene variant in neuropsychiatric systemic lupus erythematosus. Ann. Rheum. Dis., 69: 1886–1887

de Weerd, N.A., Samarajiwa, S.A., and Hertzog, P.J. (2007). Type I interferon receptors: biochemistry and biological functions. J Biol Chem *282*, 20053-20057.

Diebold S. S., Montoya M., Unger H., …, and Reis e Sousa C. (2003). Viral infection switches non-plasmacytoid dendritic cells into high interferon producers. Nature 424: 324–328
Diner, E.J., Burdette, D.L., Wilson, S.C., ..., and Vance, R.E. (2013). The innate immune DNA sensor cGAS produces a noncanonical cyclic dinucleotide that activates human STING. Cell Rep *3*, 1355-1361.

Dinkla, K., Rohde, M., Jansen, W.T., ..., and Talay, S.R. (2003). Streptococcus pyogenes recruits collagen via surface-bound fibronectin: a novel colonization and immune evasion mechanism. *Mol Microbiol* 47:861-869.

Dougherty, J.P., Samanta, H., Floyd-Smith, G., ..., and Lengyel, P. (1981). Enzymology of interferon action. The (2'-5')(A)n synthetase-RNase L pathway. Tex Rep Biol Med *41*, 443-451.

Du, W., and Maniatis, T. (1992). An ATF/CREB binding site is required for virus induction of the human interferon beta gene [corrected]. Proc Natl Acad Sci U S A *89*, 2150-2154.

Du Z, Shen, Y., Yang, W., ..., and Ivashkiv, L.B. (2005). Inhibition of IFN-α signaling by a PKC- and protein tyrosine phosphatase SHP-2-dependent pathway. Proc. Natl Acad. Sci. USA.102:10267–10272.

Duan, X., Ponomareva, L., Veeranki, S., ..., and Choubey, D. (2011). Differential roles for the interferon-inducible IFI16 and AIM2 innate immune sensors for cytosolic DNA in cellular senescence of human fibroblasts. Mol Cancer Res *9*, 589-602.

Epe, B., Ballmaier, D., Roussyn, I., ..., and Sies, H. (1996). DNA damage by peroxynitrite characterized with DNA repair enzymes. Nucleic Acids Res *24*, 4105-4110.

Ermert D., Urban C. F., Laube B., ..., and Brinkmann V. (2009) Mouse neutrophil extracellular traps in microbial infections. J. Innate Immun. 1, 181–193.

Evans, C.J., and Aguilera, R.J. (2003). DNase II: genes, enzymes and function. Gene *322*, 1-15.

Fabbri, P., Cardinali, C., Giomi, B., and Caproni, M. (2003). Cutaneous lupus erythematosus: diagnosis and management. Am J Clin Dermatol *4*, 449-465.

Fauzi, A.R., Kong, N.C., Chua, M.K., …, and Azizah, R. (2004). Antibodies in systemic lupus antineutrophil cytoplasmic erythematosus: prevalence, disease activity correlations and organ system associations. Med J Malaysia. 59:372–377.

Feng, G.S., Chong, K., Kumar, A., and Williams, B.R. (1992). Identification of double-stranded RNA-binding domains in the interferon-induced double-stranded RNA-activated p68 kinase. Proc Natl Acad Sci U S A *89*, 5447-5451.

Ferguson, B.J., Mansur, D.S., Peters, N.E., ..., and Smith, G.L. (2012). DNA-PK is a DNA sensor for IRF-3-dependent innate immunity. Elife *1*, e00047.

Fernandes-Alnemri, T., Yu, J.W., Datta, P., ..., and Alnemri, E.S. (2009). AIM2 activates the inflammasome and cell death in response to cytoplasmic DNA. Nature *458*, 509-513.

Floyd, R.A., West, M.S., Eneff, K.L., …, and Tingey, D.T. (1988). Hydroxyl free radical mediated formation of 8-hydroxyguanine in isolated DNA. Arch Biochem Biophys *262*, 266-272.

Franz, S., Gaipl, U.S., Munoz, L.E., ..., and Herrmann, M. (2006). Apoptosis and autoimmunity: when apoptotic cells break their silence. Curr Rheumatol Rep *8*, 245-247.

Fuchs, G., Stein, A.J., Fu, C., ..., and Wolin, S. (2006). Structural and biochemical basis for misfold RNA reconition by the Ro autoantigen. Nat Struct Mol Bio 13, 1002-1009

Fuchs T. A., Abed U., Goosmann C., ..., Zychlinsky A. (2007) Novel cell death program leads to neutrophil extracellular traps. J. Cell Biol. 176, 231–241.

Fuchs A, .Vermi, W., Lee, J.S., ..., and Colonna, M. (2013). Intraepithelial type 1 innate lymphoid cells are a unique subset of IL-12- and IL-15-responsive IFN-γ-producing cells. Immunity 38(4):769-81

Fujita,T., Kimura, Y., Miyamoto, M., ..., and Taniguchi, T. (1989). Induction of endogenous IFN-alpha and IFN-beta genes by a regulatory transcription factor, IRF-1. Nature *337*, 270-272.

Fujita,T., Sakakibara, J., Sudo, Y., ..., and Taniguchi, T. (1988). Evidence for a nuclear factor(s), IRF-1, mediating induction and silencing properties to human IFN-beta gene regulatory elements. EMBO J *7*, 3397-3405.

Gall, A., Treuting, P., Elkon, K.B., ..., and Stetson, D.B. (2012). Autoimmunity initiates in nonhematopoietic cells and progresses via lymphocytes in an interferon-dependent autoimmune disease. Immunity 36(1):120–131.

Gao, P., Ascano, M., Wu, Y., …, and Patel, D.J. (2013a). Cyclic [G(2',5')pA(3',5')p] is the metazoan second messenger produced by DNA-activated cyclic GMP-AMP synthase. Cell *153*, 1094-1107.
Gao, P., Ascano, M., Zillinger, T., …, and Patel, D.J. (2013b). Structure-function analysis of STING activation by c[G(2',5')pA(3',5')p] and targeting by antiviral DMXAA. Cell *154*, 748-762.

GeurtsvanKessel C. H., Willart M. A., van Rijt L. S., …, and Lambrecht, B.N. (2008). Clearance of influenza virus from the lung depends on migratory langerin^{+}CD11b^{-} but not plasmacytoid dendritic cells. J. Exp. Med. 205: 1621–1634

Gehrke, N., Mertens, C., Zillinger, T., …, and Barchet, W. (2013). Oxidative Damage of DNA Confers Resistance to Cytosolic Nuclease TREX1 Degradation and Potentiates STING-Dependent Immune Sensing. Immunity 39, 482–495

Goodbourn, S., and Maniatis, T. (1988). Overlapping positive and negative regulatory domains of the human beta-interferon gene. Proc Natl Acad Sci U S A *85*, 1447-1451.

Gordon, S. (2002). Pattern recognition receptors: doubling up for the innate immune response. Cell *111*, 927-930.
Gracias, D. T., Stelekati, E., Hope, J.L., …, and Katsikis, P.D. (2013). The microRNA miR-155 controls CD8+ T cell responses by regulating interferon signaling. Nature Immunol. 14, 593–602

Grollman, A.P., and Moriya, M. (1993). Mutagenesis by 8-oxoguanine: an enemy within. Trends Genet *9*, 246-249.

Guiducci, C., Coffman, R.L. and Barrat, F.J. (2009). Signalling pathways leading to IFN-alpha production in human plasmacytoid dendritic cell and the possible use of agonists or antagonists of TLR7 and TLR9 in clinical indications. J Intern Med. 265(1):43-57

Gürtler, C., and Bowie, A.G. (2013). Innate immune detection of microbial nucleic acids. Trends Microbiol *21*, 413-420.

Hahne M, Rimoldi D, Schröter M, …, and Tschopp J. (1996). Melanoma cell expression of Fas(Apo-1/CD95) ligand: implications for tumor immune escape. Science. 274(5291), 1363-6.

Hakkim, A., Fürnrohr, B.G., Amann, K., ..., and Zychlinsky, A. (2010). Impairment of neutrophil extracellular trap degradation is associated with lupus nephritis. Proc Natl Acad Sci U S A. 107(21):9813-9818.

Hampton, M.B., Kettle, A.J., and Winterbourn, C.C. (1998). Inside the neutrophil phagosome: oxidants, myeloperoxidase, and bacterial killing. Blood *92*, 3007–3017.

Halliwell, B., and Aruoma, O.I. (1991). DNA damage by oxygen-derived species. Its mechanism and measurement in mammalian systems. FEBS Lett *281*, 9-19.

Harada, H., Matsumoto, M., Sato, M., …, and Taniguchi, T. (1996). Regulation of IFN-alpha/beta genes: evidence for a dual function of the transcription factor complex ISGF3 in the production and action of IFN-alpha/beta. Genes Cells *1*, 995-1005.

Hari, A., Flach, T.L., Shi, Y. and Mydlarski, P.R. (2010) Toll-like receptors: role in dermatological disease. *Mediators Inflamm* 2010:437246

Harley, J.B., Alarcón-Riquelme, M.E., Criswell, L.A., …, and Kelly, J.A. (2008). Genome-wide association scan in women with systemic lupus erythematosus identifies susceptibility variants in ITGAM, PXK, KIAA1542 and other loci. Nat Genet *40*, 204-210.

He, X., Jia, H., Jing, Z., and Liu, D. (2013). Recognition of pathogen-associated nucleic acids by endosomal nucleic acid-sensing toll-like receptors. Acta Biochim Biophys Sin (Shanghai) *45*, 241-258.

Heil, F., Hemmi, H., Hochrein, H., ..., and Bauer, S. (2004). Species-specific recognition of single-stranded RNA via toll-like receptor 7 and 8. Science *303*, 1526-1529.

Hellenbrand, K. M., Forsythe, K. M., Rivera-Rivas, J. J., ..., and Aulik, N. A. (2013). *Histophilus somni* causes extracellular trap formation by bovine neutrophils and macrophages. Microb. Pathog. 54, 67–75.

Herrmann, M., Voll, R.E., Zoller, O.M., …, and Kalden, J.R. (*1998).* Impaired phagocytosis of apoptotic cell material by monocyte-derived macrophages from patients with systemic lupus erythematosus. Arthritis Rheum 41*:* 1241–50.

Hershey, J.W. (1989). Protein phosphorylation controls translation rates. J Biol Chem *264*, 20823-20826.

Hewicker M., Kromschroder E., and Trautwein G. (1990) Detection of circulating immune complexes in MRL mice with different forms of glomerulonephritis. *Z. Versuchstierk.* 33, 149-156.

Hogle, J.M. (2002). Poliovirus cell entry: common structural themes in viral cell entry pathways, Annu. Rev. Microbiol. 56:677–702.

Horan, K.A., Hansen, K., Jakobsen, M.R., …, and Paludan, S.R. (2013). Proteasomal degradation of herpes simplex virus capsids in macrophages releases DNA to the cytosol for recognition by DNA sensors. J Immunol *190*, 2311-2319.

Hornung, V., Ablasser, A., Charrel-Dennis, M., ..., and Fitzgerald, K.A. (2009). AIM2 recognizes cytosolic dsDNA and forms a caspase-1-activating inflammasome with ASC. Nature *458*, 514-518.

Hornung, V., Ellegast, J., Kim, S., …, and Hartmann, G. (2006). 5'-Triphosphate RNA is the ligand for RIG-I. Science *314*, 994-997.

Hornung, V., Guenthner-Biller, M., Bourquin, C., …, and Hartmann, G. (2005). Sequence-specific potent induction of IFN-alpha by short interfering RNA in plasmacytoid dendritic cells through TLR7. Nat Med *11*, 263-270.

Hornung, V., Rothenfusser, S., Britsch, S., ..., and Hartmann, G. (2002). Quantitative expression of toll-like receptor 1-10 mRNA in cellular subsets of human peripheral blood mononuclear cells and sensitivity to CpG oligodeoxynucleotides. J Immunol *168*, 4531-4537.

Hoshino, K., Kaisho, T., Iwabe, T., ..., and Akira, S. (2002). Differential involvement of IFN-beta in Toll-like receptor-stimulated dendritic cell activation. Int Immunol *14*, 1225-1231.

Hovanessian, A.G. (1989). The double stranded RNA-activated protein kinase induced by interferon: dsRNA-PK. J Interferon Res *9*, 641-647.

Hu, J. J., Dubin, N., Kurland, D., Ma, B. L., and Roush, G. C. (1995). The effects of hydrogen peroxide on DNA repair activities. *Mutat. Res.* **336,** 193–201

Huangfu, W.-C. *et al*. (2011). Inflammatory signaling compromises cell responses to interferon alpha. *Oncogene* 31, 161–172

Hurtado, P. and Peh, C.A. (2010). LL-37 promotes rapid sensing of CpG oligodeoxynucleotides by B lymphocytes and plasmacytoid dendritic cells. J Immunol. 184(3):1425-35.

Huynh, L., Wang, L., Shi, C., ..., and Ivashkiv, L. B. (2012). ITAM-coupled receptors inhibit IFNAR signaling and alter macrophage responses to TLR4 and *Listeria monocytogenes. J. Immunol.* 188, 3447–3457

Hönigsmann, H. (2001). Phototherapy for psoriasis. Clin Exp Dermatol *26*, 343-350.

Höss, M., Robins, P., Naven, T.J., ..., and Lindahl, T. (1999). A human DNA editing enzyme homologous to the Escherichia coli DnaQ/MutD protein. EMBO J *18*, 3868-3875.

Imai, Y., Kuba, K., Neely, G.G., ..., and Penninger, J.M. (2008). Identification of oxidative stress and Toll-like receptor 4 signaling as a key pathway of acute lung injury. Cell. 133: 235–249.

Isaacs, A., and Lindemann, J. (1957). Virus interference. I. The interferon. Proc R Soc Lond B Biol Sci *147*, 258-267.

Ishii, K.J., Coban, C., Kato, H., .., and Akira, S. (2005). A Toll-like receptor-independent antiviral response induced by double-stranded B-form DNA. Nat Immunol *7*, 40-48.

Ishii, K.J., Suzuki, K., Coban, C., ..., and Klinman, D.M. (2001). Genomic DNA released by dying cells induces the maturation of APCs J. Immunol. 167, 2602- 2607.

Ishikawa, H. and Barber, G.N. (2008). STING is an endoplasmic reticulum adaptor that facilitates innate immune signalling. Nature. 455(7213):674-678

Ishikawa, H., Ma, Z., and Barber, G.N. (2009). STING regulates intracellular DNA-mediated, type I interferon-dependent innate immunity. Nature *461*, 788-792.

Jacob, C.O., Zhu, J., Armstrong, D.L., .., and Mohan C. (2009). Identification of IRAK1 as a risk gene with critical role in the pathogenesis of systemic lupus erythematosus. Proc Natl Acad Sci U S A *106*, 6256-6261.

Janeway, C. (1989a). Immunogenicity signals 1,2,3 ... and 0. Immunol Today *10*, 283-286.

Janeway, C.A. (1989b). Approaching the asymptote? Evolution and revolution in immunology. Cold Spring Harb Symp Quant Biol *54 Pt 1*, 1-13.

Janeway, C.A., and Medzhitov, R. (2002). Innate immune recognition. Annu Rev Immunol *20*, 197-216.

Jensen, P.B., Sørensen, B.S., Sehested, M., ..., and Hansen, H.H. (1993). Different modes of anthracycline interaction with topoisomerase II: Separate structures critical for DNA-cleavage, and for overcoming topoisomerase II-related drug resistance, 1993, Biochemical Pharmacology, 45 (10), 2025-2035

Jewell N. A., Vaghefi N., Mertz S. E., ..., and Durbin J. E.. (2007). Differential type I interferon induction by respiratory syncytial virus and influenza a virus in vivo. J. Virol. 81: 9790–9800

Johnson, N.P., Butour, J.L., Villani, G., …, and Brabec, V. (1989). Metal antitumor compounds: the mechanism of action of platinum complexes. Prog. Clin. Biochem. Med.,10:1–24.

Jovasevic, V.M. and Mokyr , M.B¨(2001). Melphalan-Induced Expression of IFN-β in MOPC-315 Tumor-Bearing Mice and Its Importance for the Up-Regulation of TNF-α Expression. J Immunol 167 (9), 4895-4901

Jurk, M., Heil, F., Vollmer, J., ..., and Bauer, S. (2002). Human TLR7 or TLR8 independently confer responsiveness to the antiviral compound R-848. Nat Immunol *3*, 499.

Kaiser, W.J., Upton, J.W., and Mocarski, E.S. (2008). Receptor-interacting protein homotypic interaction motif-dependent control of NF-kappa B activation via the DNA-dependent activator of IFN regulatory factors. J Immunol *181*, 6427-6434.

Kang, D.C., Gopalkrishnan, R.V., Wu, Q., ..., and Fisher, P.B. (2002). mda-5: An interferon-inducible putative RNA helicase with double-stranded RNA-dependent ATPase activity and melanoma growth-suppressive properties. Proc Natl Acad Sci U S A *99*, 637-642.

Kao, J.L., Nadji, S., and Taylor, J.S. (1993). Identification and structure determination of a third cyclobutane photodimer of thymidylyl-(3'-->5')-thymidine: the trans-syn-II product. Chem Res Toxicol *6*, 561-567.

Kariuki, S.N., Franek, B.S., Kumar, A.A., ..., and Niewold, T.B. (2010). Trait-stratified genome-wide association study identifies novel and diverse genetic associations with serologic and cytokine phenotypes in systemic lupus erythematosus. Arthritis Res Ther *12*, R151.

Kasai, H. (1997). Analysis of a form of oxidative DNA damage, 8-hydroxy-2'-deoxyguanosine, as a marker of cellular oxidative stress during carcinogenesis. Mutat Res *387*, 147-163.

Kasai, H., Hayami, H., Yamaizumi, Z., …, and Nishimura, S. (1984). Detection and identification of mutagens and carcinogens as their adducts with guanosine derivatives. Nucleic Acids Res *12*, 2127-2136.

Kasai, H., Yamaizumi, Z., Yamamoto, F., ..., and Cadet, J. (1992). Photosensitized formation of 8-hydroxyguanine (7,8-dihydro-8-oxoguanine) in DNA by riboflavin. Nucleic Acids Symp Ser, 181-182.

Kato, H., Takeuchi, O., Mikamo-Satoh, E., ..., and Akira, S. (2008). Length-dependent recognition of double-stranded ribonucleic acids by retinoic acid-inducible gene-I and melanoma differentiation-associated gene 5. J Exp Med *205*, 1601-1610.

Kato, H., Takeuchi, O., Sato, S., …, and Akira, S.(2006). Differential roles of MDA5 and RIG-I helicases in the recognition of RNA viruses. Nature *441*, 101-105.

Kavanagh, D., Spitzer, D., Kothari, P.H., ..., and Atkinson, J.P. (2008). New roles for the major human 3'–5' exonuclease TREX1 in human Disease. *Cell Cycle*. 7(12): 1718–1725.

Kawai, T., Adachi, O., Ogawa, T., ..., and Akira, S. (1999). Unresponsiveness of MyD88-deficient mice to endotoxin. Immunity *11*, 115-122.

Kawai, T. and Akira, S. (2007). TLR signaling. Semin Immunol. 19(1):24-32

Kawai, T., Sato, S., Ishii, K.J., …, and Akira, S. (2004). Interferon-alpha induction through Toll-like receptors involves a direct interaction of IRF7 with MyD88 and TRAF6. Nat Immunol *5*, 1061-1068.

Kawai, T., Takahashi, K., Sato, S., ..., and Akira, S. (2005). IPS-1, an adaptor triggering RIG-I- and Mda5-mediated type I interferon induction. Nat Immunol *6*, 981-988.

Kawai, T., Takeuchi, O., Fujita, T., ..., and Akira, S. (2001). Lipopolysaccharide stimulates the MyD88-independent pathway and results in activation of IFN-regulatory factor 3 and the expression of a subset of lipopolysaccharide-inducible genes. J Immunol *167*, 5887-5894.

Kawane, K., Ohtani, M., Miwa, K., ..., and Nagata, S. (2006). Chronic polyarthritis caused by mammalian DNA that escapes from degradation in macrophages. Nature 443:998–1002.

Kelley, V.E. and Roths, J.B. (1985) Interaction of mutant *lpr* gene with background strain influences renal disease. Clinical Immunology and Immunopathology 37, 220-29
Kerr, J.F., Wyllie, A.H., and Currie, A.R. (1972). Apoptosis: a basic biological phenomenon with wide-ranging implications in tissue kinetics. Br J Cancer *26*, 239-257.

Keshari, R.S., Verma, A., Barthwal, M.K. and Dikshit, M. (2013). Reactive oxygen species-induced activation of ERK and p38 MAPK mediates PMA-induced NETs release from human neutrophils. J Cell Biochem. 114(3):532-540.

Kim, S.T., Heelis, P.F., and Sancar, A. (1992). Energy transfer (deazaflavin-->FADH2) and electron transfer (FADH2-->T <> T) kinetics in Anacystis nidulans photolyase. Biochemistry *31*, 11244-11248.

Kim,T., Pazhoor, S., Bao, M., ..., and Liu, Y.J. (2010). Aspartate-glutamate-alanine-histidine box motif (DEAH)/RNA helicase A helicases sense microbial DNA in human plasmacytoid dendritic cells. Proc Natl Acad Sci U S A *107*, 15181-15186.

Kindl, G., and Raab, W. (1998). Licht und Haut, Vol 4 (Govi-Verlag).

Kirou, K.A. and Gkrouzman, E. (2013). Anti-interferon alpha treatment in SLE. Clinical Immunology 148 (3), 303- 312

Knight, E., and Korant, B.D. (1979). Fibroblast interferon induces synthesis of four proteins in human fibroblast cells. Proc Natl Acad Sci U S A *76*, 1824-1827.

Kockritz-Blickwede, M., Goldmann, O., Thulin, P., ..., and Medina, E. (2008). Phagocytosis-independent antimicrobial activity of mast cells by means of extracellular trap formation. Blood 111: 3070–3080.

Kohda, K., Nakagawa, T., and Kawazoe, Y. (1990). Singlet oxygen takes part in 8-hydroxydeoxyguanosine formation in deoxyribonucleic acid treated with the horseradish peroxidase-H2O2 system. Chem Pharm Bull (Tokyo) *38*, 3072-3075.

Kohda, K., Tada, M., Kasai, H., ..., and Kawazoe, Y. (1980). Formation of 8-hydroxyguanine residues in cellular DNA exposed to the carcinogen 4-nitroquinoline 1-oxide. Biochim. Biophys. Res., Commun *139*, 7.

Kohn, K.W. (1981). Molecular mechanisms of crosslinking of alkylating agents and platinum complexes, in Sartorelli AC,Lazo JS, Bertino JR (eds): Molecular Actions and Targets for Cancer Chemotherapeutic Agents. San Diego, Academic, 3-16

Kondo, T., Kobayashi, J., Saitoh, T., ..., and Kawai, T. (2013). DNA damage sensor MRE11 recognizes cytosolic double-stranded DNA and induces type I interferon by regulating STING trafficking. Proc Natl Acad Sci U S A *110*, 2969-2974.

Krieg, A.M. (1996). An innate immune defense mechanism based on the recognition of CpG motifs in microbial DNA. J Lab Clin Med *128*, 128-133.

Krieg, A.M. (2010). AIMing 2 defend against intracellular pathogens. Nat Immunol *11*, 367-369.

Krieser, R.J., and Eastman, A. (1998). The cloning and expression of human deoxyribonuclease II. A possible role in apoptosis. J Biol Chem *273*, 30909-30914.

Krieser, R.J., MacLea, K.S., Longnecker, D.S.,…, and Eastman, A, (2002). Deoxyribonuclease II alpha is required during the phagocytic phase of apoptosis and its loss causes perinatal lethality. Cell Death Differ 9:956–962.

Krug, A., Towarowski, A., Britsch, S., ..., and Hartmann, G. (2001). Toll-like receptor expression reveals CpG DNA as a unique microbial stimulus for plasmacytoid dendritic cells which synergizes with CD40 ligand to induce high amounts of IL-12. Eur J Immunol *31*, 3026-3037.

Krutmann, J. (2003). Premature skin aging by ultraviolet radiation and other environmental hazards. The molecular basis. Hautarzt *54*, 809-817.

Kuechle, M.K., and Elkon, K.B. (2007). Shining light on lupus and UV. Arthritis Res Ther *9*, 101.

Kuerbitz, S.J., Plunkett, B.S., Walsh, W.V., and Kastan, M.B. (1992). Wild-type p53 is a cell cycle checkpoint determinant following irradiation. Proc Natl Acad Sci U S A *89*, 7491-7495.

Kuhn, A., Herrmann, M., Kleber, S., ..., and Kolb-Bachofen, V. (2006). Accumulation of apoptotic cells in the epidermis of patients with cutaneous lupus erythematosus after ultraviolet irradiation. Arthritis Rheum 54:939-50

Lacks, S.A. (1981). Deoxyribonuclease I in mammalian tissues. Specificity of inhibition by actin, J Biol Chemi 256 (6): 2644–2648

LaFleur, D.W., Nardelli, B., Tsareva, T., …, and Moore, P.A. (2001). Interferon-kappa, a novel type I interferon expressed in human keratinocytes. J Biol Chem *276*, 39765-39771.

Lande, R., Gregorio, J., Facchinetti, V., …, and Gilliet, M. (2007). Plasmacytoid dendritic cells sense self-DNA coupled with antimicrobial peptide. Nature *449*, 564-569.

Larner, A.C., Jonak, G., Cheng, Y.S., ..., and Darnell, J.E. (1984). Transcriptional induction of two genes in human cells by beta interferon. Proc Natl Acad Sci U S A *81*, 6733-6737.

Laskowski, M. (1971) in The enzymes (Boyer, P. D., Landy, H. & Myrbäck, K., eds) Academic Press, New York 4: 289–311

Leblanc, J.F., Cohen, L., Rodrigues, M., and Hiscott, J. (1990). Synergism between distinct enhanson domains in viral induction of the human beta interferon gene. Mol Cell Biol *10*, 3987-3993.

Lee, C.H., Wu, S.B., Hong, C.H., ..., and Wei, Y.H. (2013). Molecular Mechanisms of UV-Induced Apoptosis and Its Effects on Skin Residential Cells: The Implication in UV-Based Phototherapy. Int J Mol Sci *14*, 6414-6435.

Lee, P.Y., Weinstein, J.S., Nacionales, D.C., ..., and Reeves, W.H. (2008). A novel type I IFN-producing cell subset in murine lupus. J Immunol. 180(7):5101-8.

Lee, S.B., and Esteban, M. (1993). The interferon-induced double-stranded RNA-activated human p68 protein kinase inhibits the replication of vaccinia virus. Virology *193*, 1037-1041.

Lee-Kirsch, M.A., Gong, M., Chowdhury, D., …, and Hübner, N. (2007). Mutations in the gene encoding the 3'-5' DNA exonuclease TREX1 are associated with systemic lupus erythematosus. Nat Genet *39*, 1065-1067.

Lee-Kirsch, M.A., Gong, M., Schulz, H., ..., and Linné, M. (2006). Familial chilblain lupus, a monogenic form of cutaneous lupus erythematosus, maps to chromosome 3p. Am J Hum Genet *79*, 731-737.

Limoli, C.L., Giedzinski, E., Bonner, W.M., and Cleaver, J.E. (2002). UV-induced replication arrest in the xeroderma pigmentosum variant leads to DNA double-strand breaks, gamma -H2AX formation, and Mre11 relocalization. Proc Natl Acad Sci U S A *99*, 233-238.

Lindahl, T., Gally, J.A., and Edelman, G.M. (1969). Properties of deoxyribonuclease 3 from mammalian tissues. J Biol Chem *244*, 5014-5019.

Lippke, J.A., Gordon, L.K., Brash, D.E., and Haseltine, W.A. (1981). Distribution of UV light-induced damage in a defined sequence of human DNA: detection of alkaline-sensitive lesions at pyrimidine nucleoside-cytidine sequences. Proc Natl Acad Sci U S A *78*, 3388-3392.

Lippmann, J., Rothenburg, S., Deigendesch, N., …, and Opitz, B. (2008). IFNbeta responses induced by intracellular bacteria or cytosolic DNA in different human cells do not require ZBP1 (DLM-1/DAI). Cell Microbiol *10*, 2579-2588.

Liu, J., HuangFu, W.-C., Suresh Kumar, K.G., …, and Fuchs, S.Y. (2009). Virus-induced unfolded protein response attenuates antiviral defenses via phosphorylation-dependent degradation of the type I interferon receptor. Cell Host Microbe 5, 72–83

Liu, Y.J. (2005). IPC: professional type 1 interferon-producing cells and plasmacytoid dendritic cell precursors. Annu Rev Immunol *23*, 275-306.

Loo, Y.M., Fornek, J., Crochet, N., ..., and Gale, M. (2008). Distinct RIG-I and MDA5 signaling by RNA viruses in innate immunity. J Virol *82*, 335-345.

Lund, F.E. (2008). Cytokine-producing B lymphocytes-key regulators of immunity. Curr Opin Immunol *20*, 332-338.

Lund, J., Sato, A., Akira, S., …, and Iwasaki, A.(2003). Toll-like Receptor 9–mediated Recognition of Herpes Simplex Virus-2 by Plasmacytoid Dendritic Cells. J Exp Med. 198(3): 513–520.

Lund, J.M., Alexopoulou, L., Sato, A., ..., and Flavell, R.A. (2004). Recognition of single-stranded RNA viruses by Toll-like receptor 7. Proc Natl Acad Sci U S A *101*, 5598-5603.

Malathi, K., Dong, B., Gale, M., and Silverman, R.H. (2007). Small self-RNA generated by RNase L amplifies antiviral innate immunity. Nature *448*, 816-819.

Maltzman, W., and Czyzyk, L. (1984). UV irradiation stimulates levels of p53 cellular tumor antigen in nontransformed mouse cells. Mol Cell Biol *4*, 1689-1694.

Mandal, M. and Lee, K.D. (2002). Listeriolysin O-liposome-mediated cytosolic delivery of macromolecule antigen in vivo: enhancement of antigen-specific cytotoxic T lymphocyte frequency, activity, and tumor protection, Biochim. Biophys. Acta 1563:7–17.

Mantovani, A., Cassatella, M.A., Costantini, C., and Jaillon, S. (2011). Neutrophils in the activation and regulation of innate and adaptive immunity. Nat Rev Immunol *11*, 519-531.

Mantovani, A., Sica, A., Sozzani, S., ..., and Locati, M. (2004). The chemokine system in diverse forms of macrophage activation and polarization. *Trends Immunol* 25(12):677-686

Marian, V., and Anolik, J.H. (2012). Treatment targets in systemic lupus erythematosus: biology and clinical perspective. Arthritis Res Ther *14 Suppl 4*, S3.

Marié, I., Durbin, J.E., and Levy, D.E. (1998). Differential viral induction of distinct interferon-alpha genes by positive feedback through interferon regulatory factor-7. EMBO J *17*, 6660-6669.

Martin, D.A. and Elkon, K.B. (2006). Intracellular mammalian DNA stimulates myeloid dendritic cells to produce type I interferons predominantly through a toll-like receptor 9-independent pathway. Arthritis Rheum 54 (3): 951-62

Martin, M.U., and Wesche, H. (2002). Summary and comparison of the signaling mechanisms of the Toll/interleukin-1 receptor family. Biochim Biophys Acta *1592*, 265-280.

Matzinger, P. (2002). The Danger Model: A Renewed Sense of Self. Science. 296:301–305.

Maverakis, E., Miyamura, Y., Bowen, M.P., Correa, G., Ono, Y., and Goodarzi, H. (2010). Light, including ultraviolet. J Autoimmun *34*, J247-257.

Mazur, D.J., and Perrino, F.W. (1999). Identification and expression of the TREX1 and TREX2 cDNA sequences encoding mammalian 3'-->5' exonucleases. J Biol Chem *274*, 19655-19660.

McCartney, S.A., Thackray, L.B., Gitlin, L., ..., and Colonna, M. (2008). MDA-5 recognition of a murine norovirus. PLoS Pathog *4*, e1000108.

McWhirter, S.M., Barbalat, R., Monroe, K.M., …, and Vance, R.E. (2009). A host type I interferon response is induced by cytosolic sensing of the bacterial second messenger cyclic-di-GMP. J Exp Med *206*, 1899-1911.

Medzhitov, R., Preston-Hurlburt, P., and Janeway, C.A. (1997). A human homologue of the Drosophila Toll protein signals activation of adaptive immunity. Nature *388*, 394-397.

Medzhitov, R., Preston-Hurlburt, P., Kopp, E., ..., and Janeway, C.A. (1998). MyD88 is an adaptor protein in the hToll/IL-1 receptor family signaling pathways. Mol Cell *2*, 253-258.

Meier, O. and Greber, U.F. (2003). Adenovirus endocytosis, J. Gene Med. 5:451–462.

Metzler, K.D., Fuchs, T.A., Nauseef, W.M., .., and Zychlinsky, A. (2011). Myeloperoxidase is required for neutrophil extracellular trap formation: implications for innate immunity. Blood *117*, 953-959.

Meylan, E., Curran, J., Hofmann, K., ..., and Tschopp, J. (2005). Cardif is an adaptor protein in the RIG-I antiviral pathway and is targeted by hepatitis C virus. Nature *437*, 1167-1172.

Mitchell, D.L. (1988). The relative cytotoxicity of (6-4) photoproducts and cyclobutane dimers in mammalian cells. Photochem Photobiol *48*, 51-57.

Miyamoto, M., Fujita, T., Kimura, Y., ..., and Taniguchi, T. (1988). Regulated expression of a gene encoding a nuclear factor, IRF-1, that specifically binds to IFN-beta gene regulatory elements. Cell *54*, 903-913.

Miyoshi, K., Cui, Y., Riedlinger, G., ..., and Hennighausen, L. (2001). Structure of the mouse Stat 3/5 locus: evolution from Drosophila to zebrafish to mouse. Genomics *71*, 150-155.

Moore, J.K., and Haber, J.E. (1996). Cell cycle and genetic requirements of two pathways of nonhomologous end-joining repair of double-strand breaks in Saccharomyces cerevisiae. Mol Cell Biol *16*, 2164-2173.

Morita, M., Stamp, G., Robins, P., ..., and Barnes, D.E. (2004). Gene-targeted mice lacking the Trex1 (DNase III) 3'-->5' DNA exonuclease develop inflammatory myocarditis. Mol Cell Biol *24*, 6719-6727.

Muñoz, L. E., Janko, C., Schulze, C., ..., and Herrmann, M. (2010). Autoimmunity and chronic inflammation - two clearance-related steps in the etiopathogenesis of SLE. Autoimmun Rev *10*, 38-42.

Nakanishi, K., Yoshimoto, T., Tsutsui, H. and Okamura, H. (2001). Interleukin- 18 regulates both Th1 and Th2 responses. Annu. Rev. Immunol., 19, 423–474
Napirei, M., Karsunky, H., Zevnik, B., ... and Moroy, T. (2000). Features of systemic lupus erythematosus in Dnase1-deficient mice. Nature genetics. 25:177–181

Napirei, M., Ricken, A., Eulitz, D., ..., and Mannherz, H. G. (2004). Expression pattern of the deoxyribonuclease 1 gene: lesson from the Dnase1 knockout mouse, Biochemical Journal, vol. 380, no. 3, pp. 929–937

Nathan, C. (2006). Neutrophils and immunity: challenges and opportunities. Nat Rev Immunol *6*, 173-182.

Ninomiya-Tsuji, J., Kishimoto, K., Hiyama, A., ..., and Matsumoto, K. (1999). The kinase TAK1 can activate the NIK-I kappaB as well as the MAP kinase cascade in the IL-1 signalling pathway. Nature *398*, 252-256.

Norman, A.W. (1998). Sunlight, season, skin pigmentation, vitamin D, and 25-hydroxyvitamin D: integral components of the vitamin D endocrine system. Am J Clin Nutr *67*, 1108-1110.

Odaka, C., and Mizuochi, T. (1999). Role of macrophage lysosomal enzymes in the degradation of nucleosomes of apoptotic cells. J Immunol *163*, 5346-5352.

Ohnishi, T., Mori, E., and Takahashi, A. (2009). DNA double-strand breaks: their production, recognition, and repair in eukaryotes. Mutat Res *669*, 8-12.

Okabe, Y., Kawane, K., Akira, S., ..., and Nagata, S. (2005). Toll-like receptor-independent gene induction program activated by mammalian DNA escaped from apoptotic DNA degradation. J Exp Med *202*, 1333-1339.

Okamura, W.H., Elnagar, H.Y., Ruther, M., and Dobreff, S. (1993). Thermal [1,7]-Sigmatropic Shift of Previtamin D.sub.3 to Vitamin D.sub.3: Synthesis and Study of Pentadeuterio Derivatives. J. Org. Chem *58*, 10.

Palmer, L.J., Cooper, P.R., Ling, M.R., ..., and Chapple, I.L. (2012). Hypochlorous acid regulates neutrophil extracellular trap release in humans. Clinical and experimental immunology 167(2):261-268.

Parente, R.A., Nir, S. and Szoka, F.C.(1988). pH-dependent fusion of phosphatidylcholine small vesicles, J. Biol. Chem. 263:4724–4730.

Parodi, A., and Rebora, A. (1997). ARA and EADV criteria for classification of systemic lupus erythematosus in patients with cutaneous lupus erythematosus. Dermatology *194*, 217-220.

Parvatiyar, K., Zhang, Z., Teles, R.M., …, and Cheng, G. (2012). The helicase DDX41 recognizes the bacterial secondary messengers cyclic di-GMP and cyclic di-AMP to activate a type I interferon immune response. Nat Immunol *13*, 1155-1161.

Patel, D.A., Patel, A.C., Nolan, W.C., ..., and Holtzman, M.J. (2012) High Throughput Screening for Small Molecule Enhancers of the Interferon Signaling Pathway to Drive Next-Generation Antiviral Drug Discovery. PLoS ONE 7(5): e36594. doi:10.1371

Patel, S., Kumar, S., Jyoti, A., ..., and Dikshit, M. (2010) Nitric oxide donors release extracellular traps from human neutrophils by augmenting free radical generation. Nitric oxide 22(3):226-234.

Pazmandi, K., Agod, Z., Kumar, B.V., ..., and Bacsi, A. (2014). Oxidative modification enhances the immunostimulatory effects of extracellular mitochondrial DNA on plasmacytoid dendritic cells. Free Radical Biology and Medicine, http://dx.doi.org/10.1016/j. freeradbiomed.2014.09.028

Peng, S.L., Madaio, M.P. and Craft, J. (1996). Systemic autoimmunity in LG/J mice. Immunol Lett 53(2-3):153-5.

Peng, S.L, Moslehi, J. and Craft, J. (1997). Roles of interferon-gamma and interleukin-4 in murine lupus. J Clin Invest 99(8):1936-46.

Petricoin, E. 3rd, David, M., Igarashi, K., ..., and Larner, A.C. (1996). Inhibition of alpha interferon but not gamma interferon signal transduction by phorbol esters is mediated by a tyrosine phosphatase. Mol Cell Biol.16(4):1419-24.

Pfaffl , M.W. (2001). A new mathematical model for relative quantification in real-time RT-PCR. Nucleic Acids Res, 29(9):e45.

Pichlmair, A., Schulz, O., Tan, C.P., ..., and Reis e Sousa, C. (2006). RIG-I-mediated antiviral responses to single-stranded RNA bearing 5'-phosphates. Science *314*, 997-1001.

Pisetsky,D.S.,Caster,S.A., Roths,J.B.and Murphy, E.D. (1982).lpr gene control of the anti-DNA response. J Immunol.128:2322

Pilsczek, F.H., Salina, D., Poon, K.K., ..., and Kubes, P. (2010). A novel mechanism of rapid nuclear neutrophil extracellular trap formation in response to Staphylococcus aureus. J Immunol 185(12):7413-7425.

Platanias, L.C. (2005). Mechanisms of type-I- and type-II-interferon-mediated signalling. Nat Rev Immunol *5*, 375-386.

Pommier, Y., Leo, E., Zhang, H. and Marchand, C. (2010). DNA topoisomerases and their poisoning by anticancer and antibacterial drugs. Chem. Biol. 17 (5): 421–33.

Rasmussen, M., Skullerud, K., Bakke, S.J., ..., and Jahnsen, F.L. (2005). Cerebral thrombotic microangiopathy and antiphospholipid antibodies in Aicardi-Goutieres syndrome--report of two sisters. Neuropediatrics *36*, 40-44.

Ravanat, J.L., Douki, T., and Cadet, J. (2001). Direct and indirect effects of UV radiation on DNA and its components. J Photochem Photobiol B *63*, 88-102.

Rebsamen, M., Heinz, L.X., Meylan, E., ..., and Tschopp, J. (2009). DAI/ZBP1 recruits RIP1 and RIP3 through RIP homotypic interaction motifs to activate NF-kappaB. EMBO Rep *10*, 916-922.

Remijsen, Q., Kuijpers, T.W., Wirawan, E., ..., and Vanden Berghe, T. (2011a). Dying for a cause: NETosis, mechanisms behind an antimicrobial cell death modality. Cell Death Differ *18*, 581-588.

Remijsen, Q., Vanden Berghe, T., Wirawan, E., ..., and Vandenabeele, P. (2011b). Neutrophil extracellular trap cell death requires both autophagy and superoxide generation. Cell research 21(2):290-304.

Remmers, E.F., Plenge, R.M., Lee, A.T., …, and Gregersen, P.K. (2007). STAT4 and the risk of rheumatoid arthritis and systemic lupus erythematosus. N Engl J Med *357*, 977-986.

Rice, G., Newman, W.G., Dean, J., …, and Crow, Y.J. (2007a). Heterozygous mutations in TREX1 cause familial chilblain lupus and dominant Aicardi-Goutieres syndrome. Am J Hum Genet *80*, 811-815.

Rice, G., Patrick, T., Parmar, R., …, and Crow, Y.J. (2007b). Clinical and molecular phenotype of Aicardi-Goutieres syndrome. Am J Hum Genet *81*, 713-725.

Roberts, R.M., Liu, L., Guo, Q., ..., and Bixby, J. (1998). The evolution of the type I interferons. J Interferon Cytokine Res *18*, 805-816.

Roberts, T.L., Idris, A., Dunn, J.A., …, and Stacey, K.J. (2009). HIN-200 proteins regulate caspase activation in response to foreign cytoplasmic DNA. Science *323*, 1057-1060.

Rongvaux, A.,Jackson, R., Harman C.C., .., and Flavell, R.A. (2014). Apoptotic caspases prevent the induction of type I interferons by mitochondrial DNA. Cell 159(7):1563-77.

Rosenstein, B.S., and Mitchell, D.L. (1987). Action spectra for the induction of pyrimidine(6-4)pyrimidone photoproducts and cyclobutane pyrimidine dimers in normal human skin fibroblasts. Photochem Photobiol *45*, 775-780.

Roths, J.B. (1987). Differential expression of murine autoimmunity and lymphoid hyperplasia determined by single genes. 21-33 in New Horizons in Animal Models for Autoimmune disease

Rowland, S.L., Riggs, J,M., Gilfillan, S., ..., and Colonna, M. (2014). Early, transient depletion of plasmacytoid dendritic cells ameliorates autoimmunity in a lupus model. J Exp Med. 211(10):1977-91.

Rönnblom, L., and Alm, G.V. (2001). A pivotal role for the natural interferon alpha-producing cells (plasmacytoid dendritic cells) in the pathogenesis of lupus. J Exp Med *194*, F59-63.

Sage, E. (1993). Distribution and repair of photolesions in DNA: genetic consequences and the role of sequence context. Photochem Photobiol *57*, 163-174.

Saito, T., Hirai, R., Loo, Y.M., ..., and Gale, M. (2007). Regulation of innate antiviral defenses through a shared repressor domain in RIG-I and LGP2. Proc Natl Acad Sci U S A *104*, 582-587.

Sakurai, H. (2012). Targeting of TAK1 in inflammatory disorders and cancer. Trends Pharmacol Sci *33*, 522-530.

Samejima, K., and Earnshaw, W.C. (2005). Trashing the genome: the role of nucleases during apoptosis. Nat Rev Mol Cell Biol *6*, 677-688.

Sancar, A. (1994). Structure and function of DNA photolyase. Biochemistry *33*, 2-9.

Sandgren, S., Wittrup, A., Cheng, F., ... and Belting, M (2004). The human antimicrobial peptide LL-37 transfers extracellular DNA plasmid to the nuclear compartment of mammalian cells via lipid rafts and proteoglycan-dependent endocytosis. J Biol Chem. 279(17): 17951-6.

Sato, K., Hida, S., Takayanagi, H., ..., and Ogasawara, K. (2001). Antiviral response by natural killer cells through TRAIL gene induction by IFN-alpha/beta. Eur J Immunol *31*, 3138-3146.

Sato, S., Sugiyama, M., Yamamoto, M., ..., and Akira, S. (2003). Toll/IL-1 receptor domain-containing adaptor inducing IFN-beta (TRIF) associates with TNF receptor-associated factor 6 and TANK-binding kinase 1, and activates two distinct transcription factors, NF-kappa B and IFN-regulatory factor-3, in the Toll-like receptor signaling. J Immunol *171*, 4304-4310.

Sbarra, A.J. and Karnovsky, M.L. (1959). The biochemical basis of phagocytosis. I. Metabolic changes during the ingestion of particles by polymorphonuclear leukocytes. J Biol Chem 234: 1355–1362

Schlee, M., Roth, A., Hornung, V., …, and Hartmann, G. (2009). Recognition of 5' triphosphate by RIG-I helicase requires short blunt double-stranded RNA as contained in panhandle of negative-strand virus. Immunity *31*, 25-34.

Schoenemeyer, A., Barnes, B.J., Mancl, M.E., ..., and Golenbock, D.T. (2005). The interferon regulatory factor, IRF5, is a central mediator of toll-like receptor 7 signaling. J Biol Chem *280*, 17005-17012.

Schwarting, A., Tesch, G., Kinoshita, K., …, and Kelley, V.R. (1999). IL-12 drives IFN-gamma-dependent autoimmune kidney disease in MRL-Fas(lpr) mice. J Immunol 163(12):6884-91.

Segal, A.W. and Coade, S.B. (1978). Kinetics of oxygen consumption by phagocytosing human neutrophils. Biochem. Biophys. Res. Commun. 84:611–617.

Sentenac, A., Simon, E.J. and Fromageot P. (1968). Initiation of chains by RNA polymerase and the effects of inhibitors studied by a direct filtration technique. Biochim Biophys Acta. 161(2):299-308.

Sepehr, A., Wenson, S., and Tahan, S.R. (2010). Histopathologic manifestations of systemic diseases: the example of cutaneous lupus erythematosus. J Cutan Pathol *37 Suppl 1*, 112-124.

Seth, R.B., Sun, L., Ea, C.K., and Chen, Z.J. (2005). Identification and characterization of MAVS, a mitochondrial antiviral signaling protein that activates NF-kappaB and IRF 3. Cell *122*, 669-682.

Setlow, R.B., and Carrier, W.L. (1966). Pyrimidine dimers in ultraviolet-irradiated DNA's. J Mol Biol *17*, 237-254.

Sheppard, P., Kindsvogel, W., Xu, W., …, and Klucher, K.M. (2003). IL-28, IL-29 and their class II cytokine receptor IL-28R. Nat Immunol *4*, 63-68.

Shin, H.D., Park, B.L., Cheong, H.S., ..., and Bae, S.C. (2005). DNase II polymorphisms associated with risk of renal disorder among systemic lupus erythematosus patients. J Hum Genet 50:107–111.

Siegal, F.P., Kadowaki, N., Shodell, M., …, and .Liu, Y.J. (1999). The nature of the principal type 1 interferon-producing cells in human blood. Science.;284:1835–1837.

Sisirak, V, Ganguly, D., Lewis, K.L., ...,, and Reizis, B.(2014). Genetic evidence for the role of plasmacytoid dendritic cells in systemic lupus erythematosus. J Exp Med 211(10):1969-76.

Stacey, K.J., Sweet, M.J., and Hume, D.A. (1996). Macrophages ingest and are activated by bacterial DNA. J Immunol *157*, 2116-2122.

Steinberg, B.E. and Grinstein, S. (2007). Unconventional roles of the NADPH oxidase: signaling, ion homeostasis, and cell death. Sci STKE. 2007:e11

Stetson, D.B., Ko, J.S., Heidmann, T., and Medzhitov, R. (2008). Trex1 prevents cell-intrinsic initiation of autoimmunity. Cell *134*, 587-598.

Stetson, D.B., and Medzhitov, R. (2006). Recognition of cytosolic DNA activates an IRF3-dependent innate immune response. Immunity *24*, 93-103.

Stewart, C.R., Stuart, L.M., Wilkinson, K., …, and Moore, K.J. (2010). CD36 ligands promote sterile inflammation through assembly of a Toll-like receptor 4 and 6 heterodimer. Nat. Immunol. 11:155–161.

Strumberg, D., Pilon, A.A., Smith, M., ..., and Pommier, Y. (2000). Conversion of topoisomerase I cleavage complexes on the leading strand of ribosomal DNA into 5'-phosphorylated DNA double-strand breaks by replication runoff. Mol Cell Biol *20*, 3977-3987.

Sun, L., Wu, J., Du, F., ..., and Chen, Z.J. (2013). Cyclic GMP-AMP synthase is a cytosolic DNA sensor that activates the type I interferon pathway. Science *339*, 786-791.

Sun, W., Li, Y., Chen, L., ..., and Jiang, Z. (2009). ERIS, an endoplasmic reticulum IFN stimulator, activates innate immune signaling through dimerization. Proc Natl Acad Sci U S A *106*, 8653-8658.
Sutherland, B.M. (1974). Photoreactivating enzyme from human leukocytes. Nature *248*, 109-112.

Suzuki, K., Mori, A. Ishii, K.J., …, and Kohn, L.D. (1999). Activation of target-tissue immune-recognition molecules by double-stranded polynucleotides. Proc. Natl. Acad. Sci. USA. 96:2285–2290.

Takahashi, S. Fossati, L., Iwamoto, M., ..., and Izui, S. (1996). Imbalance towards Th1 predominance is associated with acceleration of lupus-like autoimmune syndrome in MRL mice. J Clin Invest 97(7):1597-604.

Takahasi, K., Yoneyama, M., Nishihori, T., ..., and Fujita, T. (2008). Nonself RNA-sensing mechanism of RIG-I helicase and activation of antiviral immune responses. Mol Cell *29*, 428-440.

Takaoka, A., Wang, Z., Choi, M.K., …, and Taniguichi, T. (2007). DAI (DLM-1/ZBP1) is a cytosolic DNA sensor and an activator of innate immune response. Nature *448*, 501-505.

Takaoka, A., Yanai, H., Kondo, S., …, and Taniguchi, T. (2005). Integral role of IRF-5 in the gene induction programme activated by Toll-like receptors. Nature *434*, 243-249.

Takeshita, H., Yasuda, T., Nakajima, T., ..., and Kishi, K. (1997). Mouse deoxyribonuclease I (DNase I): biochemical and immunological characterization, cDNA structure and tissue distribution, Biochemistry and Molecular Biology International 42 (1): 65–75

Takeuchi, O., and Akira, S. (2010). Pattern recognition receptors and inflammation. Cell *140*, 805-820.

Tan, E.M. (1989). Antinuclear antibodies: diagnostic markers for autoimmune diseases and probes for cell biology. Adv Immunol *44*, 93-151.

Tan, E.M., Cohen, A.S., Fries, J.F., ..., and Winchester, R.J. (1982). The 1982 revised criteria for the classification of systemic lupus erythematosus. Arthritis Rheum *25*, 1271-1277.

Tanaka, K., Pracyk, J.B., Takeda, K., ..., and Finkel, T. (1998). Expression of Id1 results in apoptosis of cardiac myocytes through a redox-dependent mechanism J. Biol. Chem. 273 , 25922–25928

Tanaka, Y., and Chen, Z.J. (2012). STING specifies IRF3 phosphorylation by TBK1 in the cytosolic DNA signaling pathway. Sci Signal *5*, ra20.

Taylor, J.S., Garrett, D.S., and Cohrs, M.P. (1988). Solution-state structure of the Dewar pyrimidinone photoproduct of thymidylyl-(3'----5')-thymidine. Biochemistry *27*, 7206-7215.

Torizawa, T., Ueda, T., Kuramitsu, S., ..., and Shimada, I. (2004). Investigation of the cyclobutane pyrimidine dimer (CPD) photolyase DNA recognition mechanism by NMR analyses. J Biol Chem *279*, 32950-32956.

Trinchieri, G. (2010). Type I interferon: friend or foe? JEM 207 (10): 2053- 2063

Unterholzner, L. (2013). The interferon response to intracellular DNA: why so many receptors? Immunobiology *218*, 1312-1321.

Unterholzner, L., Keating, S.E., Baran, M., …, and Bowie, A.G. (2010). IFI16 is an innate immune sensor for intracellular DNA. Nat Immunol *11*, 997-1004.

Vallin, H., Blomberg, S., Alm, G.V., ..., and Rönnblom, L. (1999). Patients with systemic lupus erythematosus (SLE) have a circulating inducer of interferon-alpha (IFN-α) production acting on leucocytes resembling immature dendritic cells. Clin Exp Immunol. 115:196–202

van der Leun, J.C. (2004). The ozone layer. Photodermatol Photoimmunol Photomed *20*, 159-162.

Vremec, D., Pooley, J., Hochrein H., ..., and Shortman, K. (2000). CD4 and CD8 expression by dendritic cell subtypes in mouse thymus and spleen. J Immunol 164 (6): 2978-86

Vremec, D. and Shortman, K. (1997). Dendritic cell subtypes in mouse lymphoid organs: cross-correlation of surface markers, changes on incubation and differences between thymus, spleen and lymph nodes. J. Immunol. 159: 565

Wang, Z., Choi, M.K., Ban, T., ..., and Taniguchi, T. (2008). Regulation of innate immune responses by DAI (DLM-1/ZBP1) and other DNA-sensing molecules. Proc Natl Acad Sci U S A *105*, 5477-5482.

Ward, J.F., Evans, J.W., Limoli, C.L., and Calabro-Jones, P.M. (1987). Radiation and hydrogen peroxide induced free radical damage to DNA. Br J Cancer Suppl *8*, 105-112.

Waring, P. and Müllbacher,A. (1999). Cell death induced by the Fas/Fas ligand pathway and its role in pathology. Immunology and cell biology, 77(4), 312-7, 1999
Watanabe-Fukunaga, R., Brannan, C., Copeland, N.G., …, and Nagata, S. (1992). Lymphoproliferation disorder in mice explained by defects in Fas antigen that mediates apoptosis. *Nature* 356, 314-317.

Watson, M.L., Rao, J.K., Gilkeson, G.S., …, and Seldin, M.F. (1992). Genetic analysis of MRL-*lpr* mice: relationship of *Fas* apoptosis gene to disease manifestations and renal disease-modifying loci. *J. Exp. Med.* 176, 1645-1656.

Webster, S.J., Daigneault, M., Bewley, M.A., ..., and Dockrell, D.H. (2010). Distinct cell death programs in monocytes regulate innate responses following challenge with common causes of invasive bacterial disease. J Immunol 185: 2968–2979.

Weissmann, C., and Weber, H. (1986). The interferon genes. Prog Nucleic Acid Res Mol Biol *33*, 251-300.

West, A.P., Khoury-Hanold, W., Staron, M., ..., and Shadel, G.S. (2015). Mitochondrial DNA stress primes the antiviral innate immune response. Nature. 2015 Feb 2. doi: 10.1038/nature14156

White, M.J., McArthur, K. Metcalf, D., ..., and Kile BT. (2014). Apoptotic caspases suppress mtDNA-induced STING-mediated type I IFN production. Cell 159(7):1549-62.

Wondrak, G.T., Jacobson, M.K., and Jacobson, E.L. (2006). Endogenous UVA-photosensitizers: mediators of skin photodamage and novel targets for skin photoprotection. Photochem Photobiol Sci *5*, 215-237.

Wood, M.L., Dizdaroglu, M., Gajewski, E., and Essigmann, J.M. (1990). Mechanistic studies of ionizing radiation and oxidative mutagenesis: genetic effects of a single 8-hydroxyguanine (7-hydro-8-oxoguanine) residue inserted at a unique site in a viral genome. Biochemistry *29*, 7024-7032.

Wu, J., Sun, L., Chen, X., ..., and Chen, Z.J. (2013). Cyclic GMP-AMP is an endogenous second messenger in innate immune signaling by cytosolic DNA. Science *339*, 826-830.

Wyllie, A.H., Kerr, J.F., and Currie, A.R. (1980). Cell death: the significance of apoptosis. Int Rev Cytol *68*, 251-306.

Xu, J., Gamero, A. and Gallucci, S. (2012). Type I Interferons induce TREX1 in myeloid dendritic cells. Journal Immunol 188, 108-110

Xu, L.G., Wang, Y.Y., Han, K.J., ..., and Shu, H.B. (2005). VISA is an adapter protein required for virus-triggered IFN-beta signaling. Mol Cell *19*, 727-740.

Yamamoto, M., Sato, S., Hemmi, H., ..., and Akira, S. (2003). Role of adaptor TRIF in the MyD88-independent toll-like receptor signaling pathway. Science *301*, 640-643.

Yasuda, K., Yu, P., Kirschning, C.J., ..., and Wagner, H. (2005). Endosomal translocation of vertebrate DNA activates dendritic cells via TLR9-dependent and -independent pathways. J Immunol *174*, 6129-6136.

Yasutomo, K., Horiuchi, T., Kagami, S., ..., and Kuroda, Y. (2001). Mutation of DNASE1 in people with systemic lupus erythematosus. Nature genetics. 28:313–314.

Yipp, B.G. and Kubes, P. (2013). NETosis: How Vital Is It? Blood 17;122(16): 2784-2794.

Yokoyama, H., Kreft, B. and Kelley, V.R. (1995). Biphasic increase in circulating and renal TNF-alpha in MRL-lpr mice with differing regulatory mechanisms. *Kidney Int* 47: 122–130.

Yoneyama, M., Kikuchi, M., Matsumoto, K., …, and Fujita, T. (2005). Shared and unique functions of the DExD/H-box helicases RIG-I, MDA5, and LGP2 in antiviral innate immunity. J Immunol *175*, 2851-2858.

Yoneyama, M., Kikuchi, M., Natsukawa, T., ..., and Fujita, T. (2004). The RNA helicase RIG-I has an essential function in double-stranded RNA-induced innate antiviral responses. Nat Immunol *5*, 730-737.

Yoshida, H., Nishikawa, M., Kiyota, T., ..., and Takakura, Y. (2011). Increase in CpG DNA-induced inflammatory responses by DNA oxidation in macrophages and mice, *Free Radical Biology and Medicine* 51 (2), 424–431

Yoshida, H., Okabe, Y., Kawane, K., ..., and Nagata, S. (2005). Lethal anemia caused by interferon-beta produced in mouse embryos carrying undigested DNA. Nature immunology. 6:49–56.

Yoshida, R., Takaesu, G., Yoshida, H., ..., and Kobayashi, T. (2008). TRAF6 and MEKK1 play a pivotal role in the RIG-I-like helicase antiviral pathway. J Biol Chem *283*, 36211-36220.

Yousefi, S., Gold, J.A., Andina, N., ..., and Simon, H.U. (2008). Catapult-like release of mitochondrial DNA by eosinophils contributes to antibacterial defense. Nat Med 14: 949–953.

Yousefi, S., Mihalache, C., Kozlowski, E., …, and Simon, H.U. (2009). Viable neutrophils release mitochondrial DNA to form neutrophil extracellular traps. Cell Death Differ 16:1438–1444
Yu, Y. and Su, K. (2013). Neutrophil Extracellular Traps and Systemic Lupus Erythematosus. J Clin Cell Immunol.: 139.

Zamanian-Daryoush, M., Mogensen, T.H., DiDonato, J.A., and Williams, B.R. (2000). NF-kappaB activation by double-stranded-RNA-activated protein kinase (PKR) is mediated through NF-kappaB-inducing kinase and IkappaB kinase. Mol Cell Biol *20*, 1278-1290.

Zhang, Q., Itagaki, K. and Hauser, C.J. (2010). Mitochondrial DNA is released by shock and activates neutrophils via p38 map kinase. Shock 34: 55–59.

Zhang, X., Brann, T.W., Zhou, M., …, and Imamichi, T. (2011a). Cutting edge: Ku70 is a novel cytosolic DNA sensor that induces type III rather than type I IFN. J Immunol *186*, 4541-4545.

Zhang, X., Shi, H., Wu, J., ..., and Chen, Z.J. (2013). Cyclic GMP-AMP containing mixed phosphodiester linkages is an endogenous high-affinity ligand for STING. Mol Cell *51*, 226-235.

Zhang, Z., Kim, T., Bao, M., ..., and Liu, Y.J. (2011b). DDX1, DDX21, and DHX36 helicases form a complex with the adaptor molecule TRIF to sense dsRNA in dendritic cells. Immunity *34*, 866-878.

Zhang, Z., Yuan, B., Bao, M., ..., and Liu, Y.J. (2011c). The helicase DDX41 senses intracellular DNA mediated by the adaptor STING in dendritic cells. Nat Immunol *12*, 959-965.

Zhang, Z., Yuan, B., Lu, N., ..., and Liu, Y.J. (2011d). DHX9 pairs with IPS-1 to sense double-stranded RNA in myeloid dendritic cells. J Immunol *187*, 4501-4508.

Zhong, B., Yang, Y., Li, S., ..., and Shu, H.B. (2008). The adaptor protein MITA links virus-sensing receptors to IRF3 transcription factor activation. Immunity *29*, 538-550.

Zhou, F. (2009). Molecular mechanisms of IFN-gamma to up-regulate MHC class I antigen processing and presentation. Int Rev Immunol *28*, 239-260.

Zhu, F.G., Reich, C.F. and Pisetsky. D.S. (2003). Effect of cytofectins on the immune response of murine macrophages to mammalian DNA. Immunology. 109:255–262.

6. Appendix

6.1. Abbreviations

A

Absent in melanoma 2 (AIM2)
Activating protein-1 (AP-1)
Adenosine triphosphate (ATP)
Aicardi-Goutières syndrome (AGS)
Antibody (ab)
Antigen presenting cell (APC)
Antinuclear antibodies (ANA)
AP endonucleases (APE)
Apoptosis-associated speck-like protein containing a CARD (ASC)
A proliferation inducing ligand (APRIL)

B

Base excision repair (BER)
B cell activating factor of the TNF family (BAFF)
Bcl2-Antagonist of Cell Death (BAD)
Bcl-2- associated x protein (BAX)
Blank (blk)
Bone marrow derived DCs (bmDCs)
Bovine serum albumin (BSA)

C

CARD adaptor inducing IFN-β (CARDif)
Caspase-recruitment domain (CARD)
Central nervous system (CNS)
Cluster of differentiation (CD)
Coding sequence (CDS)
Conventional DCs (cDCs)
C-terminal domain (CTD)
Cutaneous LE (CLE)
Cyclic dinucleotides (CDNs)
Cyclic GMP-AMP (cGAMP)
cGAMP synthase (cGAS)
Cycle threshold (C_t)
Cyclobutane pyrimidine dimer (CPD)
Cytotoxic T cells (T_c)

D

Damage- associated molecular pattern (DAMP)
Dendritic cells (DCs)
Desoxynucleic acid (DNA)
Desoxynucleoside triphosphate (dNTP)
Desoxyribonuclease (DNase)
Diethylpyrocarbonat (DEPC)
Dimethylsulfoxid (DMSO)
Dithiothreitol (DTT)
DNA damage response (DDR)
DNA-dependent activator of IRFs (DAI)
DNA-dependent protein kinase (DNA-PK)
DNA double-strand break (DSB)
Double stranded (ds)
Drug-induced LE (DILE)
Dulbecco's Modified Eagle's Medium (DMEM)

E

Endoplasmatic reticulum (ER)
Enhanced Chemiluminescent (ECL)
Enzyme Linked Immunosorbent Assay (ELISA)
Ethylenediaminetetraacetic acid (EDTA)

F

Familial Chilblain Lupus (FCL)
FAS-associated death domain (FADD)
Fetal Calf Serum (FCS)
Fluorescence-activated cell sorting (FACS)
Forward scatter (FSC)

G

Gene of interest (GOI)
GMP-AMP synthase (cGAS)
Granulocyte-macrophage colony-stimulating factor (GM-CSF)
Green fluorescent protein (GFP)

H

Helper T cells (T_H)
Herpes simplex virus (HSV)
High-mobility group box 1 (HMGB1)
Horseradish peroxidase (HRP)
Human immunodeficiency virus (HIV)
Hydrogen peroxide (H_2O_2)
8-Hydroxy-2'-desoxy-guanosine (8-OH-dG)
8-Hydroxy-7,8- didemethyl-5-deazariboflavin (8-HDF)

Hydroxyl radicals ($HO^{\cdot}$)
Hypochlorous acid (HOCl)

I

Inhibitor of nuclear factor kappa-B kinase (IKKβ)
Interferon (IFN)
IFN-alpha receptor (IFNAR)
IFN-inducible protein (IFI)
IFN-promoter-stimulating factor 1 (IPS-1)
IFN-regulatory factor (IRF)
IFN-stimulated gene (ISG)
IFN-stimulated gene factor (ISGF)
IFN-stimulated response elements (ISREs)
IL-1 receptor-associated kinases (IRAK)
Immunoglobulin (Ig)
Immunoreceptory tyrosine-based activation motif (ITAM)
Interleukin (IL)
Isopropyl-β-D-thiogalactopyranosid (IPTG)

J

Janus kinase (JAK)
Jun N-terminal kinase (JNK)

L

Laboratory of genetics and physiology 2 (LGP2)
Leucine rich repeat (LRR)
Lipopolysaccharide (LPS)
Lymphoproliferation (lpr)
Lupus erythematosus (LE)

M

Magnetic- activated cell sorting (MACS)
Major Histocompatibility Complex (MHC)
MAP kinase (MAPK)
Mean fluorescence intensity (MFI)
Mediator of IRF-3 activation (MITA)
Melanoma differentiation- associated gene-5 (MDA5)
Mitochondrial (mt)
Mitochondrial antiviral signalling protein (MAVS)
Mitogen activated protein (MAP)
Mouse embryonic fibroblasts (MEFs)
Meiotic recombination 11 (Mre11)
Murphy Roth Large (MRL)
Myeloid DCs (mDC)
Myeloid differentiation factor 88 (MyD88)
Myeloperoxidase (MPO)

N

NADPH oxidase (Nox)
Natural killer cells (NK)
Neutrophil Extracellular Traps (NETs)
NF-κB-activating kinase (NAK)
Nicotinamide-adenine-dinucleotide-phosphate (NADPH)
NOD-like receptors (NLRs)
Non-essential amino acids (NAAs)
Non-homologous end joining (NHEJ)
Nucleic acid (NA)
Nuclear factor kappa-light-chain-enhancer of activated B-cells (NF-κB)
Nucleotide-binding oligomerization domain (NOD)
Nucleotide excision repair (NER)

O

Oligodeoxyribonucleotide (ODN)
Open reading frame (ORF)
8-oxo-2´-desoxy-guanosine (8-oxo-dG)
Ozone (O3)

P

Pathogen- associated molecular patterns (PAMPs)
Pattern recognition receptors (PRRs)
Peripheral blood mononuclear cells (PBMC)
Phorbol-12-myristate-13-acetate (PMA)
Phosphate buffered saline (PBS)
Plasmacytoid DCs (pDCs)
Polyacrylamide gel electrophoresis (PAGE)
Polyinosine-polycytidylic acid (poly(I:C))
Polymerase (Pol)
Polymerase chain reaction (PCR)
Prostaglandin E2 (PGE2)
Psoralen plus UV-A (PUVA)
6-4 Pyrimidine-pyrimidone photoproduct (6-4-PP)

R

Reactive oxygen species (ROS)
Receptor interacting protein 1 (RIP1)
Repressor domain (RP)
Retinoic acid-inducible gene 1 (RIG-I)
Rheumatoid arthritis (RA)
Ribonuclease (RNase)
Ribonucleic acid (RNA)
RIG-I-like receptor (RLR)
Room temperature (RT)

Roswell Park Memorial Institute (RPMI)

S

Side scatter (SSC)
Single stranded (ss)
Singlet oxygen (1O2)
Signal transducer and activator of transcription (STAT)
Sodium dodecyl sulfate (SDS)
Subacute CLE (SCLE)
Stimulator of interferon genes (STING)
Sunburn cell (SBC)
Superoxide (O_2^-)
Superoxide dismutase (SOD)
Systemic lupus erythematosus (SLE)

T

TAK1- binding proteins (TAB)
TANK-binding kinase 1 (TBK1)
Tetramethylbenzidine (TMB)
Three prime repair exonuclease 1 (TREX1)
TIR domain-containing adapter molecule (TRIF)
TNFR1 associated death domain protein (TRADD)
TNF-receptor associated-factor (TRAF)
TNF-related apoptosis-inducing ligand (TRAIL)
Toll/ interleukin-1 receptor homology (TIR)
Toll-like receptor (TLR)
Topoisomerase (Top)
TRAF-family member associated NF-κB activator (TANK)
Transfer RNAs (tRNAs)
Transforming growth factor (TGF)
Transforming growth factor-beta-activated protein kinase 1 (TAK1)
Triphosphate RNA (3-P-RNA)
Tris-Acetat-EDTA buffer (TAE)
Tris-EDTA (TE)
Tumor necrosis factor alpha (TNF-α)
Tyrosine kinase (Tyk)

U

Ultraviolet (UV)
Uridine (U)
Urocanic acid (UCA)
UV radiation (UVR)
UV irradiated DNA (UV-DNA)

V

Virus-induced signaling adaptor (VISA)
Volt (V)

6.2. Figures and Tables

Figures

Tables